Snow Hydrology of Canadian Prairie Droughts: Model Development and Application

A Thesis Submitted to the College of

Graduate Studies and Research

in Partial Fulfillment of the Requirements

for the Degree of

Master of Science

in the Department of Geography

(Centre for Hydrology)

University of Saskatchewan

Saskatoon

By

Xing Fang

PERMISSION TO USE

In presenting this thesis in partial fulfillment of the requirements for a Postgraduate degree from the University of Saskatchewan, I agree that the Libraries of the University may make it freely available for inspection. I further agree that permission for copying of this thesis in any manner, in whole or in part, for scholarly purposes may be granted by the professors who supervised my thesis work or, in their absence, by the Head of the Department or the Dean of the College in which my thesis work was completed. It is understood that any copying or publication of use of this thesis or parts thereof for financial gain shall not be allowed without my written permission. It is also understood that due recognition shall be given to me and to the University of Saskatchewan in any scholarly use which may be made of any material in my thesis.

Requests for permission to copy or to make any other use of the material in this thesis in whole or in part should be addressed to:

Head of the Department of Geography
University of Saskatchewan
Saskatoon, Saskatchewan
S7N 5A5, Canada

ABSTRACT

Hydrological models have been developed to estimate snow accumulation, snowmelt and snowmelt runoff on the Canadian Prairies; however, their proper scale of application is unknown in the Prairie environment. The first objective of this thesis is to examine the proper scale for pre-melt snow accumulation as snow water equivalent (SWE) and snowmelt in a Prairie first order basin. Spatially distributed and spatially aggregated approaches were used to calculate SWE and snowmelt at St. Denis National Wildlife Area (SDNWA). Both approaches used models with similar physics, but differed in the model scale at which calculations were carried out. The simulated pre-melt SWE, cumulative seasonal SWE, and daily snowmelt from the two modelling approaches were compared to field observations of pre-melt SWE, cumulative seasonal SWE, and daily snowmelt; comparisons of areal cumulative seasonal SWE, areal snowmelt, snowmelt duration, and snow-covered area were also conducted between two modelling approaches. Results from these comparisons showed that both approaches had reasonable and similar accuracy in estimation of SWE and snowmelt. The spatially aggregated approach was more computationally efficient and was selected as a modelling scale for small-sized prairie basins.

Another objective of this thesis is to derive a snow hydrology model for the Canadian Prairies. Physically-based hydrological models were assembled in the Cold Regions Hydrological Model Platform (CRHM) using the aggregated approach. Tests of pre-melt SWE and surface snowmelt runoff

were conducted at two basins in Saskatchewan – Creighton Tributary of Bad Lake and Wetland 109, St. Denis. Results showed that the snow hydrology model had a reasonable capability to simulate SWE and snowmelt runoff to the stream and wetland.

Droughts are natural hazards that develop frequently on the Canadian Prairies. Analyzing the impact of drought on hydrological processes and water supply is another objective of this thesis. Synthetic drought scenarios were proposed for the Creighton Tributary of Bad Lake and the corresponding impacts on the snowmelt runoff-related processes were examined. Results indicated that wind redistribution of snow was very sensitive to drought conditions, sublimation of blowing snow and snow-covered period were sensitive to drought, but winter evaporation and infiltration did not show strong trend. The results also showed that drought conditions had magnified effects on the snowmelt runoff and could cause cessation of streamflow. Also, the impacts of the recent 1999-2005 drought on the snowmelt hydrology were investigated at St. Denis. Results illustrated that three-years (1999-2002) of severe winter drought were followed by a normal year (2002-03) and then a two-year (2003-05) recovery period, and then returning to normal (2005-06). Results showed that both snowfall and rainfall during hydrological winter were consistently low for severe drought and surface snowmelt runoff was very much lower during severe drought, about 45-65 mm less compared to that in the normal periods.

ACKNOWLEDGEMENTS

I would like to extend my gratitude to my supervisor, Dr. John Pomeroy for his guidance and support throughout my Graduate Studies program and for his insightful recommendation to my research. I would also like to thank my advisory committee members: Dr. Lawrence Martz and Dr. Seifu Guangul and external examiner: Dr. Charles Maule for their valuable suggestions

I wish to thank Mr. Tom Brown for his help and maintenance of the computer coding, which was essential to this study. I also want to thank Mr. Michael Solohub for his assistance in the field work, which was important part of this study. Also, thanks are owed to Ms. Joni Onclin and Dr. Julie Friddell for their administrative support to my research, which made my life easier.

I would also like to pass on my appreciation to my graduate colleagues and friends, especially to:

- Chad Ellis, James MacDonald, for their assistance in my field work,
- Robert Armstrong, for sharing data of study area,
- Pablo Dornes, Warren Helgason, Kimberely Janzen, and Gro Libaek for sharing joys and pains from hydrology,
- Laura Comeau, Chad Ellis, Dusty Guedo, Mathieu Lebel, Rui Li, Shinji Shimoura, Daniel Delury, Kinechi Yamaguchi and other friends from the Department of Sociology for the extracurricular activity.

The financial support provided by the following sources was greatly appreciated: the Canada Research Chairs Programme, the Drought Research Initiative (DRI) network funded by the Canadian Foundation for Climate and Atmosphere Sciences (CFCAS), and the Department of Geography at the University of Saskatchewan. Thanks are also owed to the Environment Canada and the Department of Soil Science at the University of Saskatchewan for sharing data. In addition, I wish to thank Dr. Richard Essery for providing blowing snow modelling code.

Social events such as the hydro-beer 30 and coffee 30 were much appreciated; they were essentially important to this study and generated many ideas to this study.

I want to pass on my appreciation to my Canadian boarding family for their support. Conducting a study on the Canadian cold regions has been a challenge but also a wonderful experience and I would not have done it without having support from my parents and friends overseas. Indeed, a very special thanks goes to them.

TABLE OF CONTENTS

List of Tables

List of Figures

Figure Con't **Page Con't**

Figure Con't **Page Con't**

List of Symbols

Acronyms:

a.s.l.	above sea-level
CRHM	Cold Regions Hydrological Modelling platform
DBSM	Distributed Blowing Snow Model
DEM	Digital Elevation Model
DRI	Drought Research Initiative
EBSM	Energy-Budget Snowmelt Model
ENSO	El Niño/Southern Oscillation
GGSH	Grass Gentle Slope Hilltop
GGSV	Grass Gentle Slope Valley
GL	Grass Level
GNGS	Grass North Gentle Slope
GNSS	Grass North Steep Slope
GSGS	Grass South Gentle Slope
GSSH	Grass Steep Slope Hilltop
GSSS	Grass South Steep Slope
GSSV	Grass Steep Slope Valley
HAWTS	Heat And Water Transport in frozen Soils
HRU	Hydrological Response Unit
IHD	International Hydrological Decade
LiDAR	Light Detection and Ranging
m	metres

MB	Model Bias
MS	Mason and Sykes
NS	Nash-Sutcliffe coefficient
NWA	National Wildlife Area
PBSM	Prairie Blowing Snow Model
PDSI	Palmer Drought Severity Index
PHDI	Palmer Hydrological Drought Index
RMSD	Root Mean Square Difference
SBSM	Simplified Blowing Snow Model
SDNWA	St. Denis National Wildlife Area
SGSH	Stubble Gentle Slope Hilltop
SGSV	Stubble Gentle Slope Valley
SL	Stubble Level
SLURP	Simple Lumped Reservoir Parametric
SNGS	Stubble North Gentle Slope
SNSS	Stubble North Steep Slope
SPI	Standardized Precipitation Index
SSGS	Stubble South Gentle Slope
SSSH	Stubble Steep Slope Hilltop
SSSS	Stubble South Steep Slope
SSSV	Stubble Steep Slope Valley
SWE	Snow Water Equivalent
SWSI	Surface Water Supply Index

W	Wetland

Roman Letters:

B	fraction of ice in a unit of wet snow (0.95 → 0.97)
C	heat capacity (J kg^{-1} K^{-1})
C_{salt}	empirical constant for saltation transport (0.68 m s^{-1})
C_P	specific heat (kJ kg^{-1} °C^{-1})
d	depth of snow (m)
D	diffusivity of water vapour (m^2 s^{-1})
D_e	bulk transfer coefficient for latent heat transfer (kJ m^{-3} °C^{-1})
D_h	bulk transfer coefficient for sensible heat transfer (kJ m^{-3} °C^{-1})
e_s	vapour pressures of the snow surface (mb)
F	fetch distance of blowing snow (m)
g	gravitational acceleration (m s^{-2})
$Evap$	actual evaporation (mm)
h^*	lower boundary of suspension (m)
h_f	latent heat of fusion of ice (333.5 kJ kg^{-1})
h_{il}	enthalpy change from ice to liquid (J kg^{-1})
I	snow age index
INF	total snowmelt infiltration into unsaturated frozen soil (mm)
k	von Kármán's constant (0.4) thermal conductivity (W m^{-1} °C^{-1})
L_s	latent heat of sublimation (2.838×10^6 J kg^{-1})
M	molecular weight of water (18.01 kg mol^{-1})

Nu	Nusselt number
p_a	vapour pressures of air (mb)
P	precipitation rate (kg m^{-2} s^{-1})
P_r	depth of rain (mm day^{-1})
Q_A	blowing snow accumulation flux (kg m^{-2} s^{-1}) small-scale advection from patches of soils in horizontal direction (W m^{-2})
Q_{dfo}	diffuse radiation under clear sky (W m^{-2})
Q_{dfs}	diffuse radiation with cloud cover (W m^{-2})
Q_{dro}	direct beam short-wave radiation under clear sky (W m^{-2})
Q_{drs}	direct beam short-wave radiation with cloud cover (W m^{-2})
Q_e	convective flux of latent heat (W m^{-2})
Q_E	blowing snow sublimation flux (kg m^{-2} s^{-1})
Q_g	conductive flux of ground flux (W m^{-2})
Q_h	convective flux of sensible heat (W m^{-2})
Q_{ln}	net long-wave radiation flux (W m^{-2})
Q_{lno}	clear sky net long-wave radiation (W m^{-2})
$Q_{l\downarrow}$	downward long-wave radiation emitted by the atmosphere (W m^{-2})
$Q_{l\uparrow}$	upward long-wave radiation emitted by the surface (W m^{-2})
Q_m	energy flux available for snowmelt (W m^{-2})
Q_n	net radiation flux (W m^{-2})
Q_p	advection from rain in vertical direction (W m^{-2})
Q_r	radiative energy absorbed by the particle (J s^{-1} m^{-2}) short-wave flux reflected by the surface (W m^{-2})

Q_R	blowing snow transport flux (kg m^{-2} s^{-1})
Q_s	incident short-wave flux received by the surface (W m^{-2})
Q_{salt}	saltation transport rate (kg m^{-1} s^{-1})
Q_{sn}	net short-wave radiation flux (W m^{-2})
Q_{so}	clear sky short-wave radiation (W m^{-2})
Q_{susp}	suspension transport rate (kg m^{-1} s^{-1})
r	radius of a snow particle possessing mass, m (μm)
R	snowmelt runoff (mm) universal gas constant (8313 J mol^{-1} K^{-1})
Sh	Sherwood number
S_I	soil saturation of the top 400 mm soil layer (mm^3 mm^{-3})
S_0	surface saturation (mm^3 mm^{-3})
T	ambient atmospheric temperature (K)
T_a	air temperature (°C)
T_g	ground temperature (°C)
T_I	initial temperature of top 400 mm soil layer (K)
T_m	mean snow temperature (°C)
t_0	infiltration opportunity time (h)
T_r	temperature of the rain (°C)
T_s	temperature of the snow surface (°C)
u^*	atmospheric friction velocity (m s^{-1})
u_{mean}	mean wind speed (m s^{-1})
u_n^*	friction velocity applied to non-erodible surface element (m s^{-1})

u_t^*	threshold friction velocity (m s^{-1})
u_z	wind speed at height of z (m s^{-1})
U	internal energy of snow (W m^{-2})
X_s	horizontal distance between upwind and downwind edges of snowcovers (m)
z_b	upper boundary of suspension (m)
z_0	aerodynamic roughness height (m)

Greek Letters:

α_s	albedo of snow
δ	standard deviation of wind speed u
$\eta(z)$	mass concentration of suspended snow (kg m^{-3}) at height z
λ	pore size distribution index
λ_T	thermal conductivity of the atmosphere (J s^{-1} m^{-1} K^{-1})
ρ	atmospheric density (kg m^{-3}) density (kg m^{-3})
ρ_w	density of water (1000 kg m^{-3})
ρ_s	saturation density of water vapour (kg m^{-3})
σ	ambient atmospheric undersaturation of water vapour with respect to ice
Φ	porosity of soil
ψ_0	air entry potential (m)

Chapter 1

1.0 Introduction and Objectives

1.1 Introduction

The Prairies of Canada lie in the southern part of provinces of Alberta, Saskatchewan, and Manitoba and are characterized with relatively low precipitation especially in the west part due to the barrier effect imposed by the Rockies. Snow is an important water resource on the Canadian Prairies. Annual precipitation in the prairie region of Saskatchewan ranges from 300-400 mm (Pomeroy *et al*., 2007a); approximately one third of that occurs as snow, which produces 80% or more of annual local surface runoff (Gray and Landine, 1988). The Prairies are a cold region of Canada that has a long snow-covered, frozen season. Great variation in the hydrology exists across the Prairies, with relatively well-drained, semi-arid basins in the southwestern part and with many wetlands and lakes in the sub-humid east-central part (Pomeroy *et al*., 2007a). Some of unique hydrological features of the Prairies are:

- long winters (usually 4-5 months) with mid-winter melt (frequent in the southwest and infrequent in the northeast) (Pomeroy *et al*., 2007a),

- wind redistribution and sublimation of snow and heterogeneous distribution of snow accumulation due to local topography and land covers (Pomeroy *et al*., 1993),
- high surface runoff from snowmelt as a result of frozen mineral soils (Gray *et al*., 1985),
- melt water from shallow snowcovers forming a major source of water supply and also resulting in local flooding (Norum *et al.*, 1976), which is controlled by both snow accumulation and snowmelt infiltration (Gray *et al.*, 1985),
- numerous small depressions such as wetlands, potholes and dugouts that are internally drained, resulting in closed drainage basins (Hayashi *et al*., 2003), which are non-contributing areas to prairie streamflow (Godwin and Martin, 1975).

Studies on the modelling of the hydrological processes on the Canadian Prairies have been conducted for decades. Wind redistribution of snow has been investigated extensively; the Prairie Blowing Snow Model (PBSM) was developed by Pomeroy (1988) and many studies were conducted to advance the knowledge of snow accumulation in the windy prairie environment (Pomeroy *et al*., 1993; Pomeroy and Gray, 1995; Li and Pomeroy, 1997a, 1997b). The recent development of PBSM showed reasonable estimations of areal snow accumulation on the Prairies (Pomeroy and Li, 2000). The Energy-Budget Snowmelt Model (EBSM) was developed by Gray and Landine (1988) and was used to estimate snowmelt on the

Canadian Prairies. Through intense field studies of snowmelt infiltration into the unsaturated frozen prairies soils, Gray *et al.* (1985) derived an equation for estimating snowmelt infiltration of limited infiltrability soils on the Prairies; a parametric equation for snowmelt infiltration was developed by Zhao and Gray (1999) and was used for areal estimation of infiltration over the prairie regions (Gray *et al*., 2001). These models were assembled in the Cold Regions Hydrological Model Platform (CRHM) with the Granger-Gray evaporation expression for actual evaporation from unsaturated surfaces (Granger and Pomeroy, 1997), a soil moisture balance model (Leavesley *et al.*, 1983), Clark's lag and route runoff timing estimation procedure (Clark, 1945) along with models for radiation estimation and albedo changes (Garnier and Ohmura, 1970; Gray and Landine, 1987; Granger and Gray, 1990). CRHM runs on basins which are broken down into Hydrological Response Units (HRUs) spatial units. HRUs are the smallest land units having definable hydrological characteristics such as land cover, slope, aspect, and elevation and need not directly drain to any stream or wetland – hence they can be used to determine contributing area for medium sized basins. Preliminary tests have been conducted to evaluate the performance of CRHM in calculating the water balances for cold regions, showing reasonable results for estimates of snow accumulation, snowmelt, spring snowmelt runoff, and streamflow when compared to recorded data (Dornes *et al*., 2006; Pomeroy *et al*., 2007b).

Runoff generation in the Prairies is affected by the climate variation over the region. Much of the Prairies lies in the Palliser Triangle, where

droughts develop frequently. Over half the years of three decades, 1910-1920, 1930-1939, and 1980-1989 were in drought (Nkemdirim and Weber, 1999) and the drought of 1999-2004 was the most recent (Bonsal and Wheaton, 2005). Many Prairie winter hydrological processes: blowing snow transport, blowing snow sublimation, snowmelt, snowmelt infiltration, and snowmelt runoff are sensitive to meteorological and hydrological changes during the drought. Springtime stream discharge drops under warmer and drier conditions during the drought. Thus, water supply to the prairie streams and wetlands which are natural habitats for wildlife is under tremendous stress during the drought.

1.2 Objectives

Due to the importance of snow and snowmelt water for the water resources of the Canadian Prairies, it is necessary to improve and verify the estimating method for snow accumulation and snowmelt. The Canadian Prairies have many internally drained basins, thus deriving a physically-based runoff model that is relevant to this type of basin is essential. Also, improving the understanding of drought impacts on prairie hydrology is important to providing better management of water resources to cope with future drought. In light of these issues, the objectives of this thesis are to:

1. Compare the spatially modelling scale for snow accumulation and snowmelt and recommend an appropriate scale for a Prairie first order basin.

2. Derive and test a Prairie snow hydrology model.
3. Analyze the impact of drought on hydrological processes that control snowmelt runoff generation in respect to Prairie drainage basins.

Chapter 2

2.0 Literature Review

2.1 Snow Accumulation

Snow is an important water resource on the Canadian Prairies. Approximately one third of annual precipitation occurs as snowfall, which produces 80% or more of annual local surface runoff (Gray and Landine, 1988; Pomeroy and Goodison, 1997). There are three scales describing the spatial variability of snow accumulation – micro (10 to 100 m), meso (100 m to 10 km), and macro (10 to 1,000 km) (Pomeroy and Gray, 1995). Snow accumulation is highly heterogeneous at micro and meso scales on the Canadian Prairies, due to wind redistribution of snow which is known as blowing snow. Redistribution is primarily from open, well exposed sites to sheltered or vegetated sites. There are three modes of movement involved in the transport of blowing snow – creep, saltation, and suspension (Pomeroy and Gray, 1995). Even though small scale heterogeneity in snow accumulation is caused by snow transport; sublimation of blowing snow contributes substantially to over-winter ablation. Seasonal sublimation of blowing snow is equivalent to 15%-40% of the seasonal snowfall on the Canadian Prairies (Pomeroy and Gray, 1995). Blowing snow can transport and sublimate as

much as 75% of annual snowfall from open, exposed fallow fields in southern Saskatchewan (Pomeroy and Gray, 1995).

On the Canadian Prairies topography and land cover strongly influence blowing snow, because both induce variations in wind speed. In absence of vegetation cover, a leeward slope has much higher snow accumulation than does a windward slope (Steppuhn, 1981; Pomeroy and Gray, 1995). Studies among others by Lapen and Martz (1996) also showed similar findings, suggesting that the spatial distribution of snow depth in a Prairie agricultural landscape was strongly affected by the orientation of slopes with respect to directions of wind transport, and their relative position to other topographic features. Different land covers impose variations in surface roughness, which in turn causes wind speed and snow accumulation to change. Pomeroy *et al.* (1990) found in southern Saskatchewan wheat stubble fields had substantially less loss to blowing snow compared to fallow fields. Vegetation height in these agricultural fields plays important roles. As the stubble height increased from 1 to 40 cm on agricultural fields nearby Regina, the loss by blowing snow decreased by about 22% of the mean seasonal snowfall (Pomeroy *et al.*, 1990). At Bad Lake, Saskatchewan, snow accumulation in the depressions with tall shrubs increased by approximately 50% to 100% of seasonal snowfall attributed to transport of blowing snow (Pomeroy *et al.*, 1998).

The Prairie Blowing Snow Model (PBSM) was developed by Pomeroy (1988), assembling physically based algorithms to estimate seasonal snow accumulation on Canadian Prairies. The algorithms estimate snow

accumulation flux, Q_A, by calculating saltation, suspension and sublimation rates of blowing snow described by Pomeroy *et al.* (1998; 1999) as:

$$Q_A(F) = P - \frac{Q_R(F) - Q_R(0)}{F} - Q_E \qquad [2.1]$$

where P is precipitation rate (kg m^{-2} s^{-1}), F is fetch distance of blowing snow (m) which is the distance with non-disruptive wind distribution, Q_R is downwind blowing snow transport (saltation and suspension) flux (kg m^{-2} s^{-1}), creep is not counted because it comprises a very small portion of total transport, and Q_E is sublimation flux (kg m^{-2} s^{-1}). A control volume concept shown in Figure 2.1 is applied to estimate the mass fluxes of blowing snow over a component of the landscape (Pomeroy and Li, 2000).

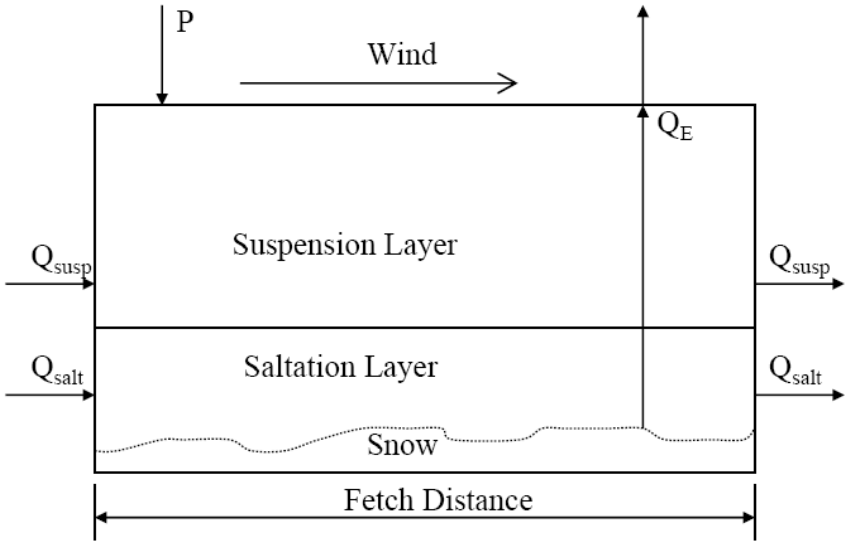

Figure 2.1 Cross-sectional view of control volume for blowing snow mass fluxes.

Individual fluxes of blowing snow are described by Pomeroy *et al*.

(1993) in the Prairie Blowing Snow Model (PBSM), which calculates the fluxes of transport by the following equation:

$$Q_R = Q_{salt} + Q_{susp} \quad [2.2]$$

where Q_{salt} and Q_{susp} are the fluxes of saltation and suspension, respectively.

The flux of saltation is estimated by the following equation:

$$Q_{salt} = \frac{C_{salt}\rho u_t^*}{u^* g}\left(u^{*2} - u_n^{*2} - u_t^{*2}\right) \quad [2.3]$$

where: Q_{salt} = saltation transport rate (kg m^{-1} s^{-1}),
C_{salt} = empirical constant (0.68 m s^{-1}),
ρ = atmospheric density (kg m^{-3}),
g = gravitational acceleration (m s^{-2}),
u^* = atmospheric friction velocity (m s^{-1}),
u_n^* = friction velocity applied to non-erodible surface elements (m s^{-1}), and
u_t^* = threshold friction velocity (m s^{-1}).

Equation [2.3] was formulated by Pomeroy and Gray (1990); it applied Bagnold's framework (1954) for calculating the transport rate of saltating sand to saltating snow and included the total atmospheric shear stress, τ, shear stress applied to non-erodible surface elements, τ_n, and shear stress applied to erodible surface elements, τ_t, to estimate the mean weight of saltating snow. The various types of shear stress are related to the corresponding friction velocity – u^*, u_n^*, and u_t^*. The atmospheric friction velocity is calculated as a function of the wind speed profile:

$$u^* = \frac{u_z k}{\ln[\frac{z}{z_0}]} \quad [2.4]$$

where: u_z = wind speed at height of z (m s^{-1}),

k = von Kármán's constant (0.4),
z_0 = aerodynamic roughness height (m).

The non-erodible friction velocity, u_n^*, was found to be equal to zero for complete snowcovers without exposed vegetation; the threshold friction velocity, u_t^*, is the friction velocity at which transport ceases and was found in the range of 0.07-0.25 m s^{-1} for fresh, loose snow and a higher range of 0.25-1.0 m s^{-1} for old, dense snow (Pomeroy and Gray, 1990). Li and Pomeroy (1997a) derived a relation between u_t^* and air temperature (°C), T at the two metre height:

$$u^*_t = 0.35 + \frac{T}{150} + \frac{T^2}{8200} \qquad [2.5]$$

The equation [2.5] provides a direct method to calculate threshold condition for blowing transport from meteorological data.

The flux of suspension is estimated by the following equation:

$$Q_{susp} = \frac{u^*}{k} \int_{h^*}^{z_b} \eta(z) \ln(\frac{z}{z_0}) dz \qquad [2.6]$$

where: Q_{susp} = suspension transport rate (kg m^{-1} s^{-1}),
u^* = atmospheric friction velocity (m s^{-1}),
k = von Kármán's constant (0.4),
z_b = upper boundary of suspension (m),
h^* = lower boundary of suspension (m),
$\eta(z)$ = mass concentration of suspended snow (kg m^{-3}) at height z, and
z_0 = aerodynamic roughness height (m).

Pomeroy and Gray (1990) found an expression for the aerodynamic roughness height over complete snowcovers as a function of atmospheric friction velocity, u^*:

$$z_0 = 0.1203\frac{u^{*2}}{2g} \qquad [2.7]$$

The lower boundary of suspension, h^*, which defines the saltation-suspension interface, was found to relate to atmospheric friction velocity, u^*:

$$h^* = 0.08436u^{*1.27} \qquad [2.8]$$

Pomeroy and Male (1992) developed an analytical expression relating the mass concentration of suspended snow to height, z, and atmospheric friction velocity, u^*:

$$\eta(z) = 0.8\exp[-1.55(4.784u^{*-0.544} - z^{-0.544})] \qquad [2.9]$$

PBSM models sublimation rate based on the energy equilibrium of radiation, convection of snow particles, water vaporation from snow particles, and sublimation (Pomeroy, 1988). The sublimation rate is approximated by the following equation:

$$\frac{dm}{dt} = \frac{2\pi r\sigma - \frac{Q_r}{\lambda_T TNu}\left(\frac{L_s M}{RT} - 1\right)}{\frac{L_s}{\lambda_T TNu}\left(\frac{L_s M}{RT} - 1\right) + \frac{1}{D\rho_s Sh}} \qquad [2.10]$$

where:
- r = radius of a snow particle possessing mass, *m* (μm),
- σ = ambient atmospheric undersaturation of water vapour with respect to ice (dimensionless),
- Q_r = radiative energy absorbed by the particle (J s^{-1} m^{-2}),
- L_s = latent heat of sublimation (2.838 × 10^6 J kg^{-1}),
- M = molecular weight of water (18.01 kg mol^{-1}),
- λ_T = thermal conductivity of the atmosphere (λ_T = 0.00063T + 0.0673) (J s^{-1} m^{-1} K^{-1}),
- Nu = Nusselt number (dimensionless),
- R = universal gas constant (8313 J mol^{-1} K^{-1}),
- T = ambient atmospheric temperature (K),
- ρ_s = saturation density of water vapour at T (kg m^{-3}),

D = diffusivity of water vapour ($m^2\ s^{-1}$), and
Sh = Sherwood number (dimensionless).

Estimation of the blowing snow fluxes based on Equations [2.3], [2.6], and [2.10] with an assumption of horizontal steady flow, does not generate adequate and accurate information of snow accumulation over landscapes having different fetch and land use. Upscaling of blowing snow transport and sublimation estimations is related to the variability of blowing snow transport and sublimation over open snow areas, increase in transport and sublimation with fetch and the influence of exposed vegetation on available shear stress to drive transport (Pomeroy and Li, 2000). Pomeroy *et al*. (1997) developed a simple scheme to address the calculation of areal snow mass balance based on monthly climatologic expressions of blowing snow transport and sublimation, which are not directly applicable for other atmospheric and hydrological models due to their empirical nature and monthly time step but provide the basis to distribute blowing snow over landscape (Pomeroy and Li, 2000).

Li and Pomeroy (1997b) found that the probability of blowing snow occurrence followed a cumulative normal distribution with regard to the mean wind speed, u_{mean}, and the standard deviation δ of wind speed, u, as:

$$p = \frac{1}{\delta\sqrt{2\pi}} \int_0^u \exp^{-\frac{(u_{mean}-u)^2}{2\delta^2}} du \qquad [2.11]$$

Based on an extensive study on the Canadian Prairies, they found the mean wind speed and the standard deviation of wind speed were functions of snow conditions and air temperature. For wet snow, the values of 21 and 7 m s^{-1}

were found for the mean and standard deviation of wind speed, respectively. For dry snowpacks, the mean and variance of wind speed were associated to air temperature (°C), T, and snow age index, I, as follows:

$$u_{mean} = 0.365T + 0.00706T^2 + 0.9I + 11.2 \quad [2.12]$$

$$\delta = 0.145T + 0.00196T^2 + 4.3 \quad [2.13]$$

Equation [2.11] allows the application of blowing snow fluxes calculation from the meteorological data and provides a technique for approximating areal blowing snow fluxes from a point. The estimation of snow mass balance using this technique was conducted in the Canadian Arctic and Prairies (Pomeroy and Li, 2000).

Other methods have been developed and applied to simulate seasonal snow accumulation. The Simplified Blowing Snow Model (SBSM), an efficient parametric routine for estimating snow mass owing to surface roughness change based on the physically-based PBSM, reproduces PBSM results closely with less computational cost (Essery *et al*., 1999). The windflow model can be used to estimate the wind speed variation due to local topography, which is important in simulating areal snow accumulation. The model of Mason and Sykes (1979), referred as MS, is a computational routine for estimating windflow over three-dimensional topography, which is extended from a two-dimensional theory of Jackson and Hunt (1975) for turbulent flow over a shallow hill. The MS windflow model is based on Fourier transform techniques and has a division of the inner and outer flow

regions. The MS model is linearized and thus only applies to low hills; it assumes neutral thermal stratification and uniform surface roughness within the simulation region. The MS model calculates normalized westerly and southerly wind components along with normalized wind speed due to changing topography. The normalized wind speed is inputted in the snow mass simulation model to adjust the wind speed. The MS model is potentially computational costly and Walmsley *et al*. (1989) derived a simple parametric version of the MS model for estimating wind speed variation induced by small-scale topographic features; this version simplified the calculation procedures and data requirement and is only applied to calculations at a coarse scale. At coarse scales, it has very similar results compared to those from the MS model (Walmsley *et al*., 1989). The Distributed Blowing Snow Model (DBSM) is a physically-based model that simulates the development of snowcovers affected by wind over landscapes having variations in topography and vegetation cover. DBSM was developed by combining SBSM with Walmsley's windflow model and showed reasonable capability to simulate seasonal snow accumulation in Canadian arctic open environments (Essery *et al.*, 1999). A detailed description of DBSM is given by Essery *et al.* (1999), Essery and Pomeroy (2004). Essery (2006) developed the latest portable version of DBSM, which includes the MS windflow model as a windflow simulating component and SBSM as a snow mass simulating component. This version of DBSM computes wind speed and snow accumulation on the same

grid cells; it has not yet been evaluated in Canadian prairie open environment or Canadian arctic open environment.

2.2 Snowmelt

Snowmelt is one of the most important hydrological events on Canadian Prairies. Meltwater from snow recharges soil moisture and groundwater storage through infiltration, and replenishes reservoirs, lakes, and rivers through surface runoff (Norum *et al.*, 1976). The amount of water from snowmelt is controlled by the net energy flux at the snow surface, and meltwater is produced when snow pack is at a temperature of 0°C (Male and Gray, 1981) or even when temperature of snow pack is below 0°C (Marsh and Woo, 1984). Snowmelt involves phase changes and hence the energy equation is the physical framework for snowmelt estimation (Granger *et al.*, 1977; Granger and Male, 1978; Gray and Landine, 1988). The energy equation is based upon the law of conservation of energy for a control volume of snow, and this volume has a snow-ground interface and a snow-air interface as its lower and upper boundaries, respectively (Figure 2.2). The energy budget for calculating snowmelt involves energy and mass fluxes via radiation, convection, conduction, and advection along with a change in internal energy (Gray and Landine, 1988). The equation for the energy budget is expressed as:

$$Q_m = Q_n + Q_h + Q_e + Q_g + Q_p + Q_A - \Delta U/\Delta t \qquad [2.14]$$

where: Q_m = energy flux available for snowmelt (W m^{-2}),
Q_n = net radiation flux (W m^{-2}),
Q_h = convective flux of sensible heat (W m^{-2}),

Q_e = convective flux of latent heat (W m^{-2}),
Q_g = conductive flux of ground flux (W m^{-2}),
Q_p = advection from rain in vertical direction (W m^{-2}),
Q_A = small-scale advection from patches of soils in horizontal direction (W m^{-2}),
$\Delta U/\Delta t$ = rate of change in internal energy (W m^{-2}).

In applying Equation [2.14], the fluxes of energy directed towards the snow pack are taken as positive. Individual terms in the energy budget equation can be determined by existing equations.

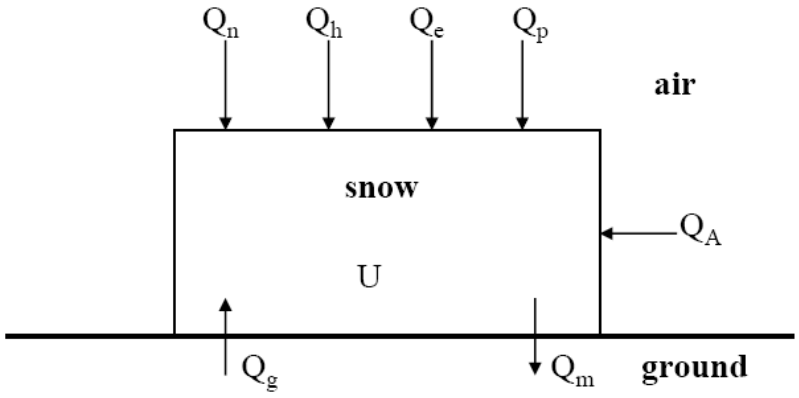

Figure 2.2 Cross-sectional view of control volume for snowmelt energy.

Net radiation, Q_n, is the total of the net short-wave, Q_{sn}, and net long-wave, Q_{ln}, expressed as:

$$Q_n = Q_{sn} + Q_{ln} \qquad [2.15]$$

where the net long-wave is normally negative and the energy fluxes directed towards the snow pack are considered as positive. The net short-wave is the incident short-wave flux received by the surface, Q_s, less the short-wave flux reflected by the surface, Q_r; the reflected short-wave energy is a fraction of

the incident short-wave, which is expressed as the albedo of snow, α_s, normally in the range of 0.65-0.95 depending on the age of snow. Thus, the net-short wave is expressed as:

$$Q_{sn} = Q_s(1 - \alpha_s) \quad [2.16]$$

The incident short-wave flux, Q_s, is the sum of direct beam, Q_{drs}, and diffuse, Q_{dfs} components, expressed as:

$$Q_s = Q_{drs} + Q_{dfs} \quad [2.17]$$

With cloud cover, the amount of direct beam short-wave flux is reduced and can be found to be a function of the direct beam short-wave radiation under clear sky, Q_{dro}, as:

$$Q_{drs} = Q_{dro}[a + b(\frac{n}{N})^c] \quad [2.18]$$

where n/N is the sunshine ratio; a, b, and c are coefficients and were found to equal 0.024, 0.974, and 1.35, respectively, for the southwestern prairie region of Saskatchewan (Granger and Gray, 1990). The direct beam short-wave radiation under clear sky, Q_{dro}, can be estimated by the expression developed by Garnier and Ohmura (1970). Atmospheric constituents such as dust particles, water droplets, and ice crystals, reduce the transmissivity for beam radiation and increase scattering and diffusion. Granger and Gray (1990) derived a relation for estimating the diffuse flux with cloud cover, Q_{dfs}, as a function of diffuse radiation under clear sky, Q_{dfo}, and the sunshine ratio, n/N, as:

$$Q_{dfs} = Q_{dfo}[2.68 + 2.2(\frac{n}{N}) - 3.85(\frac{n}{N})^2] \quad [2.19]$$

The clear-sky diffuse radiation, Q_{dfo}, can be the expression derived by Granger and Gray (1990) that relates Q_{dfo} to the atmospheric pressure ratio, cosine of the angle of incidence of the sun's rays on a slope, and day of year. The net long-wave flux, Q_{ln}, is the sum of the downward radiation emitted by the atmosphere, $Q_{l\downarrow}$, and the upward radiation emitted by the surface, $Q_{l\uparrow}$. Due to the influence of diurnal changing temperature on the internal energy content of shallow snowcovers, it is important to incorporate long-wave fluxes into the snowmelt estimation. Granger and Gray (1990) developed an expression for calculating the net long-wave flux under cloud cover, Q_{ln}, for the southwestern prairie region of Saskatchewan as:

$$Q_{\ln} = Q_{\ln o}[0.25 + 0.75(\frac{n}{N})] \quad [2.20]$$

where n/N is the sunshine ratio; Q_{lno} is the clear sky net long-wave radiation, estimated by the following expression relating to the clear sky short-wave radiation, Q_{so}:

$$Q_{\ln o} = -4.25 - 0.24Q_{so} \quad [2.21]$$

In addition to the net radiation flux, convective fluxes are also important in snowmelt calculations. Male and Gray (1981) outlined simplified bulk transfer expressions for calculating convective sensible heat flux Q_h and latent heat flux Q_e:

$$Q_h = D_h U_z (T_a - T_s) \quad [2.22]$$

$$Q_e = D_e U_z (e_s - p_a) \quad [2.23]$$

where:
- D_h = bulk transfer coefficient for sensible heat transfer (kJ m^{-3} °C^{-1}),
- D_e = bulk transfer coefficient for latent heat transfer (kJ m^{-3} °C^{-1}),
- U_z = wind speed at a reference height (m s^{-1}),
- T_a, T_s = temperature of the air and the snow surface, respectively (°C),
- p_a, e_s = vapour pressures of the air and snow surface, respectively (mb).

Ground heat flux Q_g and internal energy U are estimated by the following equations (Male and Gray, 1981):

$$Q_g = -k(\partial T_g / \partial z) \quad [2.24]$$

where:
- k = thermal conductivity (W m^{-1} °C^{-1}),
- T_g = ground temperature (°C),
- Z = depth (m).

$$U = d(\rho_i C_{Pi} + \rho_l C_{Pl} + \rho_v C_{Pv}) T_m \quad [2.25]$$

where:
- d = depth of snow (m),
- ρ = density (kg m^{-3}),
- C_P = specific heat (kJ kg^{-1} °C^{-1}),
- T_m = mean snow temperature (°C), and
- i, l, v = ice, liquid and vapor phases, respectively.

When rain falls on a melting snow pack where the rain does not freeze, the advection flux from rain is estimated by the following equation (Male and Gray, 1981):

$$Q_p = 4.2(T_r - T_s) P_r \quad [2.26]$$

where:
- T_r = temperature of the rain (°C),
- T_s = snow temperature (°C), and
- P_r = depth of rain (mm day^{-1}).

When patches of bare soils and snowcovers appear, the amount of energy transferred from the patchy bare soils to patchy snowcovers is important for

melting snow. This horizontal advection flux Q_A is estimated as the change of sensible heat from upwind edge of snowcovers to downwind edge of snowcovers over the length of snowcovers (Granger *et al.*, 2002). That is:

$$Q_A = aX_s^b \qquad [2.27]$$

where: X_s = horizontal distance between upwind and downwind edges of snowcovers (m),
a, b = Weisman's dimensionless coefficients.

The amount of melt can be calculated from Q_m by the equation:

$$M = \frac{Q_m}{\rho_w B h_f} \qquad [2.28]$$

where: ρ_w = density of water (1000 kg m^{-3}),
B = fraction of ice in a unit of wet snow (0.95 → 0.97),
h_f = latent heat of fusion of ice (333.5 kJ kg^{-1}).

On Canadian Prairies snowcovers are relatively shallow compared to mountain snowcovers and some energy components dominate melting processes while other components are minor contributors. In the Prairie environment, net radiation (short- and long-wave) is the primary factor affecting snow ablation rate and convective energy (sensible and latent heat) is usually a secondary factor as the convective fluxes are of opposite sign and similar magnitude. Ground heat is small compared to others (Granger *et al.*, 1977; Male and Granger, 1981; Gray and Landine, 1988). Average daily ground heat fluxes are within range of 0-4.6 W m^{-2} (Pomeroy *et al.*, 1998).

Many studies have been taken to develop a physically based model to estimate springtime snowmelt on Canadian Prairies for decades. Gray and Landine (1987) investigated the albedo-depletion of seasonal snow covers on

the prairies and developed algorithms for determining the onset and duration of snowmelt events. This albedo-depletion routine was applied to estimate the daily net radiation associated with prairie snowmelt (Granger and Gray, 1990). Gray and Landine (1988) suggested that temperature-index snowmelt approaches (e.g. Anderson, 1973) do not usually work properly in the open environments due to the lack of correlation between radiative and convective energy exchanges in such environments. They developed the Energy-Budget Snowmelt Model (EBSM) for estimating melt from shallow prairie snow covers by examining radiative, convective, advective, and internal energy based on standard climatological measurements. Local scale advection is also an important flux for melting snow in the patchy soil and snow-covered area. Shook (1995) demonstrated reasonable ability of the Prairie Snow Ablation Simulation (PSAS) model in estimating small-scale advective heat from snow-free patches to snow-covered patches. Following that Shook and Gray (1997) applied an adjusted version of the Penman-Monteith equation to estimate the amount of energy for snowmelt from large- and small-scale advection. Granger *et al.* (2002) developed simple parametric expression for estimating the advective energy in melting snow as warming air moving from snow-free ground to snow patches. Essery *et al.* (2006) attempted a simple advection model with parameterizations for local surface fluxes on snow patches based on estimations of flux and temperature profiles in the internal boundary layers on snow-free and snow patches.

2.3 Snowmelt Infiltration into Frozen Prairie Soils

Snowmelt infiltration into frozen soils is an important hydrological event on the Canadian Prairies. It replenishes soil moisture and groundwater storage used for plant growth, agricultural water supply, and domestic consumption. It reduces the direct surface runoff and the magnitude of peak streamflow (Male and Gray, 1981). Infiltration is defined as the process by which water flows through the soils, involving three-step sequence: entry of water into the surface of the soil, transmission through the soil, and diminishing storage capacity in soil (Musgrave and Holtan, 1964). The process is governed by the combined influence of gravity and capillary forces (Gray *et al.*, 1970; Kane and Stein, 1983). Frozen soils are common in northern high latitude regions, such as Canada and Russia. Through intense field studies of snowmelt infiltration carried out on agricultural land in Saskatchewan, Gray *et al.* (1985) proposed a classification that separates the seasonally frozen prairie soils to three groups depending on their infiltrability: restricted (no infiltration), limited (some infiltration, some runoff), and unlimited (all melt water infiltrates). It is a widely used classification (e.g. Gray *et al.*, 1986, 2001; Zhao and Gray, 1997).

An unsaturated frozen soil system is by far the most complex soil system with two solid components: soil and ice, and two fluid components: water and air and yet this system is very common (Kane and Stein, 1983). Infiltration into such a system is a complicated process involving coupled heat and mass flow with phase changes (Zhao and Gray, 1997; Zhao *et al.*, 1997;

Gray *et al.*, 2001). Infiltration into unsaturated frozen soils can be described by two regimes: a transient regime and a quasi-steady-state regime. The transient regime follows immediately after the application of water; the infiltration rate decreases rapidly during this regime. The transient regime is followed by a quasi-steady-state regime in which changes in the infiltration rate with time are relatively small (Zhao and Gray, 1997; Zhao *et al.*, 1997). The amount of unfrozen water in the soil is very important to the infiltration process. Zhao and Gray (1997) proposed a freezing point depression equation that can estimate the maximum liquid water content (θ_l) for a specific subzero temperature:

$$\theta_l = \phi[\frac{h_{il}(T-273.15)/T + CRT}{g\psi_0}]^{-1/\lambda} \qquad [2.29]$$

where:
ψ_0 = air entry potential (m),
λ = pore size distribution index (dimensionless),
Φ = porosity (dimensionless),
h_{il} = enthalpy change from ice to liquid (J kg^{-1}),
T = temperature (K),
C = heat capacity (J kg^{-1} K^{-1}),
R = gas constant (J kg^{-1} K^{-1}),
g = gravitational acceleration (m s^{-2}).

Equation [2.29] was established by Cary and Maryland (1972) based on the application of the Clausius-Clapeyron equation to the liquid-water-ice system of frozen soils assuming that unsaturated soils in unfrozen and frozen phases have the same soil matric potential function (Zhao and Gray, 1997). The amount of the unfrozen water has a direct impact on the hydraulic conductivity of frozen soils. Water transmission is strongly affected by

development of ice from freezing water in soil pores (Kane, 1980). Freezing an unfrozen soil with 91.7% water saturation can result in full ice saturation in frozen soils, because 9% of expansion in volume occurs as result of conversion of liquid water to ice (Andersland *et al.*, 1996).

Factors affecting infiltration into frozen soils are those influencing both the water entry at the surface and the downward and lateral movement of wetting front within soil profile. On Canadian Prairies the most important soil factors are surface saturation (S_0), initial soil moisture saturation in the upper soil layers (S_I), initial soil temperature (T_I), and soil cracks (macropores) (Zhao *et al.*, 2002). Infiltration is positively related to S_0 because the capillary pressure gradient rises and soil is more permeable as S_0 increases and thus increases the quantity of infiltration (Zhao and Gray, 1997). Infiltration is inversely related to S_I because increasing S_I enhances ice formation within soil, suppressing the capillary pressure gradient and making soils less permeable and consequently infiltration decreases (Zhao and Gray, 1997; Gray *et al.*, 2001). Infiltration decreases with decreasing T_I because lower temperatures can cause greater freezing, causing soils to be less permeable. T_I may be considered as a secondary factor affecting infiltration compared to S_0 and S_I (Gray *et al.*, 2001). Infiltration is greatly enhanced by cracks (Pomeroy *et al.*, 1990). Soils with development of cracks are regarded as frozen soils of unlimited infiltrability, and almost all available melting water infiltrates into these soils (Gray *et al.*, 2001). Soil texture is not a factor affecting infiltration into frozen soils of limited infiltrability; this is because the influence of

variations in soil texture on the frozen soils infiltrability is counteracted by the variations of other factors during infiltration, such as the rise in ratio of ice to liquid water (Zhao *et al.*, 2002).

Modelling the infiltration into frozen soils has been investigated worldwide for decades. Motovilov (1978) examined a physically-based mathematical model to estimate water and heat transport in frozen soils. A one-dimensional mathematical model was developed by Engelmark (1984) to simulate vertical heat and moisture transfers along with phase change. Additional research on the modelling method and theory has been conducted by Engelmark and Svensson (1993), Flerchinger and Saxton (1989a, 1989b) and Flerchinger (2000). On the Canadian Prairies Granger *et al.* (1984) developed an empirical equation for estimating cumulative infiltration (INF) of limited infiltrability frozen soils based on the SWE and average pre-melt water and ice content of 0-300 mm soil layer (S_I). Gray *et al.* (1985) derived its expression as:

$$INF = 5(1 - S_I)SWE^{0.584} \qquad [2.30]$$

Zhao *et al*. (1997) developed a physically-based finite difference numerical model, HAWTS (Heat And Water Transport in frozen Soils). The model estimates moisture movement related to sensible and latent heat transfers in frozen soils based on a set of partial differential equations. Zhao and Gray (1999) developed a parametric form of the HAWTS model that describes cumulative infiltration into frozen unsaturated soils of limited infiltrability as:

$$INF = CS_0^{2.92}(1-S_I)^{1.64}\left(\frac{273.15-T_I}{273.15}\right)^{-0.45} t_0^{0.44} \qquad [2.31]$$

where C is a constant and is found to be 2.10 and 1.14 for prairie and forest soils, respectively (Gray *et al.*, 2001). S_0 is the surface saturation (mm^3 mm^{-3}) and is assumed to be approximately equal to 1 in most situations that have low infiltration rates relative to the snowmelt rate (Gray *et al.*, 2001). S_I is the average soil saturation of the top 400 mm soil layer at the start of infiltration (mm^3 mm^{-3}) and is estimated from the average pre-melt volumetric moisture content (water + ice) (θ_I) divided by the soil porosity (Φ). θ_I can be approximated from the fall soil moisture θ_f based on empirical expressions developed from observation in the Prairies (Gray *et al.*, 1985) as:

$$\theta_I = -5.08 + 1.05\theta_f \quad \text{(for fallow fields)} \qquad [2.32]$$

$$\theta_I = 0.294 + 0.957\theta_f \quad \text{(for stubble fields)} \qquad [2.33]$$

T_I is the average initial temperature of top 400 mm of soil (K). t_0 is the infiltration opportunity time (h) and approximately equals the time required to melt the snow cover and is estimated by the following equation:

$$t_0 \cong t = \frac{SWE}{Melt} \qquad [2.34]$$

The assumptions made for the parametric equation are that the soil is homogeneous and isotropic, distributions of initial soil temperature and moisture are uniform, and melt water has a constant head at the soil surface (Zhao and Gray, 1999).

2.4 Surface Snowmelt Runoff

On the Canadian Prairies spring surface runoff from melting snow is an important resource to prairie streams and ponds. The accumulation and melt of snow is of primary importance in controlling prairie runoff generation (Norum *et al.*, 1976). Snowmelt water produces more than 80% of annual runoff on the semi-arid Canadian Prairies (Granger *et al.*, 1984; Gray and Landine, 1988; Pomeroy and Goodison, 1997). Springtime streamflow discharge and pond water levels are strongly affected by the melt water released from snowpacks (Gray *et al.*, 1985; Woo and Rowsell, 1993; Hayashi *et al.*, 2003). Snowmelt runoff volume and timing is controlled by melt rate, infiltration rate and surface storage. Runoff generation in springtime is influenced by land use (van der Kamp *et al.*, 1999; 2003). In the semi-arid prairie environment, snowmelt runoff is very sensitive to the meteorological conditions and can completely cease under drought meteorology.

Snowmelt runoff simulations usually comprise a snowmelt simulation model and a runoff routing algorithm. The snowmelt model simulates the amount of melting water from snow available for runoff and the runoff routing algorithm transfers the available water from contributing areas to basin outlet (Donald *et al.*, 1995). Digital Elevation Model (DEM) grid-based simulations have been applied in predicting runoff based on distributed energy balance calculation of snowmelt from input meteorological data and terrain information (Marks *et al.*, 1998). The simulation of runoff generation at regional scales involves the integration of Land Surface Schemes and

distributed hydrological models (e.g. Soulis *et al.*, 2000).

On the Canadian Prairies, various studies on simulating snowmelt runoff have been conducted. Gray *et al.* (1985) examined the hydrographs of streamflow from snowmelt based on modelling the loss of snowmelt to infiltration to frozen soils. Hayashi and van der Kamp (2000) developed a simple expression to estimate the volume of water in a wetland based on volume-area-depth relations. Hayashi *et al.* (2003) applied this expression to calculate the volume of water in wetlands from spring snowmelt runoff. Su *et al.* (2000) applied a semi-distributed hydrological model, SLURP (Simple Lumped Reservoir Parametric), to simulate hydrological processes in wetlands and to calculate water balance components such as precipitation, snowmelt, evaporation, surface runoff and subsurface flow. Recently, a modelling platform, Cold Regions Hydrological Model platform (CRHM) has been developed by Pomeroy *et al.* (2007b) and has been applied to prairie hydrology simulation. This modelling system incorporates all hydrological processes that are essential to snowmelt hydrology and simulates the energy and water balances of snow and soil based on physically based algorithms. CRHM has been tested showing reasonable performance in simulating prairie streamflow from surface snowmelt runoff at basin scale (Pomeroy *et al*., 2007b).

2.5 Drought on the Canadian Prairies

Drought is a natural hazard and is a normal part of climate (Wilhite

and Buchanan-Smith, 2005), but it can come to be a disaster when its impact on human society and environment becomes large (Maybank *et al.*, 1995; Wilhite and Buchanan-Smith, 2005). Drought is a subtle and slowly-developing condition, and it is difficult to declare the onset and the ending of drought (Maybank *et al.*, 1995; Wilhite and Buchanan-Smith, 2005). The common features of drought are: above average air temperature, lack of precipitation, low soil moisture, and insufficient water supplies from the surface and subsurface (Nkemdirim and Weber, 1999; Wheaton *et al.*, 1992; 2005; Wilhite and Buchanan-Smith, 2005). There is lack of accurate and well-accepted definition of drought because the definition is user and region specific (Maybank *et al.*, 1995; Wilhite and Buchanan-Smith, 2005). According to different users and sectors, four types of drought can be defined (Wilhite and Glantz, 1985):

- meteorological drought: below average precipitation over an extended period of time,
- agricultural drought: decreased availability of soil water for supporting crop growth as a result of deficiency of precipitation over some period of time,
- hydrological drought: insufficient surface and subsurface water supplies over some period of time,
- socio-economic drought: interactions of human activity and society and drought and the impacts of meteorological, agricultural, and hydrological

drought on the human society.

These types of drought are widely mentioned and used (Ripley, 1988; Wilhite and Buchanan-Smith, 2005). There are other types of drought; based on the criteria of persistence and pattern, drought can be classified as permanent drought, seasonal drought, and irregular drought (Thornthwaite, 1947; Whitmore, 2000).

To quantify the magnitude, duration, and severity of drought, drought indices are used. The drought index is derived from indicators based on meteorological and hydrological variables such as precipitation, streamflow, soil moisture, reservoir level, and groundwater level (Steinmann *et al.*, 2005). Several drought indices have been developed and they have their advantages and drawbacks depending on the users and applications. One of the simplest meteorological drought indices is the percent of normal precipitation, which describes how the precipitation from a single season compares to a long term normal. However, seasonal precipitation does not have a normal distribution, thus, it is difficult to compare amongst different locations and seasons (Steinmann *et al.*, 2005). McKee *et al.* (1993) developed another meteorological drought index, the Standardized Precipitation Index (SPI), to quantify precipitation deficits for any time scale based on probability distribution of precipitation over a long-term period. The SPI is time and location invariant, but it is not straightforward for decision makers to use (Steinmann *et al.*, 2005). The most widely used meteorological drought index is the Palmer Drought Severity Index (PDSI) (Alley, 1984; Karl, 1986;

Nkemdirim and Weber, 1999; Steinmann *et al.*, 2005). It was developed by Palmer (1965) to measure the departure of moisture supplies based on a moisture balance model, while the Palmer Hydrological Drought Index (PHDI) is a hydrological drought index derived from PDSI and is used to assess the moisture anomalies affecting streamflow, groundwater, and storage over longer period than that for PDSI (Steinmann *et al.*, 2005). The values of PDSI and PHDI vary spatially and temporally; cumulative frequencies change over regions and time periods (Guttman *et al.*, 1992; Nkemdirim and Weber, 1999; Steinmann *et al.*, 2005). The Palmer indices do not include water storage, snowfall, snow cover, and frozen ground along with human impacts, and the indices do not consider the natural lag between precipitation, moisture surplus and streamflow, making them not suitable for water management systems when dealing with droughts (Alley, 1984; Guttman *et al.*, 1992; Nkemdirim and Weber, 1999; Steinmann *et al.*, 2005). These limitations are addressed by the Surface Water Supply Index (SWSI), a hydrological drought index developed by Shafer and Dezman (1982). However, there is a need to recalculate the index once the data source or water supply source is changed (Steinmann *et al.*, 2005).

Droughts are frequent on the Canadian Prairies. Over half the years of three decades, 1910-1920, 1930-1939, and 1980-1989 were in drought (Nkemdirim and Weber, 1999) with the drought of 1961 considered as the most extensive single-year prairie drought in the 20th century (Maybank *et al.*, 1995). The drought of 1999-2004 was the most recent multi-year drought and

with 1999-2002 being the most severe on record in parts of the Prairies (Bonsal and Wheaton, 2005, Rannie, 2006).

On the Canadian Prairies, severe drought occurs most often in the southern parts, coinciding with the Palliser Triangle, named after the British explorer Captain John Palliser (Nkemdirim and Weber, 1999). This region extends from the eastern slopes of the Rocky Mountains to the southwest corner of Manitoba. It is characterized by dry conditions in the winter, especially in the western part, due to atmospheric blocking imposed by the Rockies (Agriculture and Agri-Food Canada, 1998). Drought in this region is usually associated with large-scale disruptions of the atmospheric circulation pattern and displacement of air masses (Liu *et al.*, 2004; Bonsal and Wheaton, 2005; Shabbar, 2006). During the droughts of 1961 and 1988 in the Canadian Prairies, a strong association existed between warmer and drier conditions in the wintertime and the El Niño/Southern Oscillation (ENSO). This caused the jet stream over the North Pacific to split into two branches, one flowing over the Arctic and the other flowing over the Pacific, northwest United States and southwest Canada (Bonsal and Wheaton, 2005; Shabbar *et al.*, 1997; Shabbar, 2006). However, Bonsal and Wheaton (2005) showed that the northward extension of persistent drought circulation from the continental United States was the major factor influencing the recent drought of 1999-2002.

Drought on the Canadian Prairies is featured by above-normal temperature and below-normal precipitation. During the drought of 1988, there was only 70-80% of normal snowfall east of the Rockies (Lawford,

1992); the agricultural region of prairies received less than 50% of normal snowfall (Wheaton *et al.*, 1992). During 1999-2001 part of the Prairies experienced the driest condition in the 118 year record (Sauchyn *et al.*, 2003). During the drought of 1988, mean temperatures for March, April and May were 2 to 4 °C higher than normal in most of Western Canada (Wheaton *et al.*, 1992), while slightly lower temperature anomalies, 0.5 to 1 °C above normal, existed in the recent drought of 2001-02, with the highest anomalies found in the winter season (Bonsal, 2005). Very low soil moisture reserves characterize drought (Lawford, 1992; Nkemdirim and Weber, 1999); the combination of this low soil moisture condition with drier and warmer atmospheric conditions results in little runoff from snowmelt and the drying out of wetlands and streams (Nkemdirim and Weber, 1999; Rannie, 2006).

Beyond these meteorological and hydrological impacts, tremendous socio-economic stresses have been imposed by drought. A loss in agricultural production over Canada by an estimated $3.6 billion in 2001-2002 was attributed to this drought (Wheaton *et al.*, 2005). In light of this shortfall, a new Canadian based research network, Drought Research Initiative (DRI) was established to improve the understanding of the physical characteristics and processes affecting droughts on the Canadian Prairie.

Chapter 3

3.0 Study Site and Field Observations

3.1 Study Sites Description

Two sites were chosen to conduct this study: Bad Lake, in the semi-arid, well drained prairie region and St. Denis, in the sub-humid, poorly and internally drained prairie region.

Creighton Tributary of Bad Lake International Hydrological Decade (IHD) Research Basin. Bad Lake (51º23'N, 108º26'W, 650 m a.s.l.) is an internally drained basin near Totnes in south-western Saskatchewan, Canada (Figure 3.1). Creighton is a small basin (11.4 km^2), within which silty clay and clay loams are the two dominant soils (Gray *et al.*, 1985). Approximately 85% of the basin area was cultivated land (stubble and fallow fields), and the rest of basin consisted of grassland for the periods of study (Gray *et al.*, 1985). The basin is characterized with level open land with poor drainage and highland with rolling topography; it is drained by a grassland "coulee" (sharp incised valley in the upland plain) from which flows Creighton Tributary. Bad Lake is a representative site within the Palliser Triangle. The basin has a semi-arid climate with about 300 mm of annual precipitation (Gray and Granger, 1986). The 15-year (1971-1986) average air temperature and precipitation

(rainfall and snowfall) during "winter period" (November 1 to April 30) for the basin are -6.3 ºC and 106 mm, respectively (Environment Canada, 2006a). Frozen soils and blowing snow develop over the winter, and snowmelt and meltwater runoff occur in the early spring. Major snowfall usually starts in November and continues until April; several episodes of snowmelt and runoff begin in March (Pomeroy *et al.*, 1998). The snowmelt freshet is the main streamflow event of the year at Creighton Tributary, where the stream discharges in an intermittent manner with the majority of flow during and immediately after snowmelt. At Creighton Tributary Basin, the study focuses on derivation and testing of a snow hydrology model for relatively well-drained semi-arid site and also on analyzing drought impact on snow hydrology at this site.

St. Denis National Wildlife Area (SDNWA). The SDNWA (52°02'N, 106°06'W, 545-560 m a.s.l., 3.85 km^2) is located in south-central Saskatchewan, Canada (Figure 3.1), and in a moderately rolling landscape with slope ranging from 10 to 15% (van der Kamp *et al.*, 2003). The area is dominated by small depressions with poorly-developed drainage, clay soils and glacial till substrate (Hayashi *et al.*, 1998). The SDNWA has three major land uses: native grassland, brome grassland, and cultivated land. Saskatoon Airport, located about 40 km west of the SDNWA, has a 2°C annual air temperature, with -19°C as the January mean temperature and 18°C as the July mean temperature; the 30-year (1967-1996) mean annual precipitation in Saskatoon is 358 mm with 74 mm of snowfall occurring from November to

April (van der Kamp *et al.*, 2003). Snowfall generally starts in November, and several snowmelt runoff events occur in early spring between March and April in the area (van der Kamp *et al.*, 2003). At the SDNWA, this study focuses on the modelling scale derivation and comparison for snow accumulation and snowmelt.

Basin of Wetland 109 at the SDNWA. Over 100 "pothole" depressions in which wetlands develop exist at the SDNWA, and one of them is Wetland 109 (Figure 3.1). It is a small closed depression and typifies other depressions in the area. The effective area of basin is 0.02013 km^2 with 0.00412 km^2 comprising the wetland (Hayashi and van der Kamp, 2000; Hayashi *et al.*, 2003); the effective drainage area is a portion of the drainage basin which are expected to contribute runoff. Four smaller depressions exist in the vicinity of the effective area of basin and altogether form the gross drainage of Wetland 109 (Hayashi and van der Kamp, 2000; Hayashi *et al.*, 2003). In dry years, only the meltwater in the effective area of the basin contributes to water level change in Wetland 109 during early spring period; whereas overflows from other adjacent small depressions can lead to water level rise in Wetland 109 in some wet years (van der Kamp, 2006). At the basin of Wetland 109, the study focuses on derivation and testing of a snow hydrology model for a relatively poor-drained wetland on Canadian Prairies and also on examining drought impact on snow hydrology at this site.

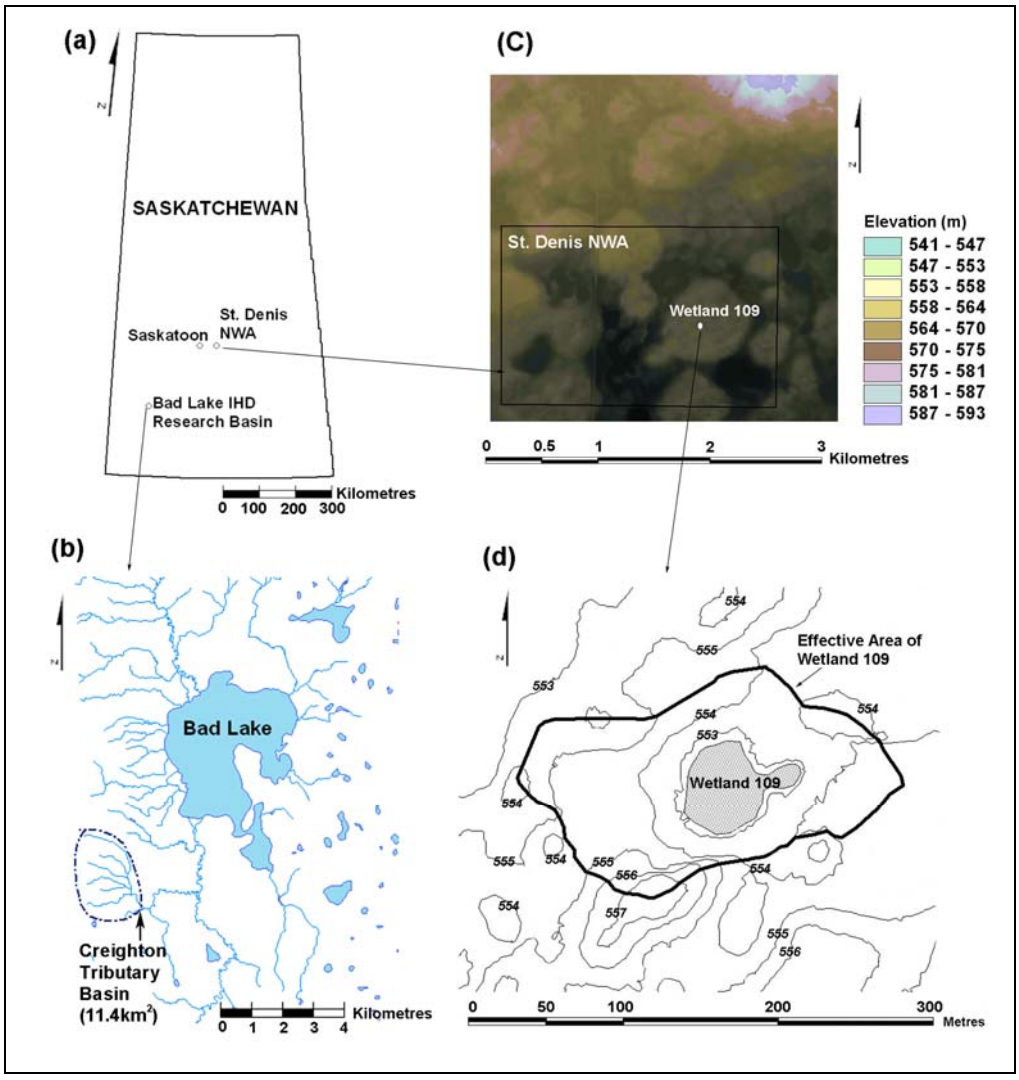

Figure 3.1 Study sites: (a) Bad Lake IHD Research Basin and St. Denis NWA, (b) Creighton Tributary of Bad Lake Research Basin, (c) LiDAR DEM of St. Denis NWA (dark solid line indicates SDNWA boundary), (d) contour map of effective area of Wetland 109 (dark solid line denotes cacthment and shaded area indicates Wetland 109).

3.2 Field Observations

At Bad Lake, field observations were carried out from the 1960s to the 1980s, including measurements from a Meteorological Service of Canada

standard meteorological station with an on-site observer, streamflow gauges and extensive snow surveys. Specialised measurements of air temperature, relative humidity, wind speed, soil temperature, precipitation, snow depth, and radiation (direct shortwave, diffuse, and net) were obtained from the meteorological station and other sites. Snow surveys were conducted in various land uses within the basin and provided measurements of snow depth and density during the winter period and melt rate during the snowmelt period. Streamflow discharge on Creighton Tributary was monitored with a stage recorder at a weir and there were frequent velocity measurements so that reliable stage-discharge relationships could be developed for the melt period.

At St. Denis, field observations were made in the 1990s and the 2000s (Figure 3.2). Measurements of air temperature, relative humidity, two-metre wind speed, and precipitation during 2005 and 2006 were collected from a precipitation gauge station. At the same time measurements of radiation (net short-wave, net long-wave, and net all) and vapour pressure were obtained from a station with eddy correlation system operated by Dr. Bing Cheng Si, Department of Soil Science, University of Saskatchewan. Measurements of air temperature, relative humidity, ten-metre wind speed, radiation, and vapour pressure from 1999 to 2006 were gathered from a ten-metre tower station operated by Environment Canada. Precipitation data from 1999 to 2005 was acquired from a nearby Meteorological Service of Canada station at Humboldt to replace precipitation collected from the ten-metre station at St. Denis.

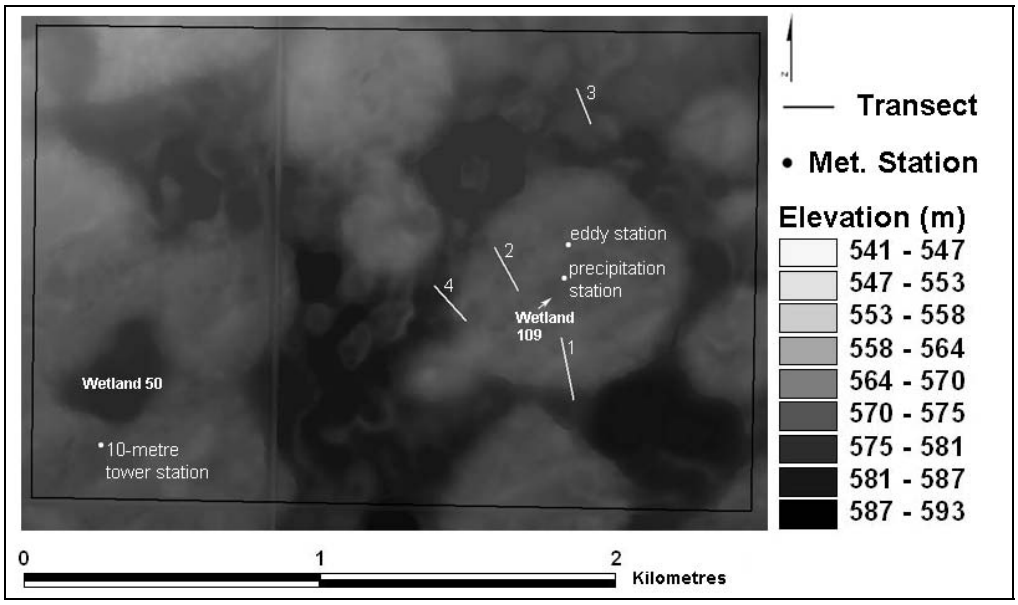

Figure 3.2 Plan of field observations at St. Denis NWA on a LiDAR DEM. Lines indicate field observation transects of soil properties, vegetation cover, and snow accumulation. Points indicate meteorological stations.

At St. Denis, field surveys of soil properties (0-40 cm volumetric soil moisture and soil porosity), vegetation cover information (stalk height, stalk density, stalk diameter, and cover type), snow accumulation information (depth and density), and pond water level were also conducted. Soil properties and vegetation cover information were surveyed along the field transects in October, 2005 (Figure 3.2); along the same transects snow survey was conducted from January-April, 2006. A brief description of these transects is shown in Table 3.1 and their photos during the field season are illustrated in Appendix A. The mean values of volumetric soil moisture, vegetation height, snow accumulation (SWE), and snow density on these transects are shown in Appendix B. In October, 1999 and November, 2000, soil properties and

Table 3.1 St. Denis field observation transect description.

Transect #	Length (m)	Sampling points	Sampling interval (m)	Description
1	220	45	5	rolling stubble field
2	170	35	5	relatively flat stubble field crossing a small wetland
3	120	25	5	relatively flat grassland area
4	160	33	5	rolling field with transition between grassland and stubble field

vegetation cover information were surveyed by Environment Canada on various land covers (cultivated land, grassland, and wetland). In October 2003 and October 2004, these surveys were carried out by Department of Soil Science, University of Saskatchewan (Pennock, 2004; Pennock *et al*., 2005). From 2000 to 2006 pre-melt snow accumulation information (usually in March) on various land covers and spring wetland water level (in April and early May) were surveyed by Environment Canada (van der Kamp *et al*., 2006a; 2006b). The methods used for the data collection at both Bad Lake and St. Denis are described in Appendix C.

At St. Denis, grids of LiDAR DEM and vegetation height that are used by the Distributed Blowing Snow Model (DBSM) were also collected. The LiDAR campaign was carried out by Applied Geomatics Research Group (AGRG) of Nova Scotia Community College and C-Clear program on August 9th, 2005. AGRG applied the Applanix proprietary 'PosPac' software environment to integrate and process GPS trajectory and inertial measurement

unit (Töyrä, 2005). Optech's proprietary 'REALM' software was used to process all data and 'flat terrain' and 'dense vegetation' options were applied to separate ground and non-ground features (Töyrä, 2005). The ground truth, conducted by Environment Canada, revealed that vegetation filtering processed by AGRG only removed the shrubs. Further filtering was conducted by Environment Canada and LiDAR explorer for ArcGIS was used to separate bard ground layer and vegetation layer based on a 3×3 kernel size and 0.2 m Z tolerance. This resulted in nine LiDAR tiles covering St. Denis NWA and surrounding area. All data in the nine LiDAR tiles was interpolated into a DEM by Dean Shaw using Inverse Distance Weighted (IDW) algorithm in ESRI ArcGIS. This results in the total number of 6201×6201 grids with grid size of 0.5 m×0.5 m for the DEM. For the modelling in DBSM, the Fast Fourier Transform routine (FFTs) in the windflow model requires any power of two numbers of grids in each direction of the DEM. Thus, a grid resample routine was conducted in ArcView GIS, resulting in 512×512 grids with a grid size of 6 m×6 m. This is the DEM grid used in the DBSM modelling.

Aerial photos and site plan along with vegetation height were used to make the vegetation height grid. A detailed vegetation survey was conducted at St. Denis NWA on October 24-26, 2005. Vegetation height was measured by ruler. Eight groups of vegetation was classified based on the height and type: fallow, short stubble, tall stubble, short grass, tall grass, shrubs, short trees, and tall trees along with non-vegetative features (roads and water bodies treated as zero height). Based on the aerial photos and site plan for St. Denis

NWA collected and compiled by Robert Armstrong and Environment Canada, vegetation height polygons were created and delineated in ArcView GIS, resulting in an ArcView GIS shape file containing vegetation height. This shape file was converted into a grid file comprising 512×512 grids with a grid size of 6 m×6 m. This is the vegetation height grid used in the DBSM modelling.

Chapter 4

4.0 Model Scale Derivation for Snow Accumulation and Snowmelt

4.1 Methods

Spatially distributed and spatially aggregated approaches were used to estimate snow accumulation (SWE) and snowmelt. Both approaches use models with similar physics, but differ in the spatial scale at which calculations were carried out. Calculations in the spatially distributed approach were conducted on small-sized Hydrological Response Units (HRU), whereas calculations in the spatially aggregated approach were based on large-sized HRU. A HRU is a spatial landscape unit assumed to have a uniform hydrological response, such that it can be described by a unique set of parameters, variables and fluxes (Pomeroy *et al*., 2007b).

4.1.1 Model Scale for Snow Accumulation

Spatially Distributed Approach. A portable version of the Distributed Blowing Snow Model (DBSM) developed by Essery (2006), which is a distributed parametric version of Prairie Blowing Snow Model (PBSM), was used in this approach. The calculation in the portable DBSM is based on gird

cells, on which the flux of snow mass is adjusted after estimation of transport and sublimation fluxes by according to Equation [2.1] (Figure 4.1).

Three inputs to this portable version of DBSM are a LiDAR DEM grid file, a grid file of vegetation height and a time-series meteorology file. The DEM grid file contains 262,144 grids of elevation with 6 m resolution over a 3100.5 × 3100.5 m area surrounding St. Denis NWA (Figure 4.2). The 6-m grids are considered as HRU based in the spatially distributed approach, and this type of HRU is the smallest possible based on location. The grid file of vegetation height stores the vegetation height on the grids with the same resolution and areal extent as DEM grids (Figure 4.2). The meteorology file contains hourly air temperature, relative humidity, wind speed, wind direction, and precipitation rate during the period of October 31, 2005 - April 30, 2006 (Figure 4.3). The final outputs are the areal distribution of SWE on the 6-m grids and are generated for the simulation period specified by users.

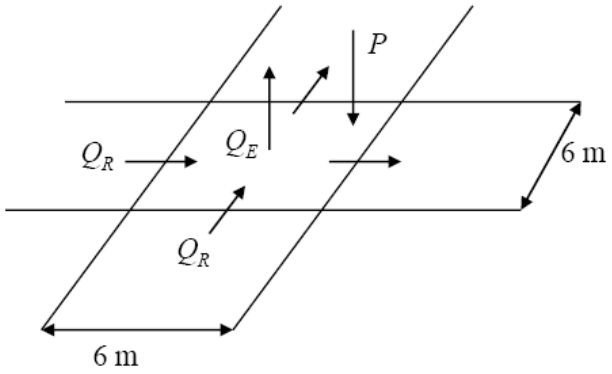

Figure 4.1 Schematics of the snow mass calculation in the spatially distributed approach. Arrows indicate fluxes of snow mass and calculations for these fluxes are based on Equation [2.1].

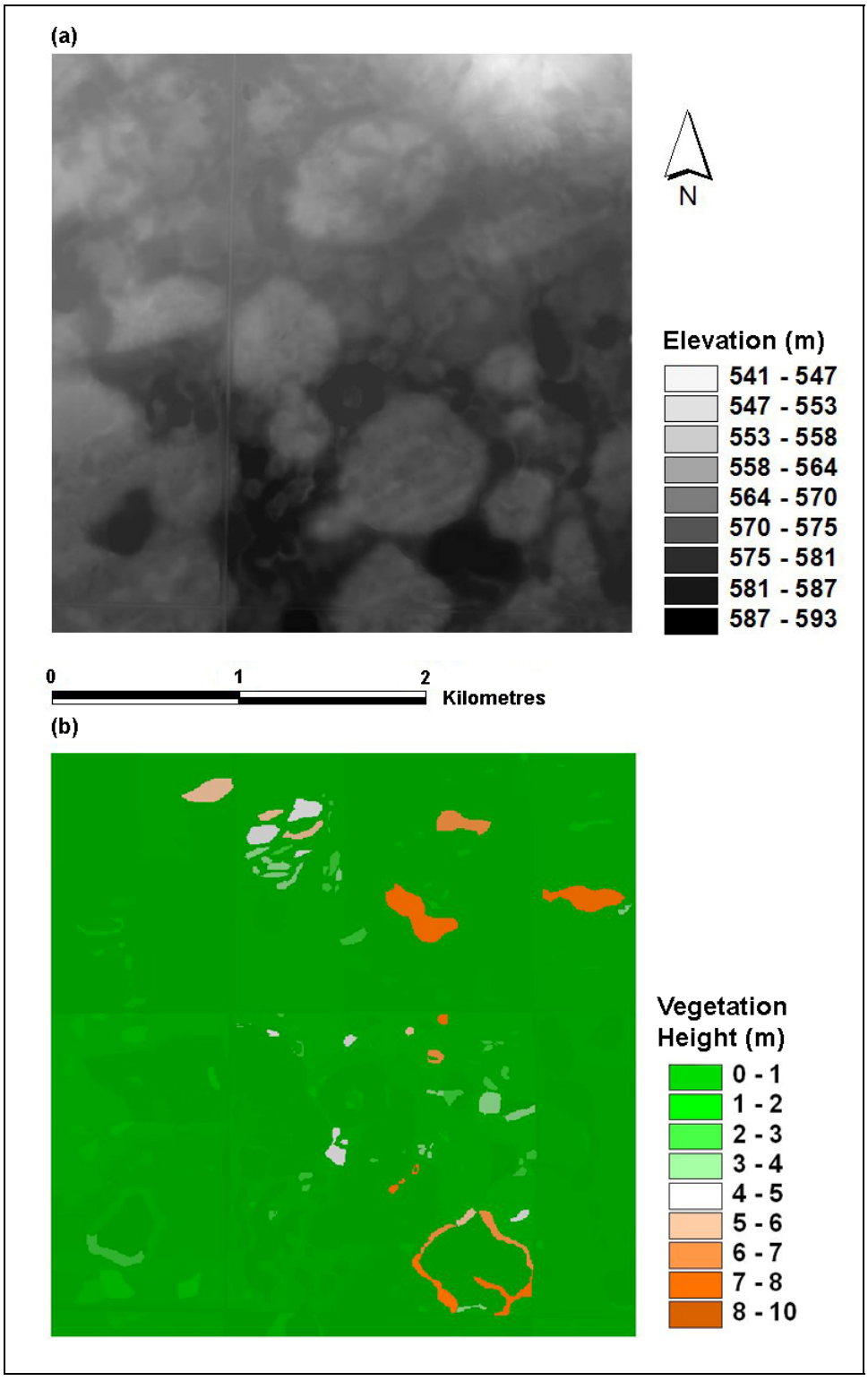

Figure 4.2 DBSM inputs for St. Denis: (a) Elevation grids, (b) Vegetation height grids.

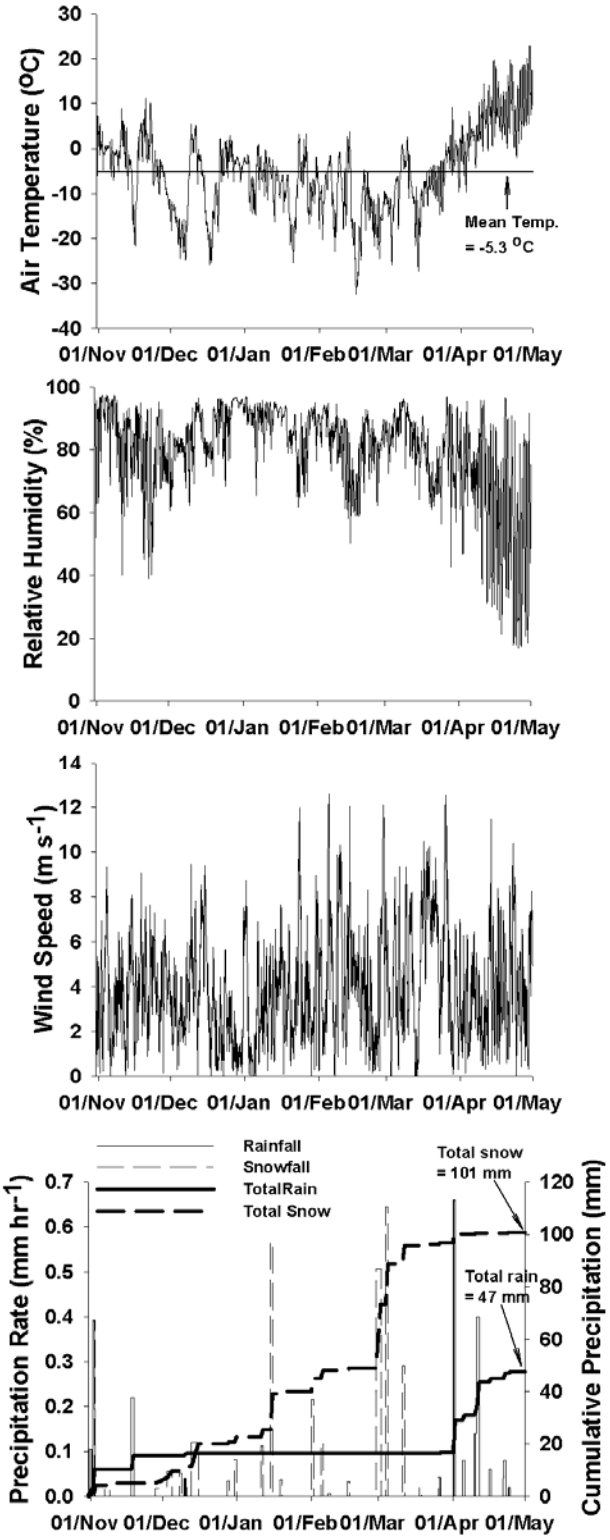

Figure 4.3 Hourly observations of temperature, humidity, wind speed, and precipitation during period of October 31, 2005 - April 30, 2006.

Spatially Aggregated Approach. The Prairie Blowing Snow Model (PBSM) of Pomeroy and Li (2000) was coupled with a windflow model in the Cold Regions Hydrological Model platform (CRHM) to estimate the redistribution of snow by wind. The windflow model is a simple parametric version of Mason and Sykes windflow model (Walmsley *et al.*, 1989). The simplified windflow model considers the effect of small scale topographical variations on wind speed and adjusts the wind speed accordingly, such that wind speeds over hilltops differ from those over depressions or flat terrain. A C++ programming code for this simplified windflow model is shown in Appendix D.

The adjusted wind speeds from the windflow model are used in PBSM. PBSM (Pomeroy and Li, 2000) uses physically-based algorithms to estimate snow accumulation based on a mass balance of snowfall and fluxes of saltation, suspension and sublimation of blowing snow. Coupling the simplified windflow model of Walmsley *et al*. with PBSM provides an estimation of snow accumulation due to changing local topography and surface roughness. The calculation is based on HRUs, in such a way that more snow accumulates in areas with rougher surfaces ('sink area') compared to those with less roughness ('source area') (Figure 4.4).

Initially, 19 HRUs were established for running the spatially aggregated approach; they were chosen based on criteria such as aspect class, slope class, and vegetation class. These criteria are similar to those in the Steppuhn's stratification system discussed by Pomeroy and Gray (1995) and

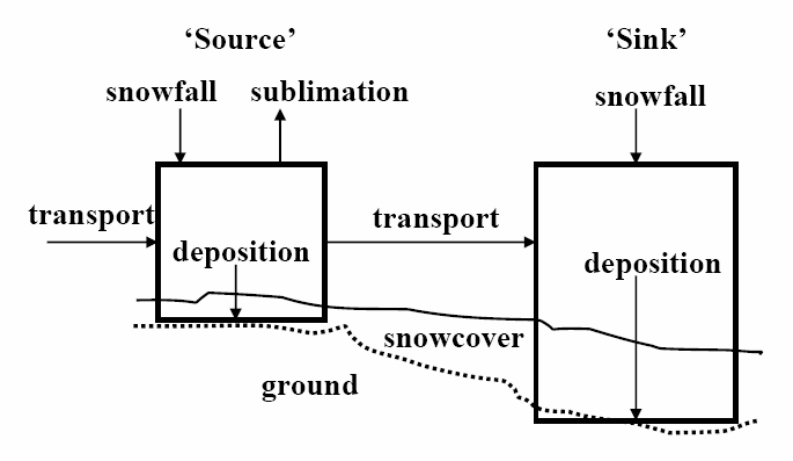

Figure 4.4 Schematics of snow mass calculation in the spatially aggregated approach.

Shook (1995); these criteria were used to divide the basin into several HRUs, on which snowcovers have independent frequency distributions of depth and water equivalent. These 19 HRUs are shown in Table 4.1; the parameters for selection were aspect, slope, elevation and aerodynamic roughness. Detailed characteristics of these parameters are shown in Appendix E. Aerial photographs and site maps were used to determine the blowing snow fetch

Table 4.1 Initial HRU for the spatially aggregated approach.

HRU Name	Symbols	HRU Name	Symbols
Stubble South Steep Slope	SSSS	Grass South Gentle Slope	GSGS
Stubble South Gentle Slope	SSGS	Grass North Steep Slope	GNSS
Stubble North Steep Slope	SNSS	Grass North Gentle Slope	GNGS
Stubble North Gentle Slope	SNGS	Grass Level	GL
Stubble Level	SL	Grass Steep Slope Hilltop	GSSH
Stubble Steep Slope Hilltop	SSSH	Grass Gentle Slope Hilltop	GGSH
Stubble Gentle Slope Hilltop	SGSH	Grass Steep Slope Valley	GSSV
Stubble Steep Slope Valley	SSSV	Grass Gentle Slope Valley	GGSV
Stubble Gentle Slope Valley	SGSV	Wetland	W
Grass South Steep Slope	GSSS		

distance shown in Appendix E; fetch distance was assumed to equal 300 m, due to the rolling terrain characteristics of field site. Preliminary runs based on these 19 HRUs were conducted to calculate snow accumulation development during pre-melt period (Oct 31, 2005 – Mar 27, 2006) (Figure 4.5). Figure 4.5 shows that some HRUs have very similar response. Based on this result, the original 19 HRUs were aggregated to seven HRU (Figure 4.6). These seven HRUs shown in Table 4.2 represent the major landscape units in St. Denis regarding the redistribution of snow by wind and the minimum complexity required to calculate snow accumulation. The map of the seven HRUs is illustrated in Figure 4.7. Areas of each HRU were determined by ground survey. Vegetation height was decided based on field surveys of vegetation; fetch distance was assumed to equal 300 m, due to the rolling terrain characteristics of field site.

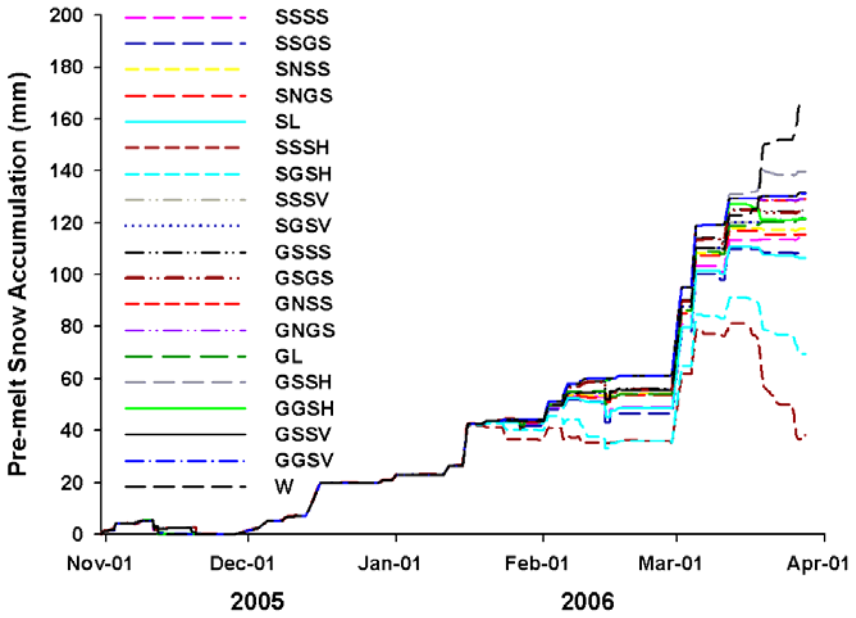

Figure 4.5 Simulated pre-melt snow accumulation for 19 HRUs at St. Denis.

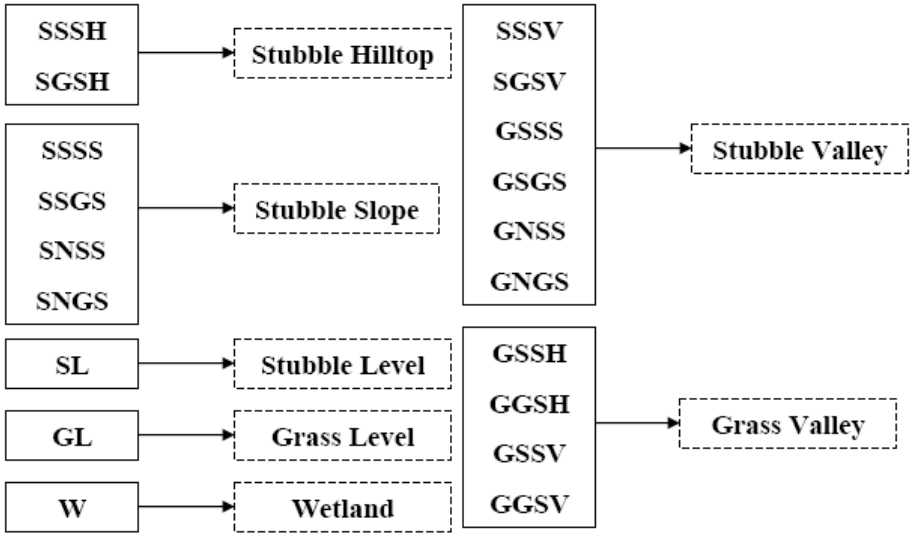

Figure 4.6 Grouping of 19 HRUs to 7 HRUs in the spatially aggregated approach.

Table 4.2 Characteristics of parameters for HRU in the spatially aggregated approach.

HRU Name	Area (km^2)	Vegetation Height (m)	Blowing Snow Fetch Distance (m)
Stubble Hilltop	0.5	0.05	300
Stubble Slope	0.4	0.12	300
Stubble Level	1	0.15	300
Stubble Valley	0.5	0.2	300
Grass Level	1	0.5	300
Grass Valley	0.3	0.5	300
Wetland	0.15	5	300

4.1.2 Model Scale for Snowmelt

The Energy-Budget Snowmelt Model (EBSM) developed by Gray and Landine (1988) was used to estimate snowmelt for both the spatially distributed and spatially aggregated approaches. The snow accumulation and snowmelt routines were linked and the outputs of daily melt were calculated.

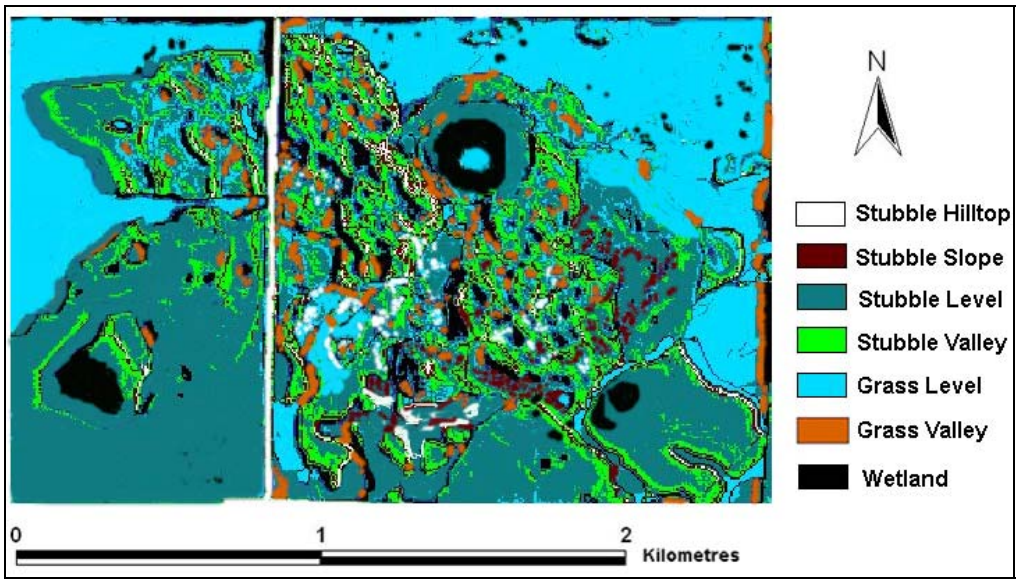

Figure 4.7 Map of seven HRUs at St. Denis NWA.

A snowmelt sensitivity analysis to slope and aspect was conducted during the melt period at St. Denis NWA. The purpose was to determine whether daily snowmelt is sensitive to changing slope or aspect in order to decide whether further disaggregation of HRUs was necessary for melt calculations. Both observed and simulated daily snowmelt rates were compared for the steepest south-facing (6.09°) and north-facing slopes (4.29°) at St. Denis (Figure 4.8). The averaged differences of daily snowmelt rate between the steepest south-facing and north-facing slopes were 9.3% and 5.8% for observation and simulation, respectively. This corresponds to mean differences of 0.68 mm/day and 0.58 mm/day for observed and simulated daily snowmelt, respectively. Such small differences indicate that the slope and aspect have only small effects on daily snowmelt at St. Denis. Hence, the

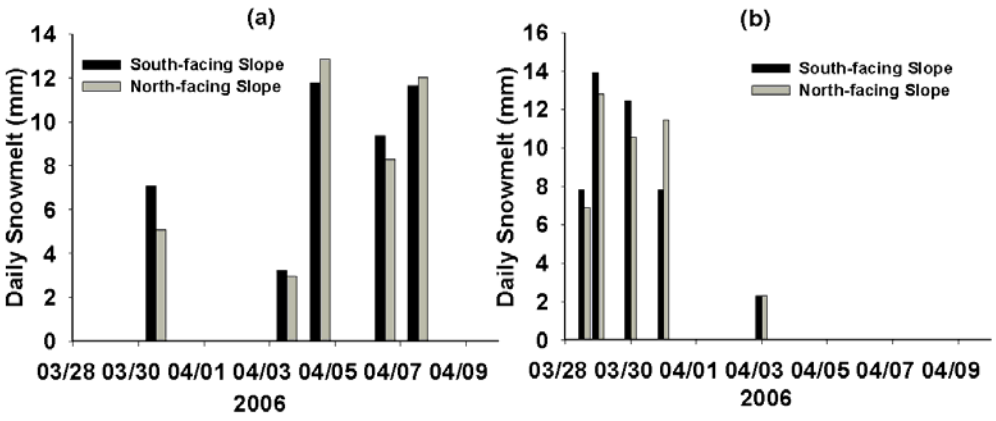

Figure 4.8 Daily snowmelt comparisons. (a) Observed daily snowmelt. (b) Simulated daily snowmelt.

criterion for determining HRU for snowmelt was not related to slope and aspect but to pre-melt snow accumulation.

In the spatially distributed approach for melting, HRU were determined initially according to the pre-melt SWE estimated from the spatially distributed snow accumulation. The maximum pre-melt SWE on March 27, 2006 over the area shown in Figure 4.2 was reclassified in ArcView GIS into 64 HRUs with unique values of pre-melt SWE. In the spatially aggregated approach, HRUs were the same seven HRUs as described in Table 4.2. A flowchart of routines for estimating snow accumulation and snowmelt for both the spatially distributed and spatially aggregated approaches is shown in Figure 4.9.

4.1.3 Model Scale Comparison

To compare the model scale, observed pre-melt SWE and daily melt

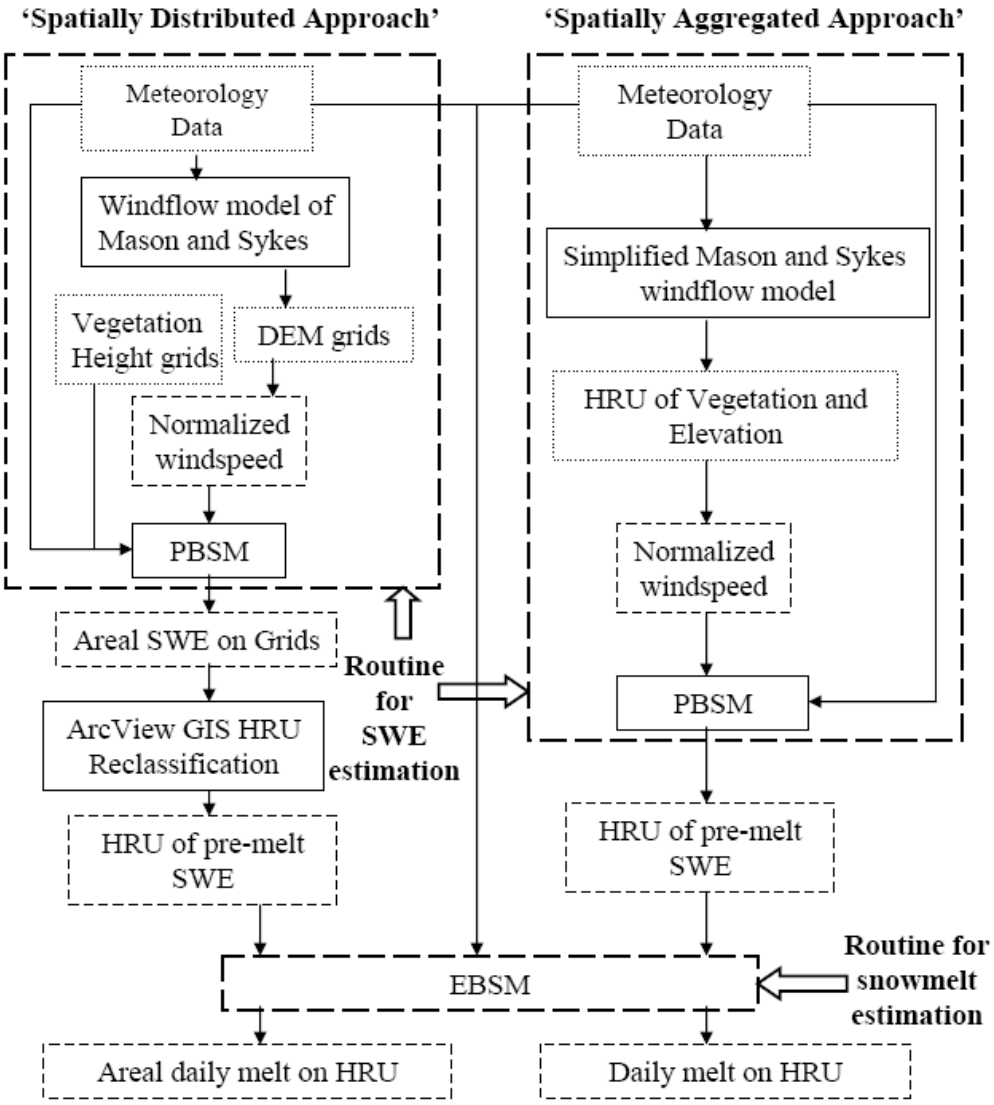

Figure 4.9 A flowchart of routines for estimating snow accumulation and snowmelt.

from the four field transects were averaged to get values of observed SWE and daily melt on the seven HRUs as described in Table 4.2. Without calibration of model parameters, average values of simulated pre-melt SWE and daily snowmelt on these seven HRUs from both approaches were

compared with the averaged observed values on the corresponding HRUs during the period of January – April, 2006.

To evaluate the performance of different modelling approaches, three statistical measures, Root Mean Square Difference (RMSD), Nash-Sutcliffe coefficient (NS) (Nash and Sutcliffe, 1970) and Model Bias (MB) were calculated as,

$$RMSD = \frac{1}{n}\sqrt{\sum (X_s - X_o)^2} \quad [4.1]$$

$$NS = 1 - \frac{\sum (X_o - X_s)^2}{\sum (X_o - \overline{X_o})^2} \quad [4.2]$$

$$MB = \frac{\sum X_s}{\sum X_o} - 1 \quad [4.3]$$

where n is number of samples, X_o, X_s, and $\overline{X_o}$ are the observed, simulated, and mean of the observed values, respectively. The Root Mean Square Difference is a weighted measure of the difference between observed and predicted values and has the same units as the observed and predicted values. A Nash-Sutcliffe coefficient measures the model efficiency with a value equal to 1 implying that model perfectly predicts pre-melt snow accumulation and daily melt with respect to observations. A value equal to 0 indicates that estimated values are not different from those observed. Hence, any positive value of this coefficient shows that the model has some predictive power, and better model performance is associated with higher values (Evans *et al.*, 2003).

The value of Model Bias evaluates the bias of the model, a positive bias indicates overprediction and a negative bias indicates underprediction.

In addition, the areal mean values of total snow accumulation on March 27 2006, daily snowmelt, snowmelt duration, and snow-covered area during melt period for St. Denis NWA were compared between the two approaches. In the spatially distributed approach, the areal mean values of these variables were determined by averaging values from 104,182 grids. The areal mean values in the spatially aggregated approach were decided based on the area-weighted values from the seven HRUs as,

$$\overline{Value}_{Areal} = \sum_{i=1}^{7} Value_{HRU(i)} \frac{Area_{HRU(i)}}{Area_{Total}} \quad [4.4]$$

where $Area_{HRU(i)}$, $Area_{Total}$, $\overline{Value}_{Areal}$, and $Value_{HRU(i)}$ are the area of HRU(i), total area of basin, areal mean value and value of HRU(i), respectively.

4.2 Results

4.2.1 Model Scale Comparison for Snow Accumulation

4.2.1.1 Pre-melt Snow Accumulation

The routines for estimating pre-melt SWE from both spatially distributed and spatially aggregated approaches were run for the 147-day period of October 31, 2005 – March 27, 2006. Cumulative snowfall was approximately 97 mm during this period. The areal distribution of snow accumulation for nine dates before melt was simulated from the spatially distributed approach (Figure 4.10). Figure 4.10 shows how snow

accumulation changed from Feb. 08, 2006 to Mar. 15, 2006; the areal snow accumulation evolved rapidly after the three major snowfalls (24 mm on Feb. 28 and Mar. 01, 15 mm on Mar. 04, and 8 mm on Mar. 11). Figure 4.10 also illustrates that deeper snow accumulation tends to occur in ditches of grid road and areas with taller vegetation.

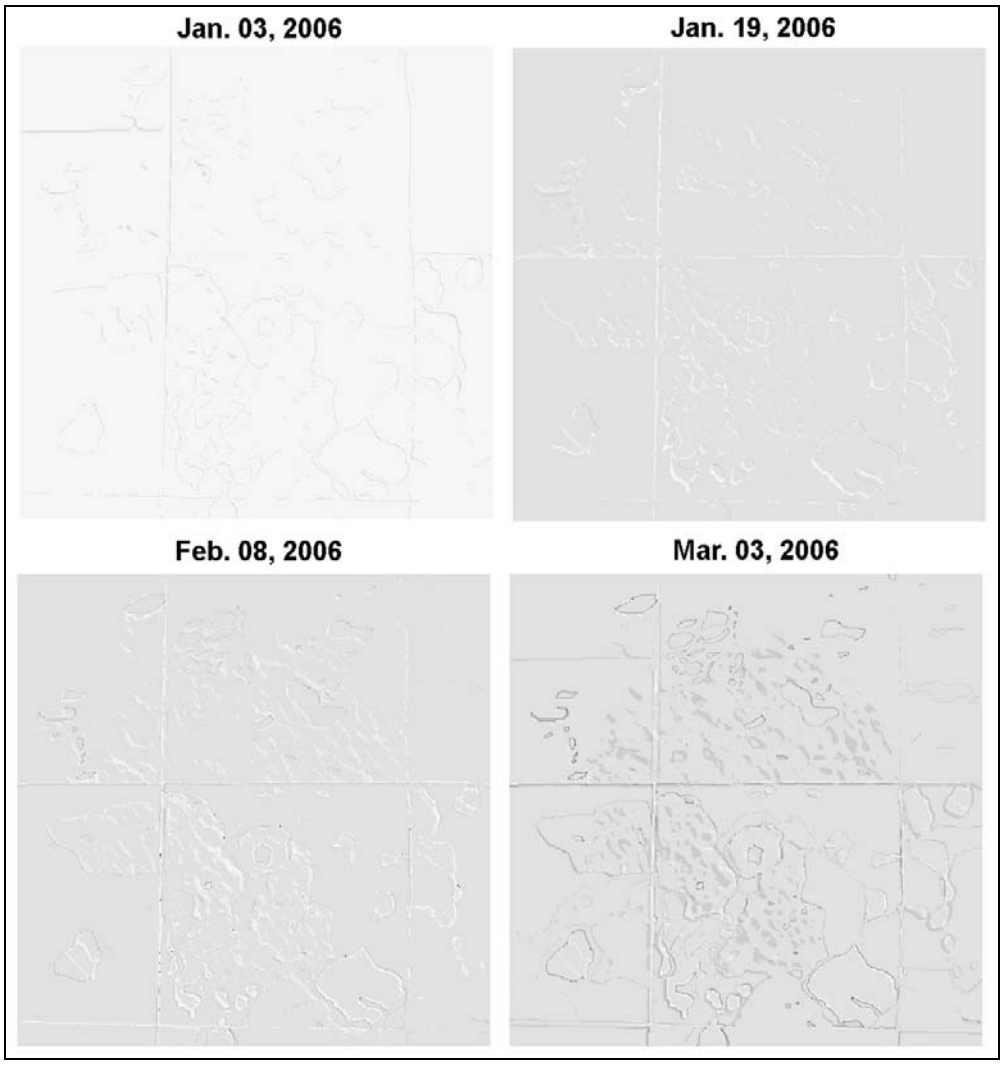

Figure 4.10 Simulated evolution of pre-melt snow accumulation from the spatially distributed approach.

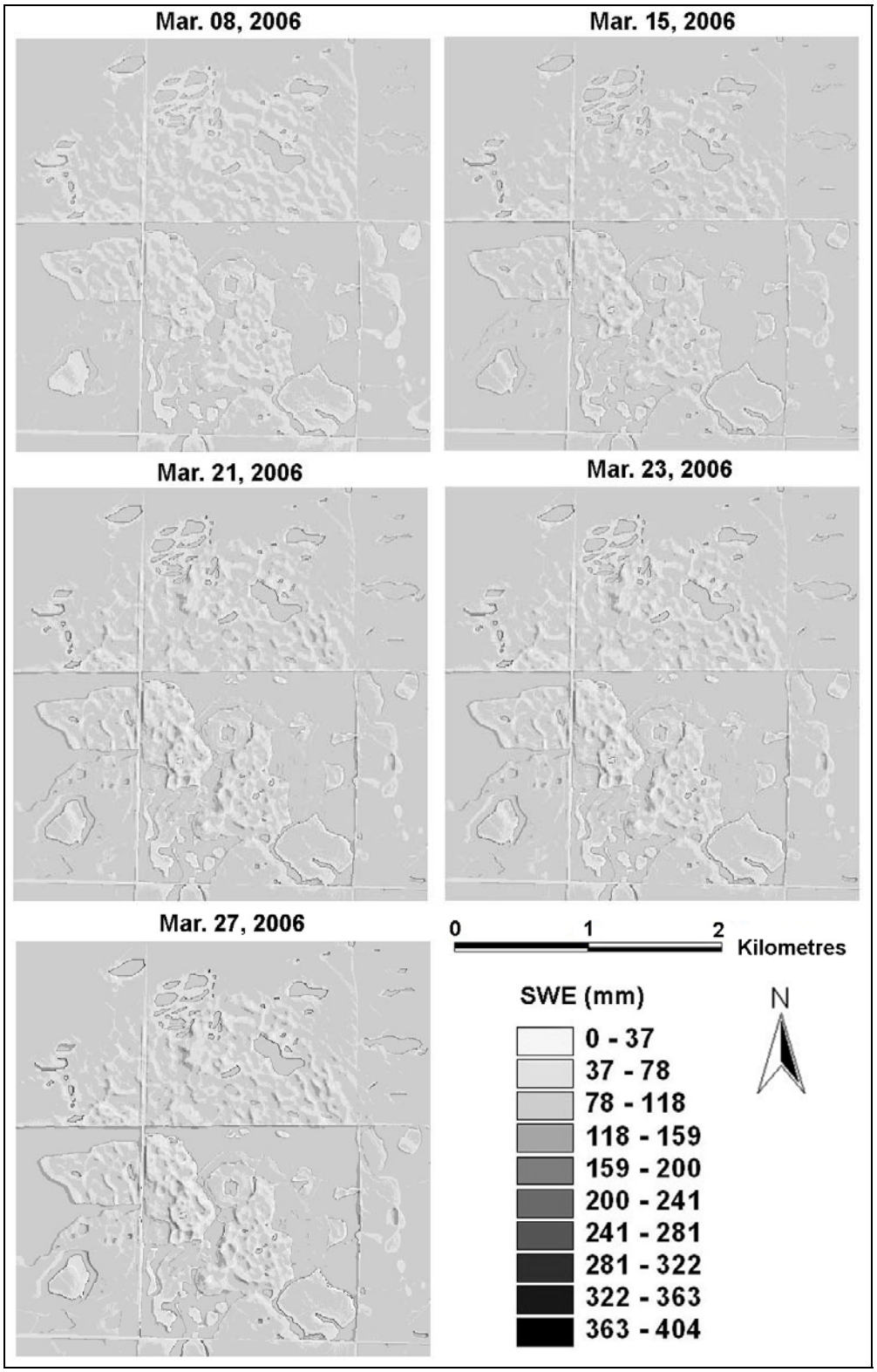

Figure 4.10 *Concluded*.

Simulated pre-melt snow accumulation on the seven HRUs is shown in Figure 4.11; it demonstrates that taller vegetation (e.g. grassland and wetland) had greater snow accumulation than did shorter vegetation (e.g. stubble fields). Also, more snow accumulated in valleys than on hilltops and slopes, because hilltops and slopes have higher wind exposure, resulting in snow being drifted from these areas to valleys. At end of the pre-melt period, about 148 mm and 237 mm of SWE were on 'grass valley' and 'wetland' areas, which was about 4 and 6 times that snow accumulation to the 'stubble hilltop' (i.e. 40 mm SWE), respectively. The 'stubble valley' area cumulated about 99 mm SWE, more than 2 times of that of the 'stubble hilltop'.

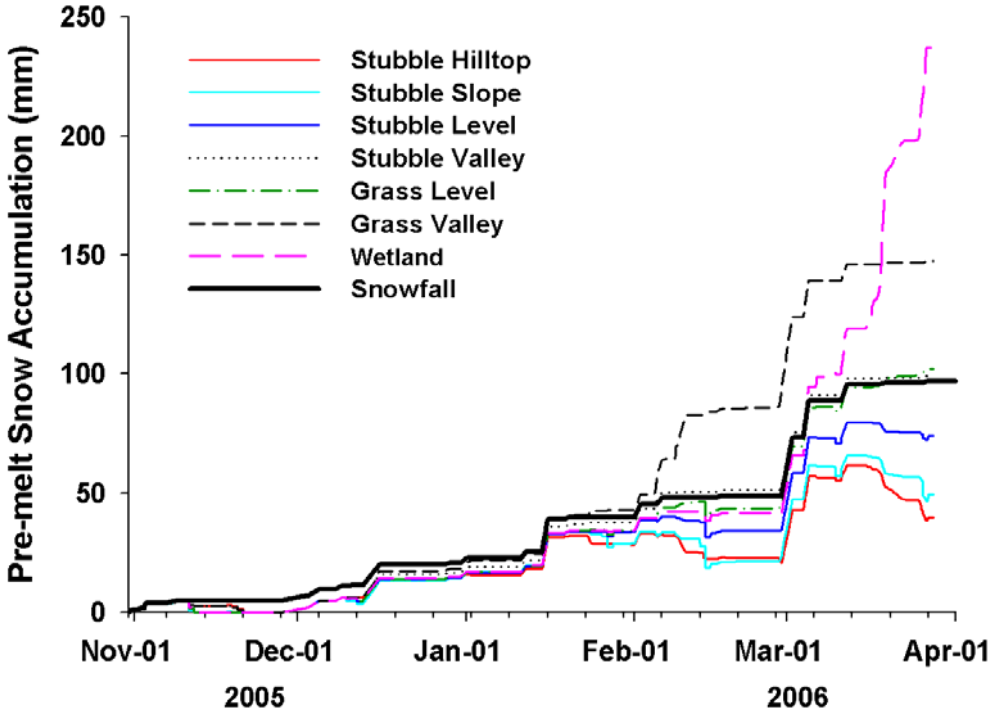

Figure 4.11 Simulated pre-melt snow accumulation evolution from the spatially aggregated approach.

4.2.1.2 Model Scale Comparison

Field transect of observations of snow depth and density were assigned to the seven HRUs and were compared to the simulated snow accumulation for pre-melt period of January - March 2006 from both the spatially distributed and spatially aggregated approaches (Figure 4.12 and Figure 4.13). They demonstrate that both approaches simulate snow accumulation fairly close to the observed ones at this scale. On the 'stubble hilltop', the spatially aggregated approach tends to simulate snowcover development well, while the spatially distributed approach tends to overestimate snow. On the 'wetland', the spatially distributed approach tends to have the best performance in predicting snow accumulation.

To quantify the difference and performance of the two model approaches in predicting snow accumulation, the Root Mean Square Difference (RMSD) and Nash-Sutcliffe coefficient (NS) were calculated for the seven HRUs (Figure 4.12), and Model Bias (MB) was also computed for the seven HRUs (Figure 4.13). Both approaches have quite similar RMSD and NS for five HRUs ('stubble slope', 'stubble level', 'stubble valley', 'grass level' and 'grass valley'), with RMSD ranging from 2.06 mm to 5.91 mm and NS ranging from 0.68 to 0.91. This indicates that both approaches simulate the development and timing of snowcovers in winter period fairly well with relatively small differences with observations. For the 'stubble hilltop', a negative value of NS for the spatially distributed approach and a positive value of NS for the spatially aggregated approach implies that the spatially

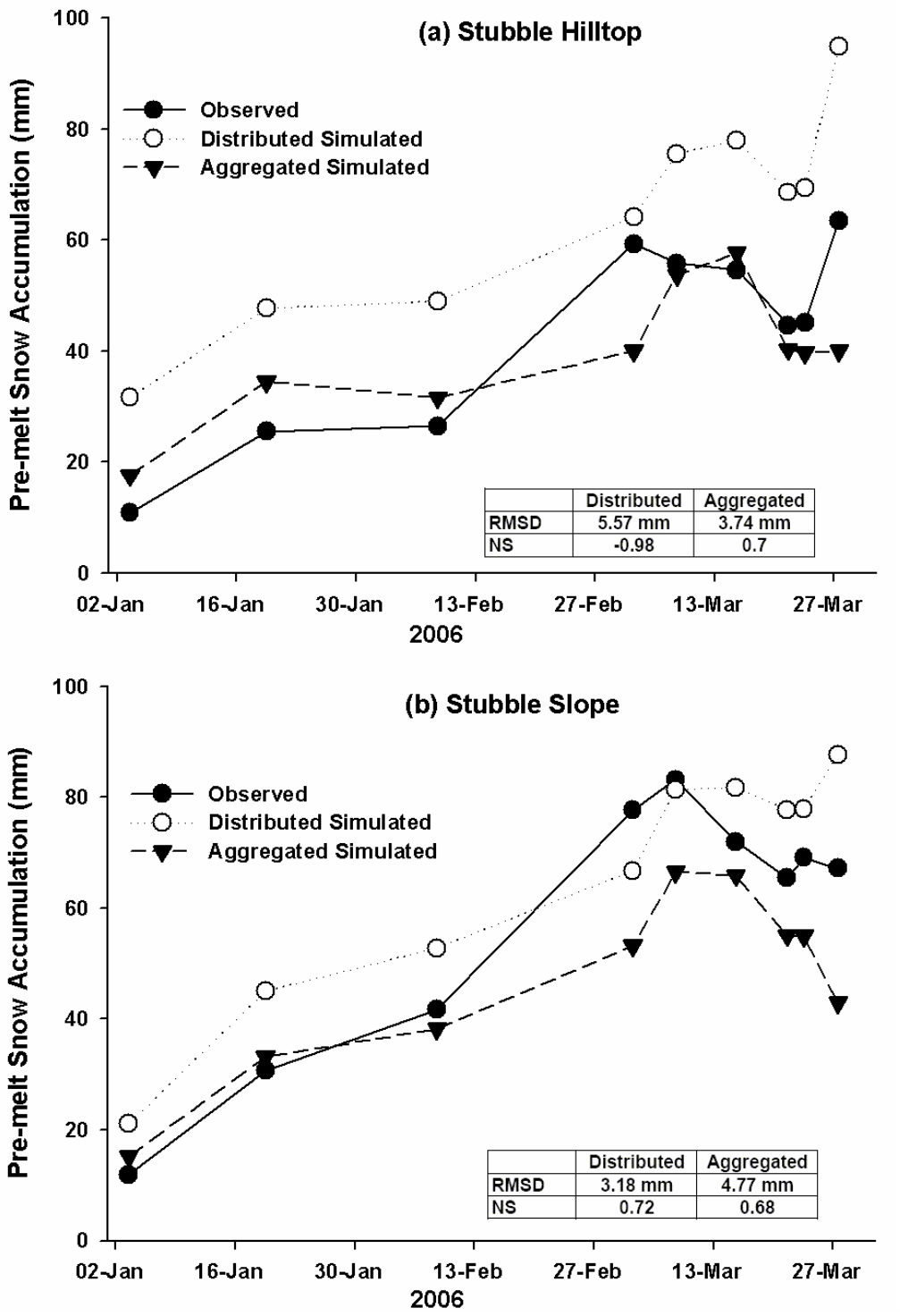

Figure 4.12 Model scale comparison for snow accumulation. (a) Stubble hilltop (b) Stubble slope (c) Stubble level (d) Stubble valley (e) Grass level (f) Grass valley (g) Wetland.

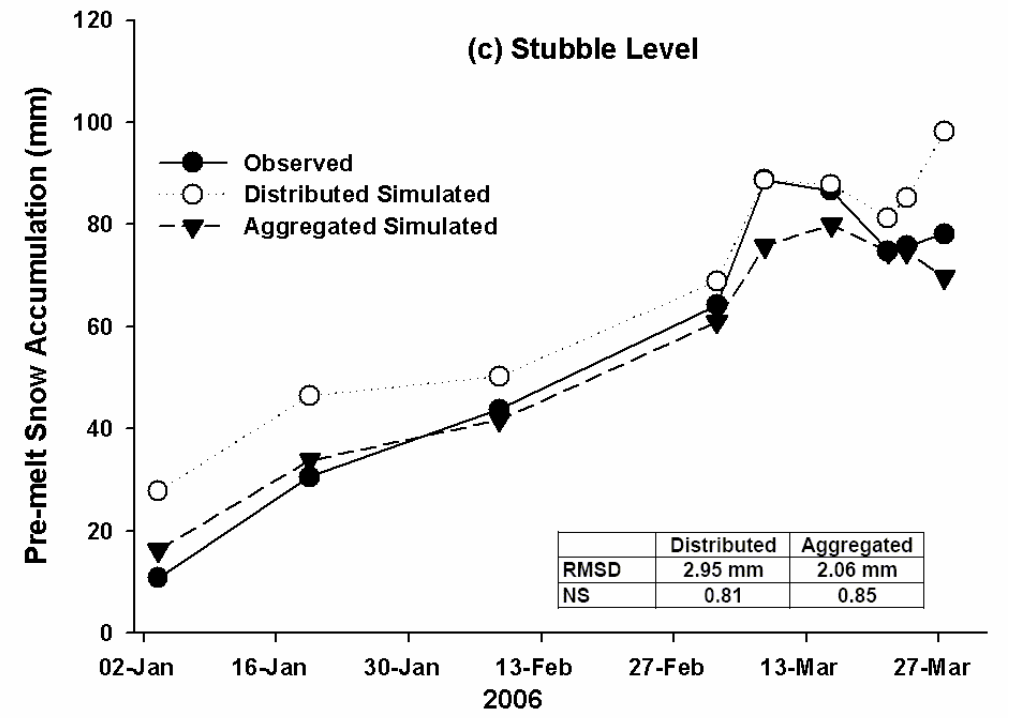

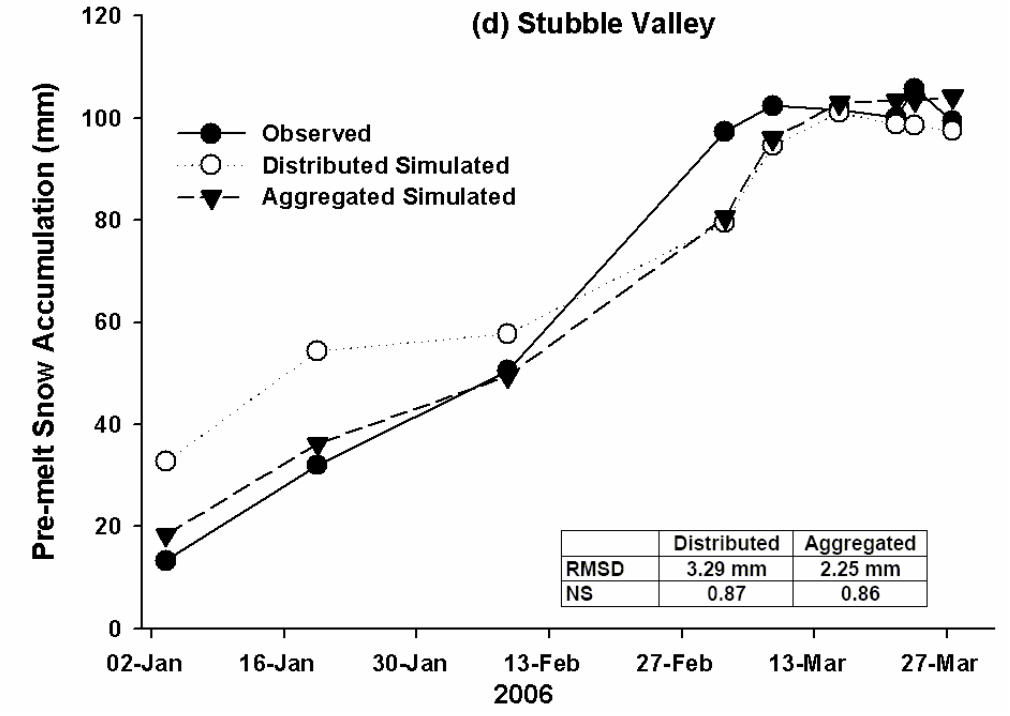

Figure 4.12 *Continued*.

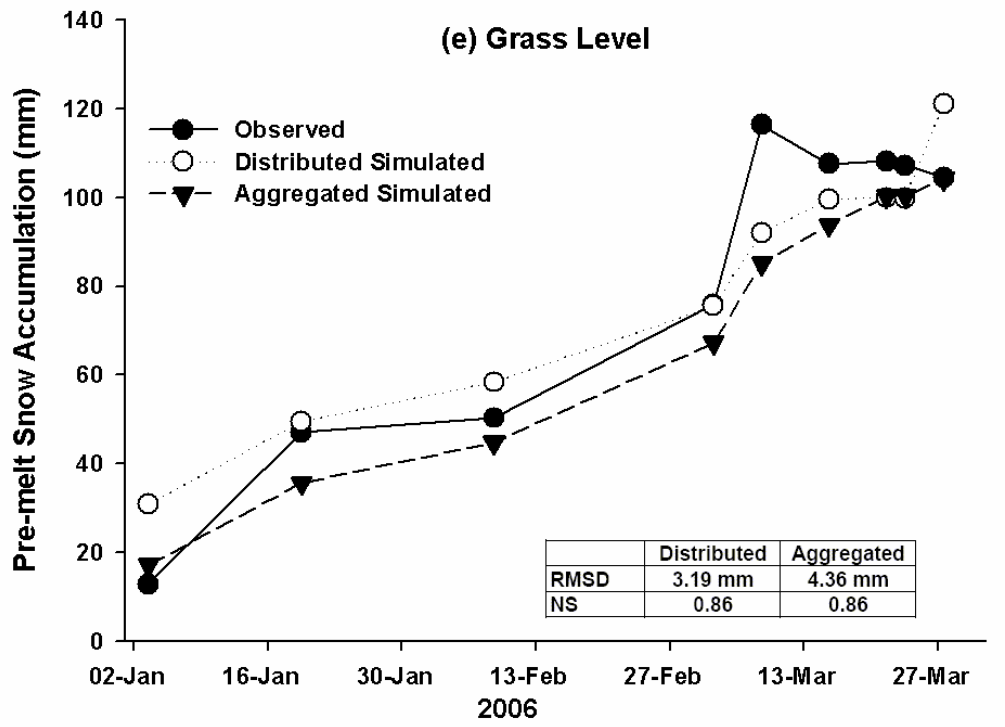

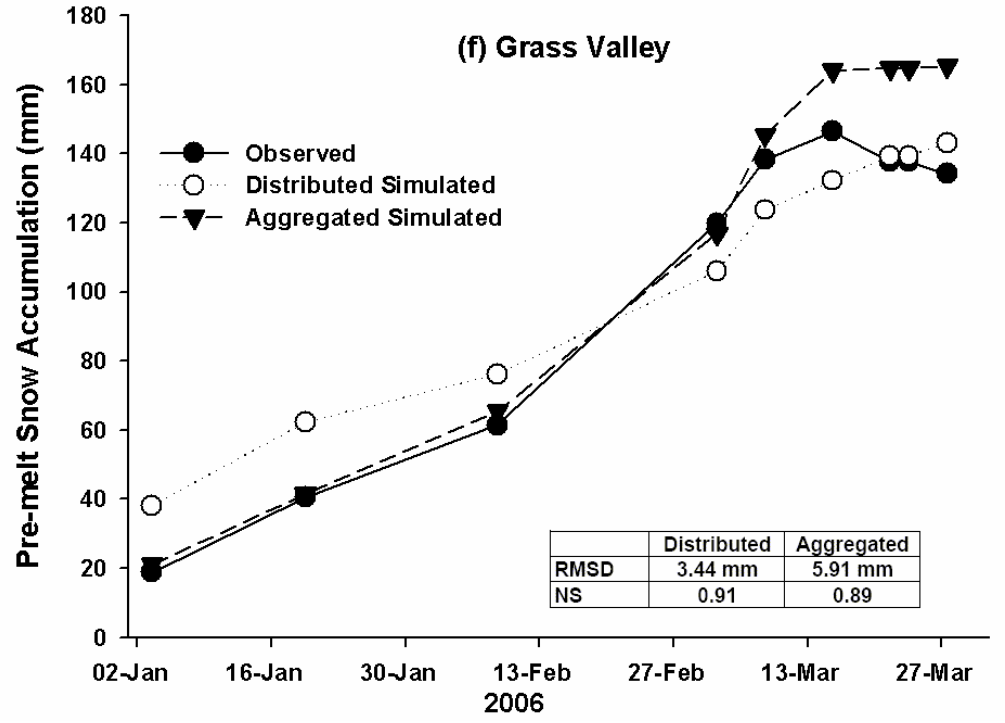

Figure 4.12 *Continued*.

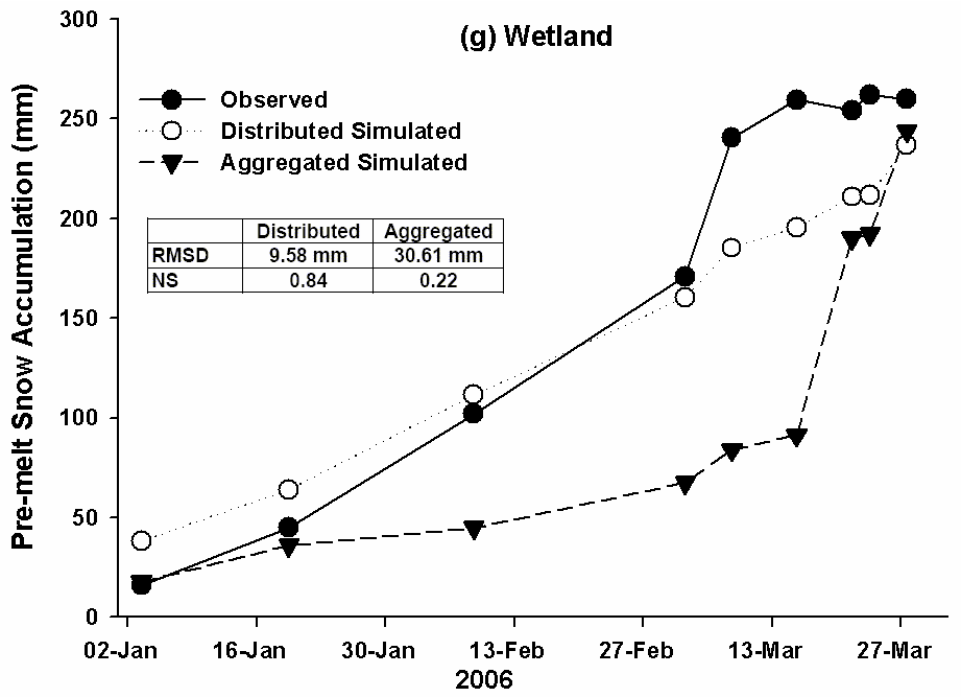

Figure 4.12 *Concluded*.

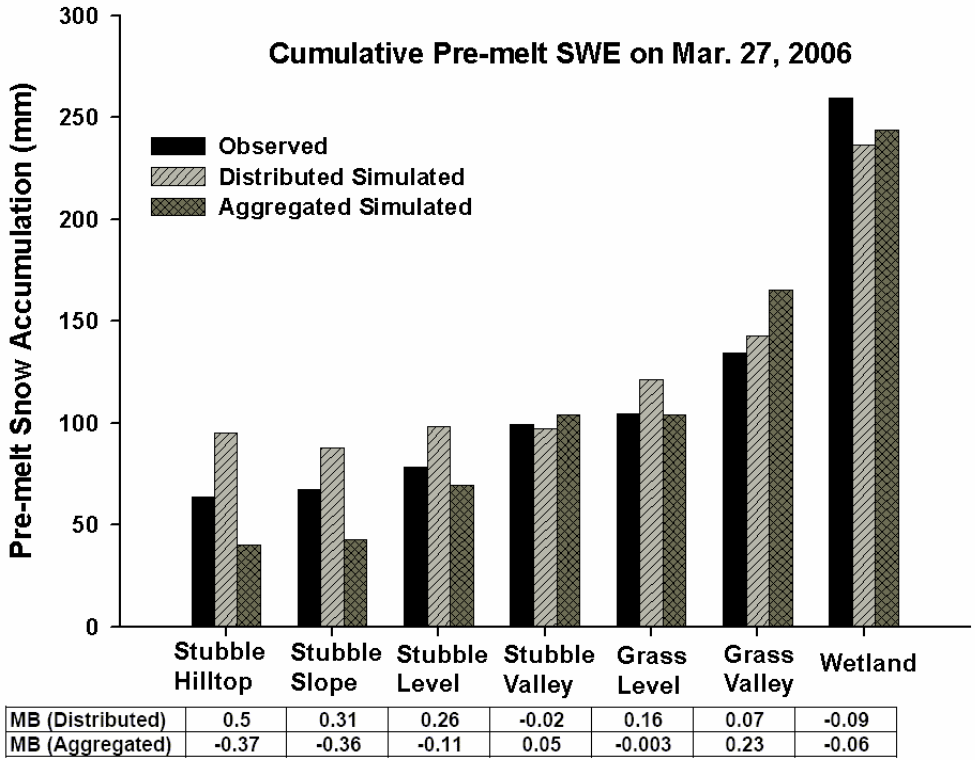

Figure 4.13 Model scale comparison for cumulative pre-melt SWE.

aggregated approach performs much better in predicting snowcover evolution here. For the 'wetland', values of NS are 0.84 and 0.22 for the spatially distributed and spatially aggregated approaches, respectively, indicating that the spatially distributed approach has better prediction power in the timing of SWE. The total end of winter snow accumulation on Mar. 27, 2006 is shown in Figure 4.13. Both approaches generate the end of winter snow mass moderately close to the observations on most HRUs; that is, the amount of overestimation or underestimation for total snow accumulation is within 30%. However, for the 'stubble hilltop' and 'stubble slope', the spatially distributed approach overestimates by more than 30%, while spatially aggregated approach underestimates by more than 30%. Topography adds some uncertainty to the modelling of blowing snow.

4.2.1.3 Areal Mean Snow Accumulation Comparison

In the spatially distributed approach, an average end of winter snow accumulation of 111 mm was calculated from 104,182 grid cells (Figure 4.14). This averaged value is more than the total winter snowfall of 97 mm; part of this difference is the blowing snow import from the outside of basin, which was about 6 mm estimated by the spatially distributed approach. In the spatially aggregated approach, an areal mean end of winter snow accumulation of 90 mm was computed according to Equation [4.4] from the seven HRUs. Compared to the spatially distributed approach, the spatially aggregated approach estimated 21 mm less SWE for the entire St. Denis

NWA. The areal mean observed snow accumulation can be roughly estimated based on area-weighted observations for the seven HRU and was approximately 97 mm. This implies that both approaches have similar accuracy in estimating areal snow accumulation with about 10% of overestimation or underestimation.

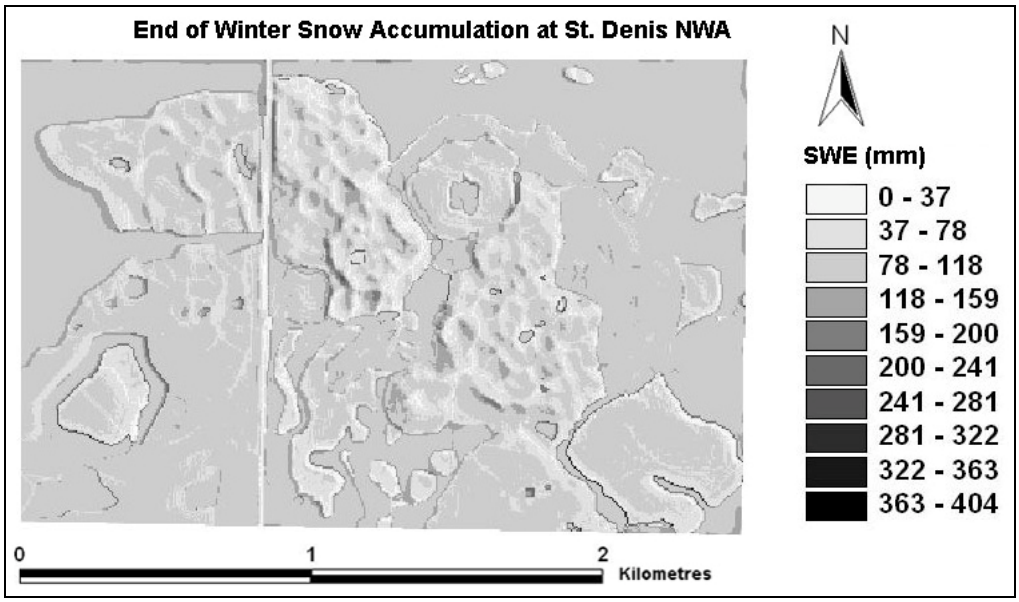

Figure 4.14 Simulated end of winter snow accumulation at St. Denis NWA.

4.2.2 Model Scale Comparison for Snowmelt

4.2.2.1 Model Scale Comparison

Snow survey observations were assigned to the seven HRU and were compared to the simulated daily snowmelt for melting period of March - April 2006 from both the spatially distributed and spatially aggregated approaches (Figure 4.15). Any negative change in snow accumulation during ablation was

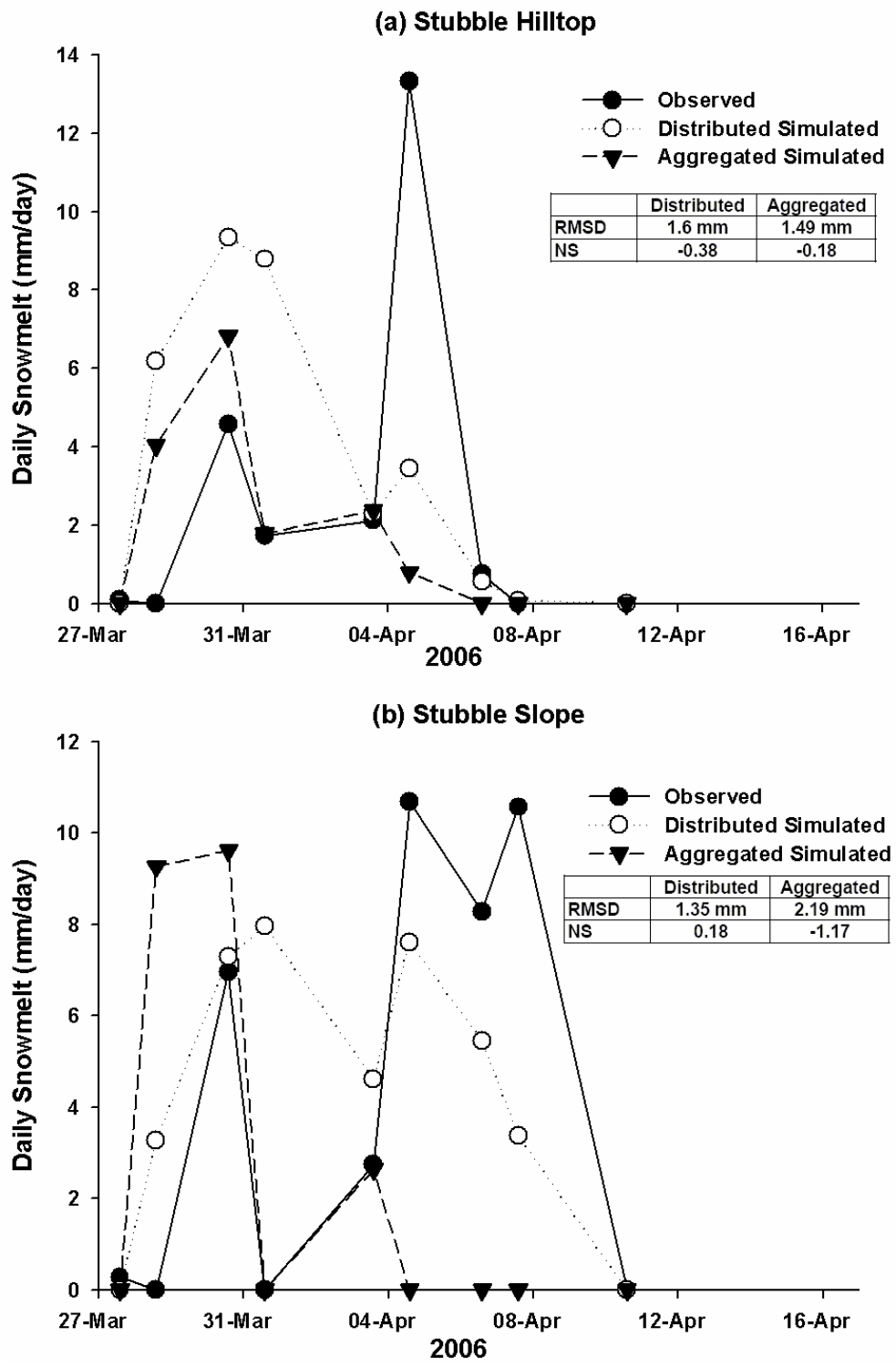

Figure 4.15 Model scale comparison for snowmelt. (a) Stubble hilltop (b) Stubble slope (c) Stubble level (d) Stubble valley (e) Grass level (f) Grass valley (g) Wetland.

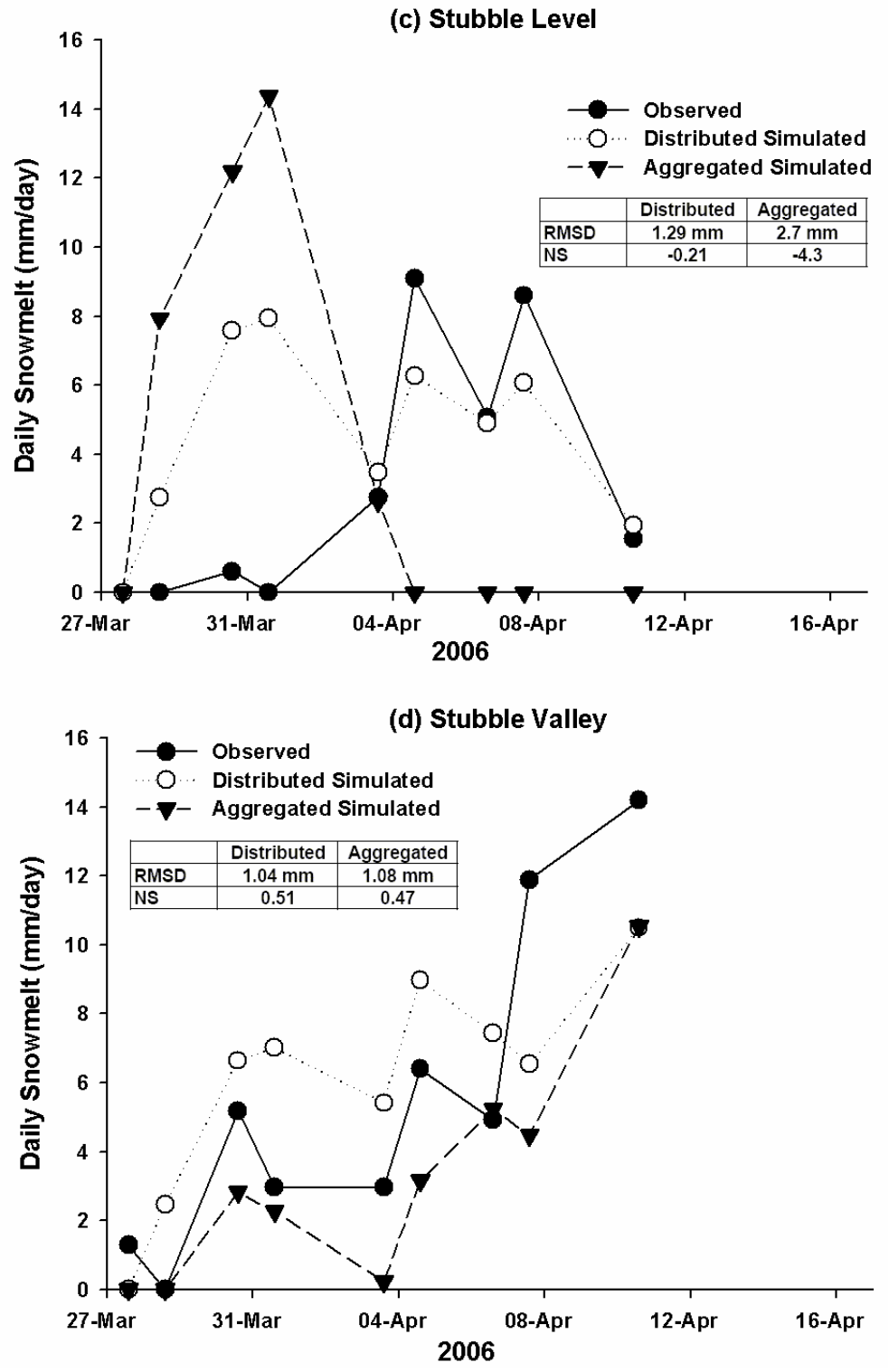

Figure 4.15 *Continued*.

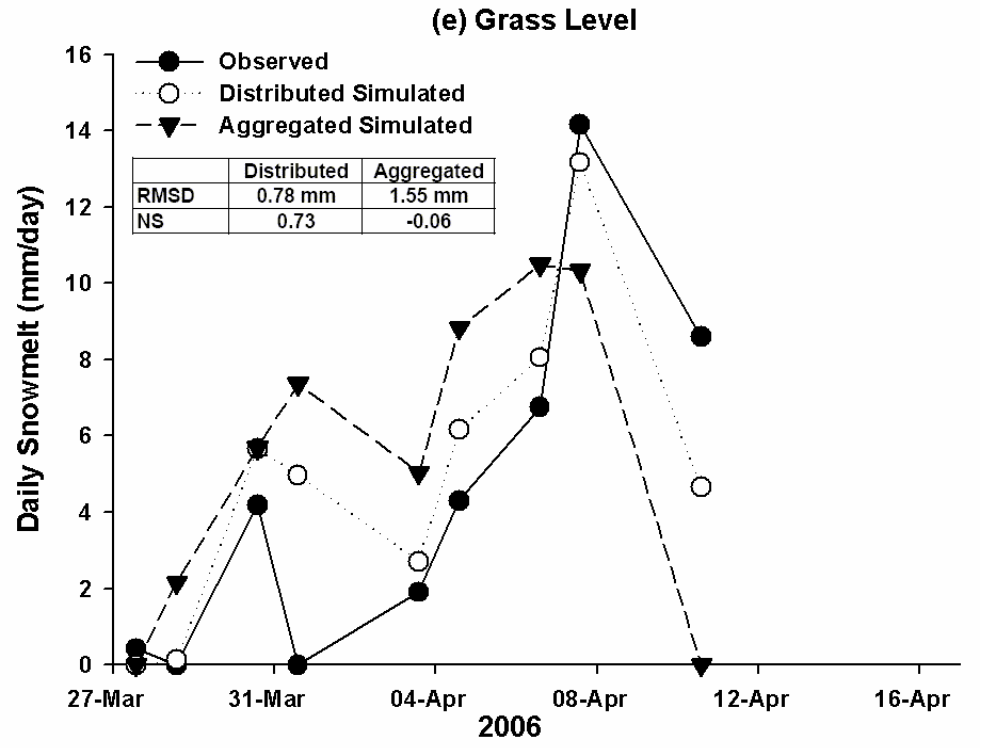

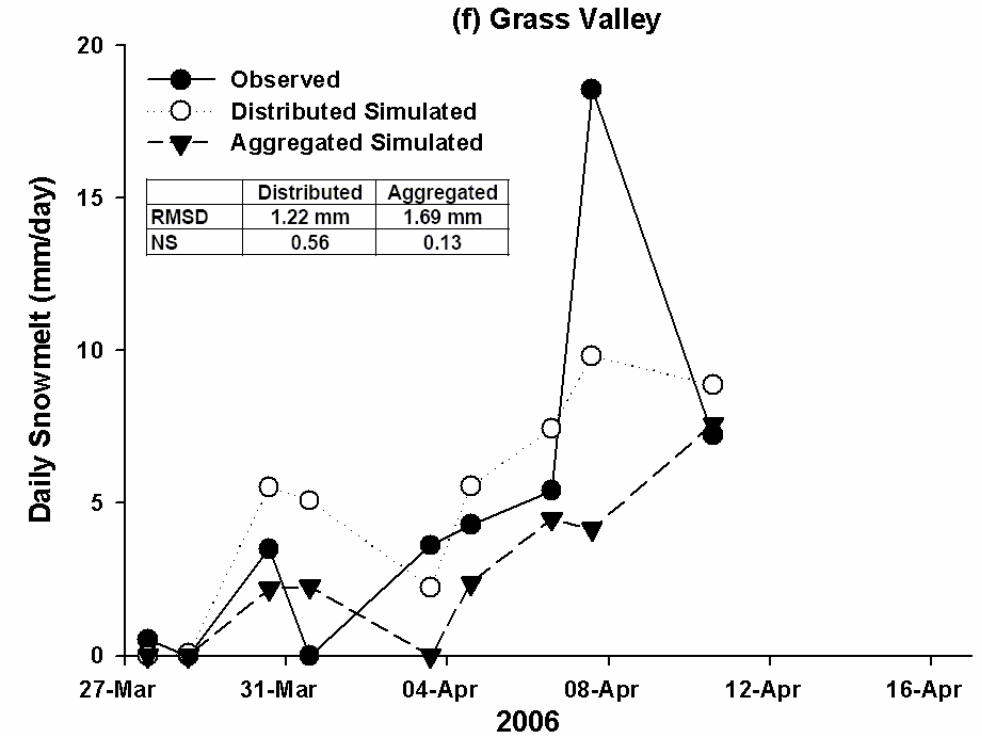

Figure 4.15 *Continued*.

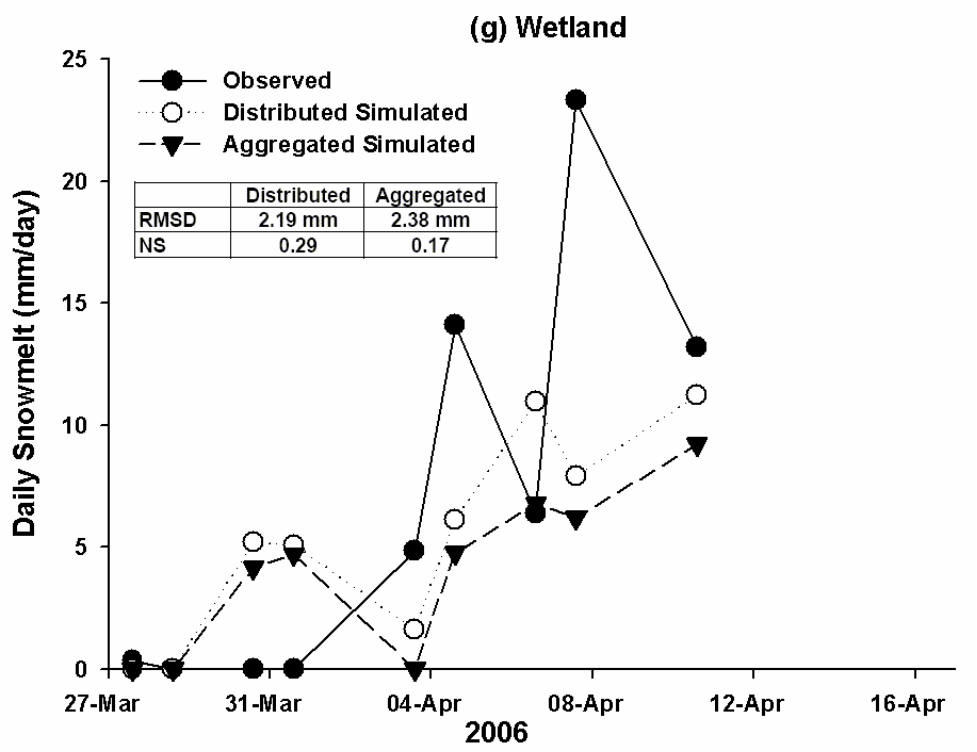

Figure 4.15 *Concluded*.

considered to be due to snowmelt. The observations show that both modelling approaches have some predictive power for snowmelt. The Root Mean Square Difference (RMSD) and Nash-Sutcliffe coefficient (NS) were calculated for the seven HRUs to evaluate the difference between the two modelling approaches in predicting snowmelt (Figure 4.15). Both approaches have RMSD within the range of 0.78 – 2.7 mm/day for the seven HRUs. This implies relatively small differences between the simulated and observed daily snowmelts. Values of NS vary with HRUs; that is, both approaches have negative values for the 'stubble hilltop', 'stubble level', indicating that both modelling approaches simulate the timing of daily snowmelt poorly at these

sites. However, both approaches predict well for the 'stubble valley' with NS of 0.51 and 0.47 for the spatially distributed and spatially aggregated approaches, respectively. The spatially distributed approach has higher values of NS than those of spatially aggregated approach for the 'stubble slope', 'grass level', 'grass valley' and 'wetland'. This suggests that the spatially distributed approach performs better in estimating the timing of snowmelt.

4.2.2.2 Areal Mean Daily Snowmelt, Snowmelt Duration, and Relative Snow-covered Area Comparison

Based on Equation [4.4], the areal mean daily snowmelt and relatively snow-covered area for St. Denis NWA were estimated from 64 HRUs in the spatially distributed approach and from the seven HRUs in the spatially aggregated approach (Figure 4.16). Figure 4.16 shows that major melt commenced on March 28, 2006; snowmelt ended on April 20 in the spatially aggregated approach, which was eight days earlier than that in spatially distributed approach. Total snowmelt of 88 mm and 109 mm was calculated for the spatially aggregated and spatially distributed approaches; this is about the same as the pre-melt snow accumulation.

Figure 4.16(a) illustrates that the majority of melt occurred during March 28 - April 14; the areal mean daily melt peaked on March 29 (about 11 mm/day) and on April 08 (about 12.5 mm/day) for the spatially aggregated and spatially distributed approaches, respectively. Both approaches estimated very similar daily snowmelt during March 28 - April 03. With more pre-melt

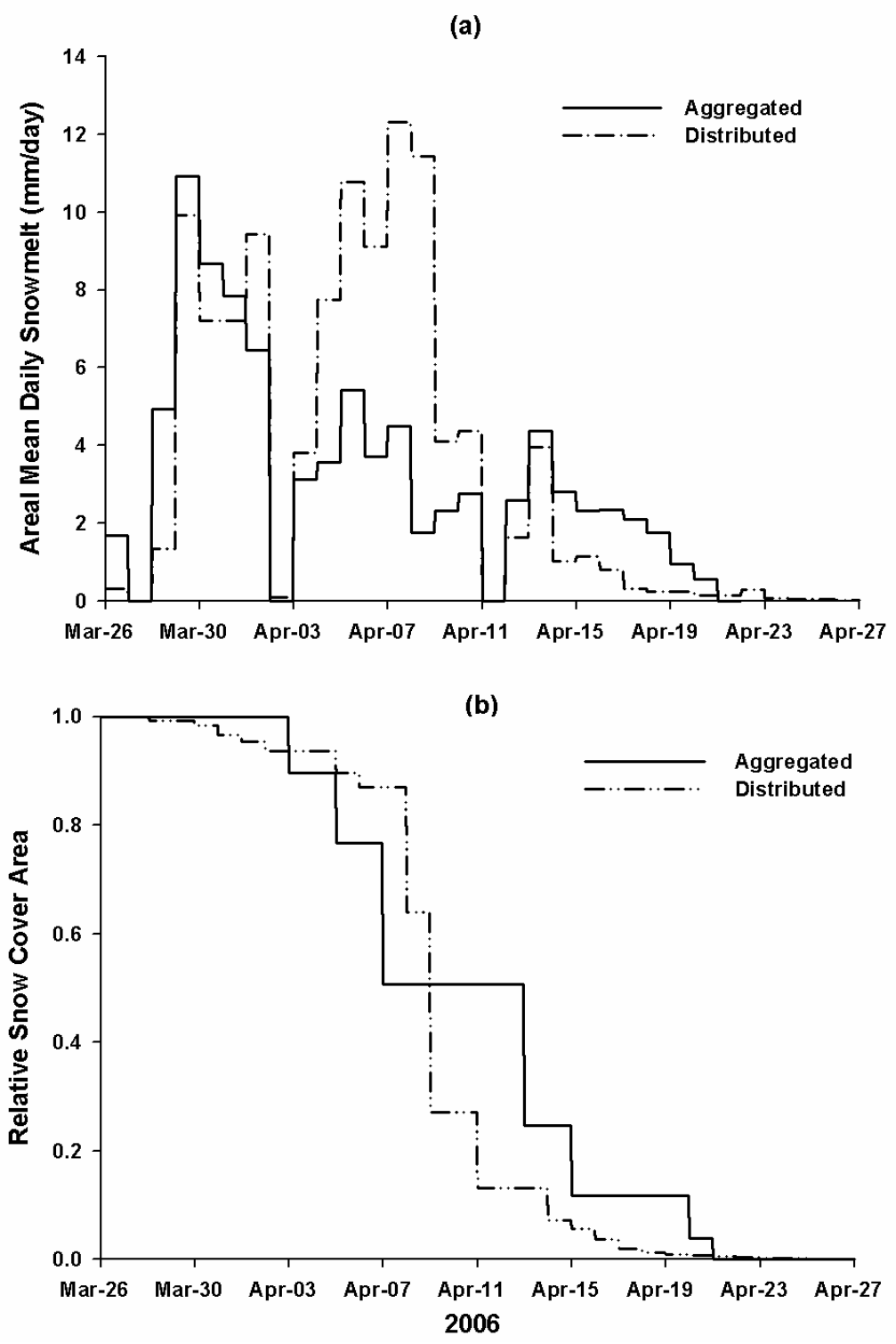

Figure 4.16 Areal snowmelt comparisons. (a) Areal mean daily snowmelt (b) Relative snow-covered area.

snow accumulation calculated in the spatially distributed approach, much higher daily melt from the spatially distributed approach during April 04 - April 11 indicates that the melt rate is closely associated with the amount of pre-melt snow accumulation. Figure 4.16(b) shows an interesting aspect of model scale on the areal snowcover depletion. Compared to the spatially aggregated approach, the snow-covered area depleted rather gradually in the spatially distributed approach. This is attributed to larger numbers of HRU in the spatially distributed approach so that snowcover depletion of individual HRU did not cause sudden reduction of snow-cover area for entire basin. The relative snow-cover area from the spatially distributed approach shown in Figure 4.16(b) is closer to snow cover depletion curves in the Prairies from aerial photographs measurement by Pomeroy *et al*. (1998).

4.3 Model Scale Selection

For the predictability of snowcover development during the winter accumulation period, Figure 4.12(a)-(g) shows that both the spatially distributed and spatially aggregated approaches have similar performance on most HRUs. The spatially distributed approach predicted the development of snow accumulation better on some HRU (e.g. 'wetland'), while the spatially aggregated approach had better performance on other HRU (e.g. 'stubble hilltop'). However, the end of winter snow accumulation is the most important snow variable in the water balance. Figure 4.13 shows that both scales provided similar predictability of the end of winter snow accumulation when

compared to the observations of cumulative winter snow accumulation. This is also confirmed in the areal mean snow accumulation comparison, indicating that both approaches had similar accuracy. However, the computational time for the spatially distributed approach was about 30-50 minutes, while the spatially aggregated approach took about 1 minute. For the purpose of estimating the timing of pre-melt snow accumulation and total snow accumulation in a small-sized Canadian prairie basin, the spatially aggregated approach was sufficiently accurate and is computationally efficient. However, the spatially distributed approach provides much more detailed information on the location of deep snow drifts and scour zones.

With respect to the sequence of daily snowmelt, Figure 4.15(a)-(g) demonstrates that both approaches have some prediction power and that their simulated results are analogous. Compared to the spatially aggregated approach, the spatially distributed approach performed better in reproducing the timing of daily snowmelt for some HRUs (e.g. 'stubble slope', 'grass level', 'grass valley' and 'wetland'). There were differences between two approaches in the timing of areal snowmelt, snow-covered area, and duration of areal snowcovers (Figure 4.16). However, the spatially aggregated approach takes only the half computational time of the spatially distributed approach, hence it is more efficient to use the spatially aggregated approach for the estimation of snowmelt for a small-sized Canadian prairie basin.

Chapter 5

5.0 Snow Hydrology Model Derivation and Test for Canadian Prairies

A snow hydrology model for Canadian Prairies was run at two drainage basins: Creighton Tributary of Bad Lake, Saskatchewan and Wetland 109 at St. Denis NWA, Saskatchewan. The former basin is semi-arid and has relatively well-developed drainage, while the latter one is sub-humid, partly wooded and relatively poorly-drained site with many small depressions like Wetland 109. The basins represent the range of conditions in the Canadian Prairies.

5.1 Model Derivation and Evaluation at Bad Lake, Saskatchewan

5.1.1 Methods

5.1.1.1 Model Derivation

The Cold Regions Hydrological Modelling platform (CRHM) was used to estimate the water balance during winter and spring for Creighton Tributary of Bad Lake. CRHM is based on a modular, object-oriented structure in which component modules represent basin descriptions, observations, or physically-based algorithms for calculating hydrological processes. Full details of CRHM are described by Pomeroy *et al.* (2007b).

Relevant modules for simulation of surface snowmelt runoff include the Prairie Blowing Snow Model (Pomeroy, 1989; Pomeroy *et al*., 1993; Pomeroy and Li, 2000), the Energy-Budget Snowmelt Model (Gray and Landine, 1988), Gray's expression for snowmelt infiltration (Gray *et al.*, 1985), Granger-Gray evaporation expression for estimating actual evaporation from unsaturated surfaces (Granger and Gray, 1989; Granger and Pomeroy, 1997), a soil moisture balance model for calculating soil moisture balance and drainage (Leavesley *et al.*, 1983), and Clark's lag and route runoff timing estimation procedure (Clark, 1945). These modules were assembled along with modules for radiation estimation and albedo changes (Garnier and Ohmura, 1970; Gray and Landine, 1987; Granger and Gray, 1990) into CRHM "projects" which are basin-specific models. Detailed schematics of these modules for the snow hydrology model are shown in Appendix F.

Assembling these modules in CRHM enabled the estimation of snow accumulation (SWE) after wind redistribution, snowmelt rate, cumulative snowmelt, cumulative snowmelt infiltration into unsaturated frozen soils (INF), and actual evaporation (Evap). Evaporation is calculated using the method of Granger and Pomeroy (1997), which is entirely an atmospheric energy balance and feedback approach. The approach is then modified by CRHM in that actual evaporation (Evap) is limited by a surface mass balance; when interception storage and soil moisture reserves are depleted evaporation cannot proceed. Snowmelt runoff over the event (R) was estimated based on a simplified conservation equation:

$$R = SWE - INF - Evap \quad [5.1]$$

where all terms are in mm of water equivalent.

Calculations in CRHM are made on Hydrological Response Units (HRUs). Based on the major land uses in the basin and on physiography, three HRUs (fallow field, stubble field, and grassland [coulee]) were chosen for the snowmelt runoff simulation (Table 5.1). The total snowmelt runoff from these HRUs provided the cumulative basin snowmelt runoff as,

$$R_{basin} = R_{fallow} \frac{Area_{fallow}}{Area_{basin}} + R_{stubble} \frac{Area_{stubble}}{Area_{basin}} + R_{grassland} \frac{Area_{grassland}}{Area_{basin}} \quad [5.2]$$

where R_{basin}, R_{fallow}, $R_{stubble}$, and $R_{grassland}$ are basin snowmelt runoff, snowmelt runoff over fallow field, stubble field, and grassland, respectively; all runoff are in mm of water equivalent; $Area_{basin}$, $Area_{fallow}$, $Area_{stubble}$, and $Area_{grassland}$ are area of basin, fallow field, stubble field, and grassland, respectively. The definition of these HRUs within a basin permits consideration of effects due to variable contributing area – HRUs are only part of the contributing area for streamflow when they produce surface runoff.

5.1.1.2 Model Evaluation

The simulated snow accumulation was compared to field observations of snow depth and density in Bad Lake Research Basin taken during period of January - April 1982. With no calibration of parameters from streamflow observations, the simulated total streamflow discharge during snowmelt period was tested against cumulative streamflow discharge in the snowmelt

Table 5.1 Characteristics of major module parameters at Creighton Tributary. These parameters are used for three HRUs (fallow field, stubble field, and grassland coulee) to test model in both 1974-75 and 1981-82.

HRU Name	Area (km^2)	Soil Type	Fall Soil Moisture (m^3 water/m^3 soil)	Porosity (ratio)	Vegetation Height (m)	Blowing Snow Fetch Distance (m)	Routing Lag (hour)	Routing Storage (day)
Fallow Field	3.58	Clay Loam	0.23	0.5	0.05	1500	8	1
Stubble Field	6.13	Clay Loam	0.27	0.5	0.2	2000	8	1
Grassland	1.68	Clay Loam	0.22	0.5	0.25	2000	3	0.5

period in the spring of 1975. For the snow accumulation simulations (1981-82) only fetch length and vegetation height were important to the simulation and these were recorded from field observations made at the time. For the basin discharge simulation (1974-75), parameters observed and reported by Gray *et al.* (1985) or noted in field observations at the time were used and are listed in Table 5.1. Porosity was determined from soil type and values recommended by Dingman (1994). Blowing snow fetch distance was decided from maps and contemporary aerial photographs of the area. The method to estimate routing lag and storage was discussed by the Division of Hydrology (1977) in evaluating the U.S. National Water Service River Forecast System and their values were chosen based on the HRU size and shape and landform type. The fetch length and vegetation heights in 1981-82 were similar to that in 1974-75.

Two statistical measures, the Nash-Sutcliffe coefficient (NS) (Nash and Sutcliffe, 1970) and Model Bias (MB) were used to evaluate the performance of CRHM in simulating snow accumulation over the winter and streamflow discharge. NS and MB were calculated as,

$$NS = 1 - \frac{\sum (X_o - X_s)^2}{\sum (X_o - \overline{X_o})^2} \qquad [5.3]$$

$$MB = \frac{\sum X_s}{\sum X_o} - 1 \qquad [5.4]$$

where X_o, X_s, and $\overline{X_o}$ are the observed, simulated, and mean of the observed values, respectively.

5.1.2 Results

The values of 28 snow depth and density surveys on fallow and stubble fields were compared to simulated snow accumulation from CRHM for January - April 1982 (Figure 5.1). They show that the difference in snow accumulation between fallow and stubble field was well simulated over the accumulation and pre-melt period. Higher accumulation developed on the stubble fields due to erosion and redistribution of snow from the fallow fields as blowing snow. The correct simulation of both the source (fallow) and sink (stubble) areas suggests that both transport and sublimation of blowing snow are correctly estimated (Pomeroy *et al.*, 1998). In the spring of 1975 the simulated streamflow discharge (all of Creighton Tributary) due to snowmelt runoff was earlier than that observed by about 2 days, and somewhat greater discharge (53 mm) was predicted by the simulation compared to the measurement (45 mm), however the cumulative discharge curves are very similar and the timing of rapid discharge was correct (Figure 5.2).

To quantify differences between observation and simulation, both Nash-Sutcliffe coefficient (NS) and Model Bias (MB) were calculated for fallow and stubble snow accumulation, and cumulative streamflow discharge during snowmelt (Figure 5.1 and Figure 5.2). The NS for snow accumulation of fallow and stubble fields, and cumulative streamflow discharge were 0.60, 0.75, and 0.90, respectively. This indicates that CRHM performed fairly well in predicting the timing of snow accumulation and very well in predicting

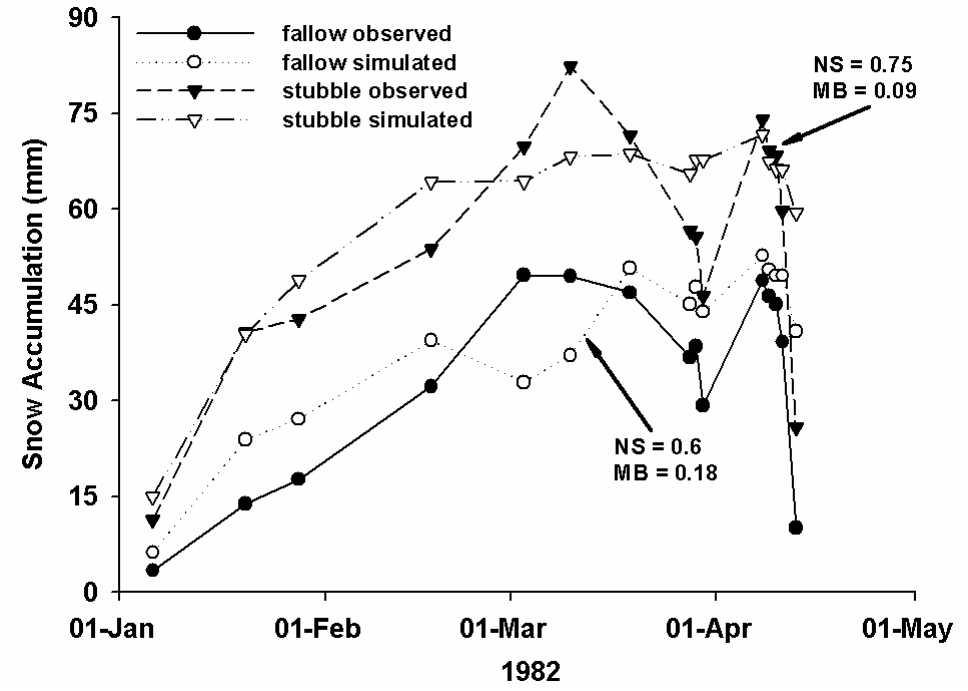

Figure 5.1 CRHM evaluation of snow accumulation in fallow and stubble field at Bad Lake during the winter of 1981-82.

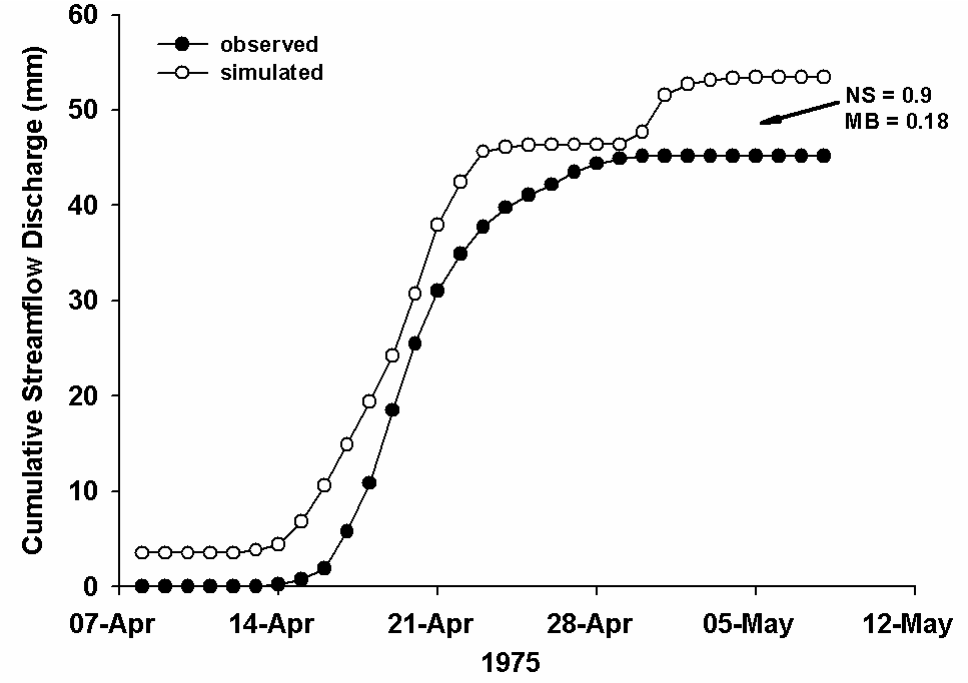

Figure 5.2 CRHM evaluation of cumulative streamflow discharge for Creighton Tributary of Bad Lake, spring 1975.

the timing of streamflow discharge due to snowmelt. Relatively small values of MB, 0.18 for both fallow snow accumulation and streamflow discharge, and 0.09 for stubble snow accumulation, represent an 18% overestimation of fallow snow accumulation and streamflow discharge and 9% overestimation of stubble snow accumulation. This implies a reasonable ability of CRHM to estimate snow accumulation in windblown prairie fields and streamflow discharge due to snowmelt over frozen soils without calibration of parameters. No calibration of parameters was attempted from the results of these comparisons, but it is presumed that the simulated hydrograph could be made to more closely mimic the observed hydrograph shape with calibration of the lag and storage parameters of the Clark unit hydrograph module.

5.1.3 Discussion

The snowmelt runoff modelling scheme in CRHM used the spatially aggregated approach. It carried out the calculations on aggregated landscape units, HRUs, by breaking down the basin into several HRUs with different properties responding to hydrological processes. The total streamflow discharge was an accumulation of the discharge resulting from snowmelt runoff on these HRUs. CRHM included all of the primary processes responsible for spring runoff generation in a prairie environment and assembled the corresponding modules in a system platform. It showed no

gross errors in calculating the water balance or interaction between HRU when compared to basin observations.

At Bad Lake, the hydrological winter seasons (November 1 to April 30) of 1974-75 and 1981-82 were both slightly colder and wetter than the 15-year (1971-1986) average: -6.3 ºC air temperature and 106 mm precipitation (Environment Canada, 2006a). The performance of CRHM when compared to diagnostic observations in these non-drought years is encouraging but does not guarantee its good performance in modelling the hydrology in drought. Any confidence in its performance under drought should be due to the physically-based modules. Bad Lake Research Basin was not operated during a severe drought and so it was not possible to test CRHM there in drought conditions. To address this, the model was set up and tested during drought years at another location; this is described in next section.

5.2 Model Derivation and Evaluation at St. Denis, Saskatchewan

5.2.1 Methods

5.2.1.1 Model Derivation

CRHM was used to estimate the water balance during winter and spring period for the basin of Wetland 109, St. Denis NWA as shown in Figure 3.1(d). The same set of physically-based modules as for the Creighton Tributary was assembled in the CRHM to simulate the surface snowmelt runoff. Full schematics of the modules for simulation of snow hydrology are

shown in Appendix G.

The estimation of snowmelt runoff was based on the Equation [5.1]. Two HRUs (cultivated field and wetland) are essential for the estimations (Table 5.2). The cultivated field HRU is the contributing area for the surface snowmelt runoff and the wetland HRU is where the runoff water accumulates. The estimations of redistribution of snow accumulation (SWE) by wind, snowmelt rate, cumulative snowmelt, cumulative snowmelt infiltration into unsaturated frozen soils, evaporation, and snowmelt runoff for the basin of Wetland 109 were based on the area-weighted approach as,

$$X_{basin} = X_{cultivated} \frac{Area_{cultivated}}{Area_{basin}} + X_{wetland} \frac{Area_{wetland}}{Area_{basin}} \quad [5.5]$$

where X_{basin}, $X_{cultivated}$, and $X_{wetland}$ are the estimated values of these variables for the basin, cultivated field, and wetland, respectively; all terms are in mm of water equivalent; $Area_{basin}$, $Area_{cultivated}$, and $Area_{wetland}$ are the areas of the basin, cultivated field, and wetland, respectively.

5.2.1.2 Model Evaluation

The simulated total pre-melt snow accumulation was tested against the field observations in the springs of 2000, 2001, 2003 and 2006. The observed total snow accumulation was derived from the snow depth and density surveys along the two transects (north-south and east-west) across the Wetland 109 (van der Kamp *et al.*, 2006a). The simulated total snowmelt runoff in the basin was tested against the observed water runoff in the springs of 2000 and 2001.

The observed snowmelt runoff was estimated based on the values reported by Hayashi *et al.* (2003) and van der Kamp *et al.* (2003).

For the snow accumulation simulations (1999-2000, 2000-01, 2002-03 and 2005-06), blowing snow fetch length and vegetation height were essential to the simulation. The fetch length can expand outside of the basin boundary; it was determined by the aerial photographs and maps of the basin and was examined in the field observations. The value for the fetch length was presumed constant for the same type of land cover over time. The vegetation cover and height information during 1999-2003 was reported by van der Kamp *et al.* (2006a), while information for 2005-06 was derived from the field survey in the fall of 2005. For the snowmelt runoff simulations (springs of 2000 and 2001), parameters observed at the time of field observations are listed in Table 5.2. The volumetric fall soil moisture was determined from the field observations by Hayashi *et al.* (2003) and van der Kamp *et al.* (2003). Porosity was estimated from the soil core samples by gravimetric method in the fall of 2005 and was assumed to have similar values for the falls of 1999 and 2000. The values presented in Table 5.2 fall in the porosity range for the clay loam soil texture reported by Dingman (1994). The method to estimate routing lag and storage was discussed by the Division of Hydrology (1977) the values were chosen based on the HRU size and shape and landform type. The routing lag and storage used here are not for the purpose of fitting hydrographs but rather for estimating the cumulative snowmelt runoff to the

Table 5.2 Characteristics of major module parameters for estimating snowmelt runoff at the Wetland 109. These parameters are used for two HRUs (cultivated field and wetland) to test model in 1999-2000, 2000-01, 2002-03 and 2005-06. Methods used for collecting and determining these parameters are described in Appendix C.

HRU Name	Area (km^2)	Soil Type	Fall Soil Moisture (m^3 water/m^3 soil)	Porosity (ratio)	Vegetation Height (m)	Blowing Snow Fetch Distance (m)	Routing Lag (hour)	Routing Storage (day)
1999 – 2000			Fall 1999					
Cultivated (stubble)	0.01601	Clay Loam	0.21	0.48	0.3	300	8	1
Wetland	0.00412	Clay Loam	0.23	0.54	5	300	0	0
2000 – 2001			Fall 2000					
Cultivated (stubble)	0.01601	Clay Loam	0.19	0.48	0.1	300	8	1
Wetland	0.00412	Clay Loam	0.22	0.54	5	300	0	0
2002 – 2003			Fall 2002					
Cultivated (fallow)	0.01601	Clay Loam	0.19	0.48	0.001	300	8	1
Wetland	0.00412	Clay Loam	0.22	0.54	5	300	0	0
2005 – 2006			Fall 2005					
Cultivated (stubble)	0.01601	Clay Loam	0.27	0.48	0.2	300	8	1
Wetland	0.00412	Clay Loam	0.32	0.54	5	300	0	0

wetland.

The Model Bias (MB) calculated based on Equation [5.4] was used to evaluate the performance of CRHM in estimating the total end of winter snow accumulation and cumulative snowmelt runoff.

5.2.2 Results

5.2.2.1 Pre-melt Snow Accumulation Test

The values of observed total pre-melt snow accumulation were derived from snow depth and density surveys at the Wetland 109 and compared to the simulated pre-melt snow accumulation for springs of 2000, 2001, 2003 and 2006 (Table 5.3). The simulated pre-melt SWE was close to the observation on the cultivated fields (source area) and wetland (sink area) for the spring of 2000. The simulations of both source and sink areas were generally in accordance with the observations for the springs of 2001, 2003, and 2006. This implies that both transport and sublimation of blowing snow were correctly simulated for springs of above years.

The cumulative pre-melt SWE for the basin was estimated from the cultivated field and wetland according to Equation [5.5] and the statistical indicator Model Bias (MB) calculated by Equation [5.4] was also calculated to quantify the differences between observation and simulation (Table 5.3). The values of MB were 0.04 and 0.06 for the springs of 2000 and 2003, respectively, representing an overestimation of 1.2 mm and 3.6 mm pre-melt

Table 5.3 CRHM evaluation of snow accumulation at St. Denis. Pre-melt snow accumulation test at the Wetland 109 for springs of 2000, 2001, 2003 and 2006.

Year	Snowfall (mm)	Observed Pre-melt SWE (mm)			Simulated Pre-melt SWE (mm)			Model Bias (MB)		
		Cultivated	Wetland	Basin	Cultivated	Wetland	Basin	Cultivated	Wetland	Basin
2000	35.2 (Feb 22)	30.9	32.4	30.9 (Feb 26)	32.4	31.2	32.1 (Feb 22)	0.05	-0.04	0.04
2001	39.8 (Mar 1)	49.1	57.4	49.1 (Mar 2-3)	38.7	46.7	40.3 (Mar 1)	-0.21	-0.19	-0.18
2003	66.8 (Mar 15)	57.1	86.7	63.1 (Mar 14)	57.7	101.9	66.1 (Mar 15)	0.01	0.18	0.06
2006	96.7 (Mar 27)	90.6	155.2	103.8 (Mar 23)	86.6	111.1	91.6 (Mar 27)	-0.04	-0.27	-0.12

Note: The date in the brackets indicates when the total snowfall, total observed and simulated pre-melt SWE are up to.

SWE for 2000 and 2003. This suggests that CRHM performed well in predicting the cumulative pre-melt snow accumulation due to wind redistribution for these two years. Values of MB, -0.18 and -0.12 for 2001 and 2006 indicates that an underestimation of 8 mm and 12 mm pre-melt SWE for 2001 and 2006. This suggests only moderate discrepancies to observations of pre-melt SWE for these years, which fall within the accuracy range of snow accumulation estimates from the blowing snow models discussed in the previous chapter.

There were total snow accumulations of 0 mm, 1.4 mm, 9.3 mm and 5.2 mm transported by blowing snow into the basin of the Wetland 109 in the hydrological winter seasons of 1999-2000, 2000-01, 2002-03, and 2005-06, respectively (Table 5.4). This indicates that CRHM has capacity of capturing the redistribution of snow by wind from outside of the basin boundary and confirms that the snow mass balance calculations in CRHM are not confined by the basin boundary.

Table 5.4 CRHM blowing snow estimations for the basin gain and loss.

Year	Total Basin Loss of Blowing Snow (mm)	Total Basin Gain of Blowing Snow (mm)	Net Gain of Blowing Snow (mm)
1999-2000	0	0	0
2000-01	0	1.4	1.4
2002-03	0	9.3	9.3
2005-06	0	5.2	5.2

5.2.2.2 Snowmelt Runoff Test

The cumulative snowmelt runoff to the Wetland 109 was simulated and compared the observed total runoff from snowmelt at the end of March in 2000 and 2001 (Table 5.5). For the simulation of snowmelt runoff at the end of March 2000, 14.9 mm of surface runoff was estimated, which is comparable with the observed snowmelt runoff. A moderate value of the Model Bias (MB), -0.17, represents an underestimation of 3 mm for the surface runoff from melting water.

Large differences were found between the observed and simulated snowmelt runoff at the end of March 2001 (Table 5.5). With similar values of fall soil moisture in 1999 and 2000 and similar values of pre-melt SWE in 2000 and 2001, the amount of snowmelt runoff at the end of March should be similar between 2000 and 2001 (Hayashi *et al.*, 2003). This is shown in Table 5.5; modelled snowmelt runoff is comparable between 2000 and 2001, 14.9 mm and 18.1 mm, respectively. However, much lower snowmelt runoff was observed in 2001. This could be related to formation of macropores or cracks in the area, which is attributed to the shrinkage of high clayey content soil during a long drying period (Hillel, 2004). Previous studies at St. Denis showed that the formation of macropores enhanced the soil infiltrability and resulted in drying-out of wetlands (van der Kamp *et al.*, 2003; Bodhinayake and Si, 2004).

The fall soil moisture in 2000 shown in Table 5.2 only describes the water content of soil and is not pertinent to infiltration in the case of

Table 5.5 CRHM evaluation of snowmelt runoff at St. Denis. Cumulative snowmelt runoff test at the Wetland 109 at the end of March in 2000 and 2001.

Year	Observed Snowmelt Runoff (mm)	Simulated Snowmelt Runoff (mm)	MB
2000	18.0	14.9	-0.17
2001	3.0	18.1	4.9

macropores in which infiltration becomes unlimited (Gray *et al*., 1985). In response, a new snowmelt runoff simulation was set up in CRHM setting unlimited infiltration for both the cultivated fields and wetland area (Table 5.6). Due to the formation of macropores under continuous cropping practices following a hot and dry growing season, more meltwater infiltrates into soils in the cultivated field, leading to much less surface runoff, approximately 3.6 mm from the contributing area to the wetland. No surface runoff was generated in the wetland where macropore development resulted in unlimited soil infiltrability, allowing all melting water to infiltrate into soils (Granger *et al.*, 1984; Gray *et al.*, 1985; 1986; 2001). Thus, the simulated snowmelt runoff

Table 5.6 CRHM snowmelt runoff simulation corresponding to the formation of macropores.

Year	Fall Soil Moisture (Volumetric Ratio)		Snowmelt Runoff (mm)		MB
	Cultivated	Wetland	Observed	Simulated	
2000-01	***0.19***	***0.22***	3.0	***18.1***	***4.9***
2000-01	*	*	3.0	3.6	0.19

Note: The italic bold represents the values of parameters and simulation for soils with no development of macropores.

Note: * indicates the soil with unlimited infiltrability.

was about 3.6 mm for the entire basin, and this is very comparable to the observation.

5.2.3 Discussion

The performance of CRHM in simulating snow accumulation during winter accumulation period and snowmelt runoff during melting period when compared to observations was very promising during the drought years (1999-2000 and 2001-02). It also performed well in estimating winter snow accumulation during non-drought years (2002-03 and 2005-06). This is likely due to the use of physically-based modules that allowed the comprehensive estimation of the primary processes for runoff generation in springtime.

The same spatially aggregated approach used in estimation of snowmelt runoff at Creighton Tributary of Bad Lake was applied in the simulation of melt runoff of the basin of Wetland 109, St. Denis. Compared to the basin of Creighton Tributary, the basin of Wetland 109 is a typical internally-drained prairie depression or pothole, resulting in poorly-drained basin. A runoff contributing area HRU (cultivated field) and a runoff accumulating area HRU (wetland) were used to estimate basin surface runoff. There are other small depressions in the vicinity of the basin; during dry years, runoff stays in these depressions without running into the central wetland, thus two HRUs (cultivated field and wetland) were sufficient for the simulating surface runoff from snowmelt at the Wetland 109. However, during wet years, the contributing area may expand and include these nearby small depressions

as runoff water exceeds their storage capacity (van der Kamp, 2006). The "fill and spill" process is common among these depressions and is critical to the delineation of basin drainage at St. Denis NWA, thus further studies are needed in order to improve understanding of water level changes in ponds and their estimation due to the surface snowmelt runoff, and discharge from pond to pond.

Throughout the evaluations of snowmelt runoff model at St. Denis, not only the variations of meteorological variables during droughts induced the change in hydrological processes responsible for the runoff generation, but the changing land use also contributed. Hence, further analysis is conducted next to address the combined effects of varying meteorology variables and land use on the water availability on Canadian Prairies during drought.

Chapter 6

6.0 Snow Hydrology Sensitivity Analysis to Drought on the Canadian Prairies

Droughts are natural hazards and frequently develop on the Canadian Prairies. Over half the years of three decades, 1910-1920, 1930-1939, and 1980-1989 were in drought (Nkemdirim and Weber, 1999) and the drought of 1999-2004 was the most recent one developed in parts of the Prairies (Bonsal and Wheaton, 2005). Droughts are characterized by lack of precipitation resulting in insufficient water supplies from surface and subsurface (Wilhite and Buchanan-Smith, 2005). Many Canadian prairie winter hydrological processes: blowing snow transport, blowing snow sublimation, snowmelt, snowmelt infiltration, and snowmelt runoff are sensitive to meteorological and hydrological changes during drought. Over 80% of annual runoff is derived from melt of snow on Canadian Prairies (Gray *et al.*, 1989). This surface meltwater runoff contributes to the water supplies in the prairie streams and wetlands that are vital resources to farmers and wildlife. This chapter examines the impacts of drought on these hydrological processes that control snowmelt runoff generation in two prairie basins: Creighton Tributary of Bad Lake and Wetland 109 at St. Denis NWA.

6.1 Synthetic Drought Impact at Bad Lake, Saskatchewan

The Bad Lake IHD research basin was operated during 1965-1986, but never under conditions of a severe drought. Synthetic drought scenarios were created to analyze the effects of drought on the snowmelt runoff-related processes at the Creighton Tributary of Bad Lake.

6.1.1 Methods

6.1.1.1 Drought Sensitivity of Winter Hydrology to Individual Parameters

A sensitivity analysis to drought was conducted to identify the influence of individual components of meteorological, soil and vegetation condition changes during drought on snowmelt runoff and its related processes. Observations at the Bad Lake IHD meteorological station from the hydrological winter (November 1-April 30) of 1974-1975 were used to drive the CRHM drought simulation runs (Figure 6.1). The soil and vegetation conditions observed at the Bad Lake basin during the same winter were also used in the simulation runs (Table 6.1). The hydrological winter of 1974-1975 was slightly colder and wetter than "average" with a mean temperature and total winter precipitation of -7 ºC and 129 mm, respectively. The 15-year (1971-1986) average temperature and precipitation (rainfall and snowfall) during the hydrological winter for the Bad Lake basin are -6.3 ºC and 106 mm, respectively (Environment Canada, 2006a). Thus, the winter of 1974-1975 was regarded as 'near-normal' in the synthetic drought scenarios.

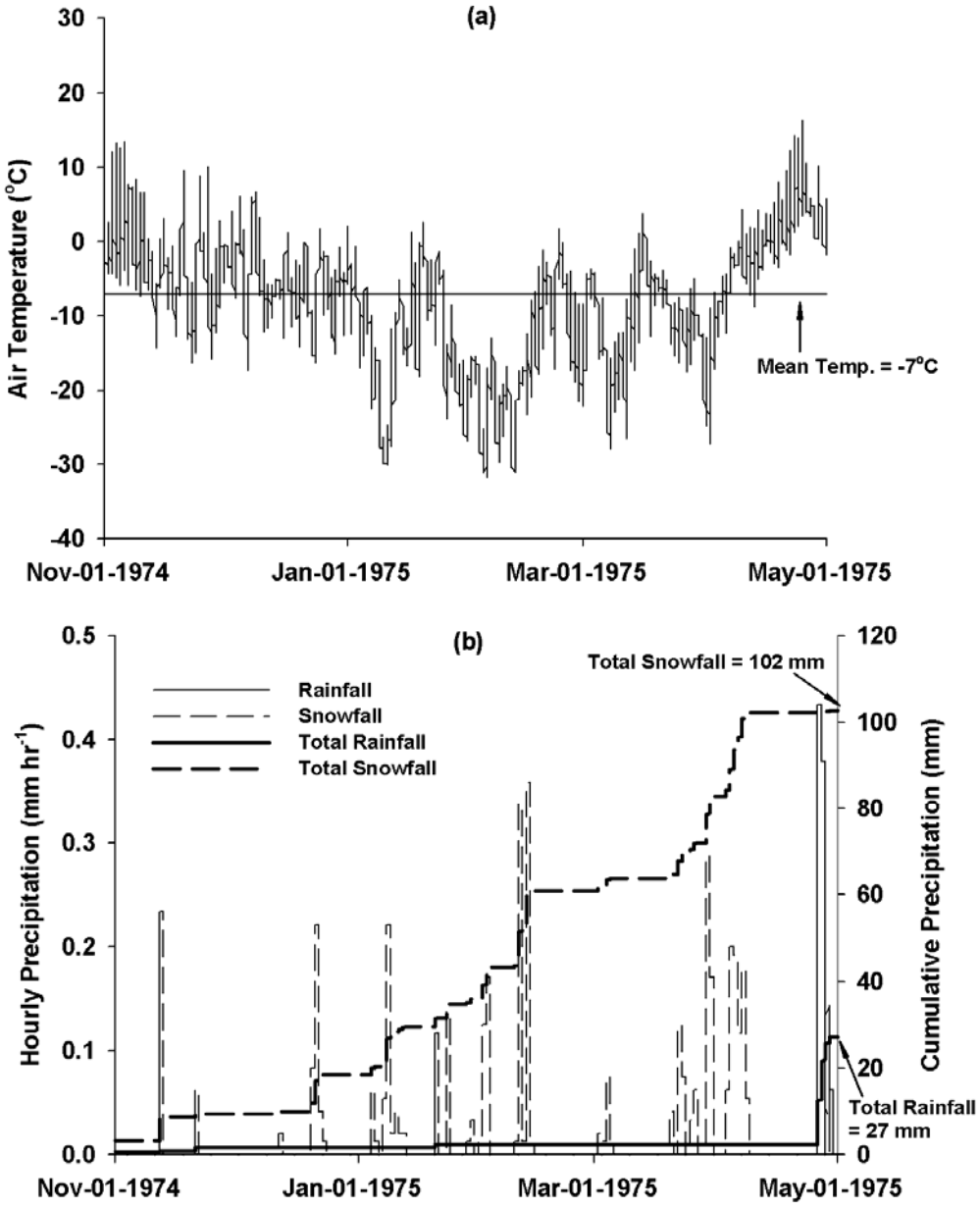

Figure 6.1 Meteorological observations in the 'normal' hydrological winter of 1974-75 at Creighton Tributary of Bad Lake. (a) air temperature, (b) precipitation as rainfall or snowfall.

To create drought scenarios, precipitation and air temperature from observed meteorological data were adjusted from observed values during the

period: November 1 1974 – April 30 1975. Fall soil moisture content and vegetation height were changed as well. 10 drought scenarios were generated by altering one observation variable or module parameter at a time whilst holding other observation variables and module parameters constant in CRHM (Table 6.2).

Table 6.1 Observed soil and vegetation conditions in the 'normal' hydrological winter of 1974-75 for three HRUs (fallow field, stubble field, and grassland coulee) at Creighton Tributary of Bad Lake.

HRU Name	Area (km^2)	Fall Soil Moisture (m^3 water/m^3 soil)	Vegetation Height (m)
Fallow Field	3.58	0.23	0.05
Stubble Field	6.13	0.27	0.20
Grassland	1.68	0.22	0.25

Table 6.2 Drought scenarios in the CRHM simulation runs.

Model Run #	Description	Model Run #	Description
1	15% decrease in winter precipitation	6	5ºC rise in winter air temperature
2	30% decrease in winter precipitation	7	25% decrease in fall volumetric soil moisture
3	50% decrease in winter precipitation	8	50% decrease in fall volumetric soil moisture
4	1ºC rise in winter air temperature	9	50% decrease in vegetation height
5	2.5ºC rise in winter air temperature	10	90% decrease in vegetation height

6.1.1.2 Prairie Hydrological Drought Progression

To examine the combined impacts of major changes in meteorology, soils, and land covers on hydrological processes and snowmelt runoff during a drought, a simplified, synthetic 'prairie hydrological drought progression' was established from the general sequence of changes in precipitation, temperature, soil moisture and vegetation that was noted during the recent drought of 1999-2004, and in previous prairie droughts (Maybank *et al.*, 1995; Nkemdirim and Weber, 1999; Wheaton *et al.*, 2005; Environment Canada, 2006b). The synthetic hydrological drought progression was also informed by winter progressions of temperature and precipitation observed at nearby Rosetown during the recent droughts of 1986-89 and 1999-2004 (Environment Canada, 2006a). They show lower winter precipitation and sometimes higher air temperatures than the long term average (Figure 6.2).

The synthetic scenarios were used to adjust CRHM parameters (soil moisture, vegetation height) or variable inputs (precipitation, temperature) in a sequence that started with no drought (Hydrological Winter 1) then a winter meteorological drought (Hydrological Winter 2), then the effects of summer drought on winter drought (Hydrological Winter 3), then the recovery from winter meteorological drought but with antecedent conditions still in drought (Hydrological Winter 4), then recovery of summer crop growing conditions, fall soil moisture and winter meteorology, but not native vegetation heights (Hydrological Winter 5). The progression is fully quantified in Table 6.3 and is summarized as follows:

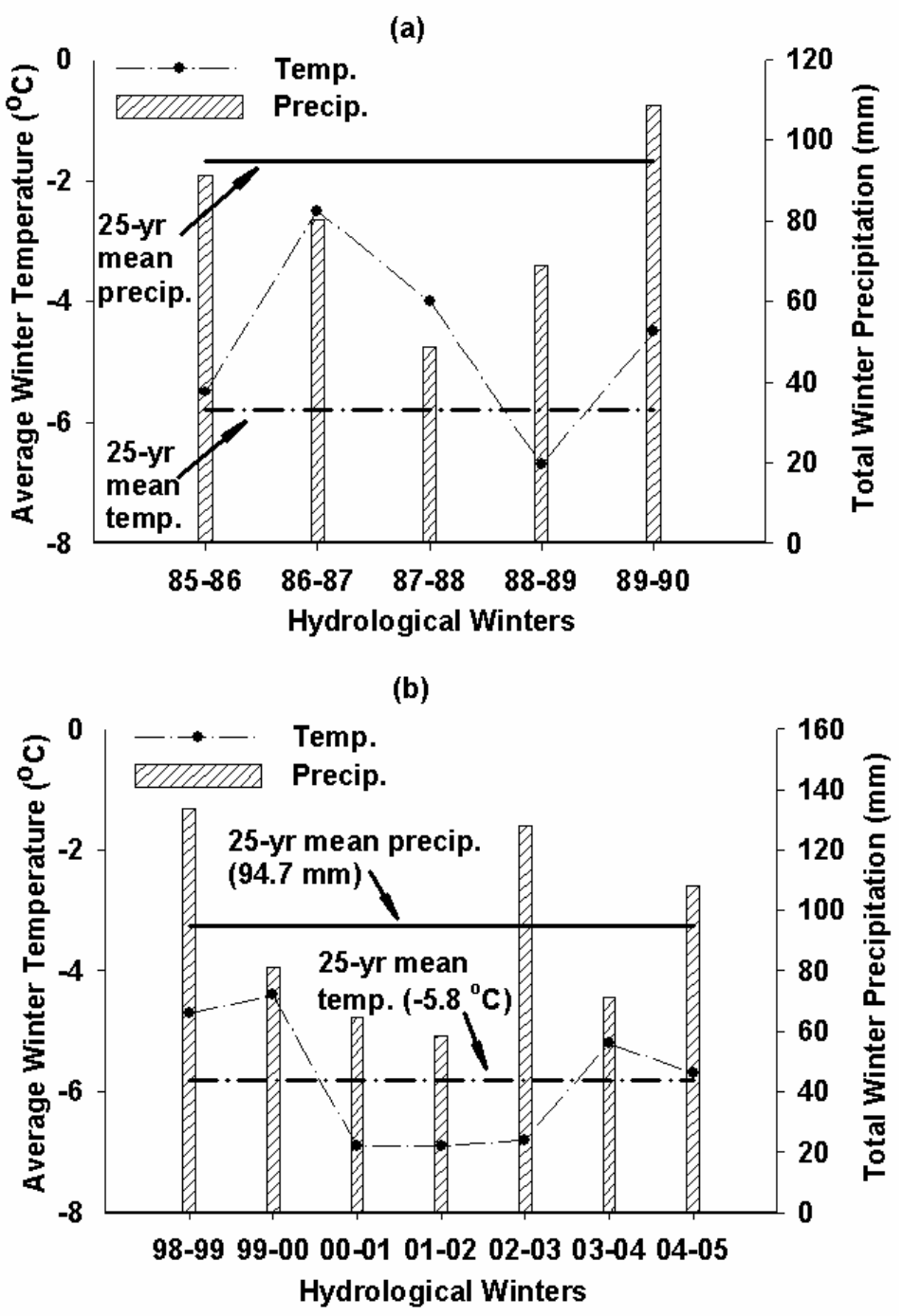

Figure 6.2 Average winter temperature and total winter precipitation (rainfall and snowfall) observed in Rosetown, Saskatchewan. during hydrological winters. (a) 1985-1990, (b) 1998-2005 with 25-year (1981-2005) hydrological winter temperature and precipitation normals (Environment Canada, 2006a).

Table 6.3 Parameters and changes in input variables for a hypothetical 'prairie hydrological drought progression'.

Drought Sequence	Fall Volumetric Soil Moisture	Vegetation Height (m)	Winter Precipitation	Winter Temperature (ºC)
Hydrological Winter 1 'normal'	normal	normal	normal	normal
Hydrological Winter 2 'severe'	normal	normal	-15%	+2.5
Hydrological Winter 3 'severe'	-45%	-60%	-30%	+2.5
Hydrological Winter 4 'recovery'	-45%	-60%	normal	normal
Hydrological Winter 5 'recovery'	normal	-35%	normal	normal

Before a drought:

Hydrological Winter 1, Normal: No drought, fall conditions shown in Table 6.1 for typical for non-drought years at Bad Lake were used (early 1970s) and the 1974-75 meteorological sequence shown in Figure 6.1 was used.

Going into a drought:

Hydrological Winter 2, Severe Winter Drought: fall soil moisture is normal and vegetation is tall, but precipitation is lower and temperature is higher over the winter. This is the first winter of meteorological drought.

Hydrological Winter 3, Severe Multi-seasonal Drought: fall soil moisture is low, vegetation is short (poor crops the previous summer reduced stubble and 'trash' on fields and native vegetation is becoming sparser), precipitation is lower, and temperatures are higher over the winter. This is the peak of the

meteorological drought which has been continuous over the previous summer and fall and extends into winter.

Coming out of a drought:

Hydrological Winter 4, Winter Recovery: fall soil moisture is low and vegetation is short, but precipitation and temperature have recovered to normal winter values. The meteorological drought is 'broken' with a return to non-drought winter meteorology; however antecedent conditions remain affected by the drought.

Hydrological Winter 5, Multi-seasonal Recovery: fall soil moisture is high, precipitation and temperature are normal over the winter but natural vegetation remains low. The meteorological drought ended the previous year and now soil moisture and cropped vegetation heights have also recovered, however native vegetation heights remain short and sparse.

6.1.2 Results

6.1.2.1 Drought Sensitivity of Winter Hydrology to Individual Parameters

Snow accumulation after wind redistribution, blowing snow sublimation, snow cover duration, evaporation, and infiltration as well as surface runoff from snowmelt were estimated from CRHM for each HRU corresponding to each of the 10 drought scenarios (lower precipitation, higher air temperature, lower soil moisture content and shorter vegetation) shown in Table 6.2. The responses of these snowmelt runoff-related processes to changes in individual parameters in the 10 drought scenarios were examined

for whole basin based on the area-weighted responses in each HRU (Figure 6.3).

Figure 6.3 shows that the basin snow accumulation after wind redistribution (pre-melt SWE) was mainly sensitive to the amount of precipitation and less to air temperature and vegetation height, and showed no sensitivity to changes in soil moisture. The decline of the basin snow accumulation with decreasing precipitation was not linear. The rate of decrease in the basin snow accumulation increased as precipitation declined. This is related to suppression of blowing snow and snow drift formation in taller vegetation area (i.e. grassland HRU). The basin snow accumulation increased initially with rising air temperature and then decreased as the temperature warmed further (after increase by more than 2.5 ºC). This is attributed to the initial temperature increases contributing to icy and wet conditions which led to suppression of blowing snow in all fields (fallow, stubble, and grassland). As temperature increased a little more (e.g. > 2.5 ºC), the occurrence of winter rainfall increased and snowfall decreased, resulting in less snow accumulation. Basin snow accumulation decreased when vegetation height decreased. Decreasing vegetation height enhanced blowing snow and redistributed more snow from shorter vegetation area (fallow and stubble) to taller vegetation area (grassland) as a result, but overall basin snow accumulation diminished because the source areas (fallow and stubble) constitute over 85% of basin, resulting in more snow exported out of basin.

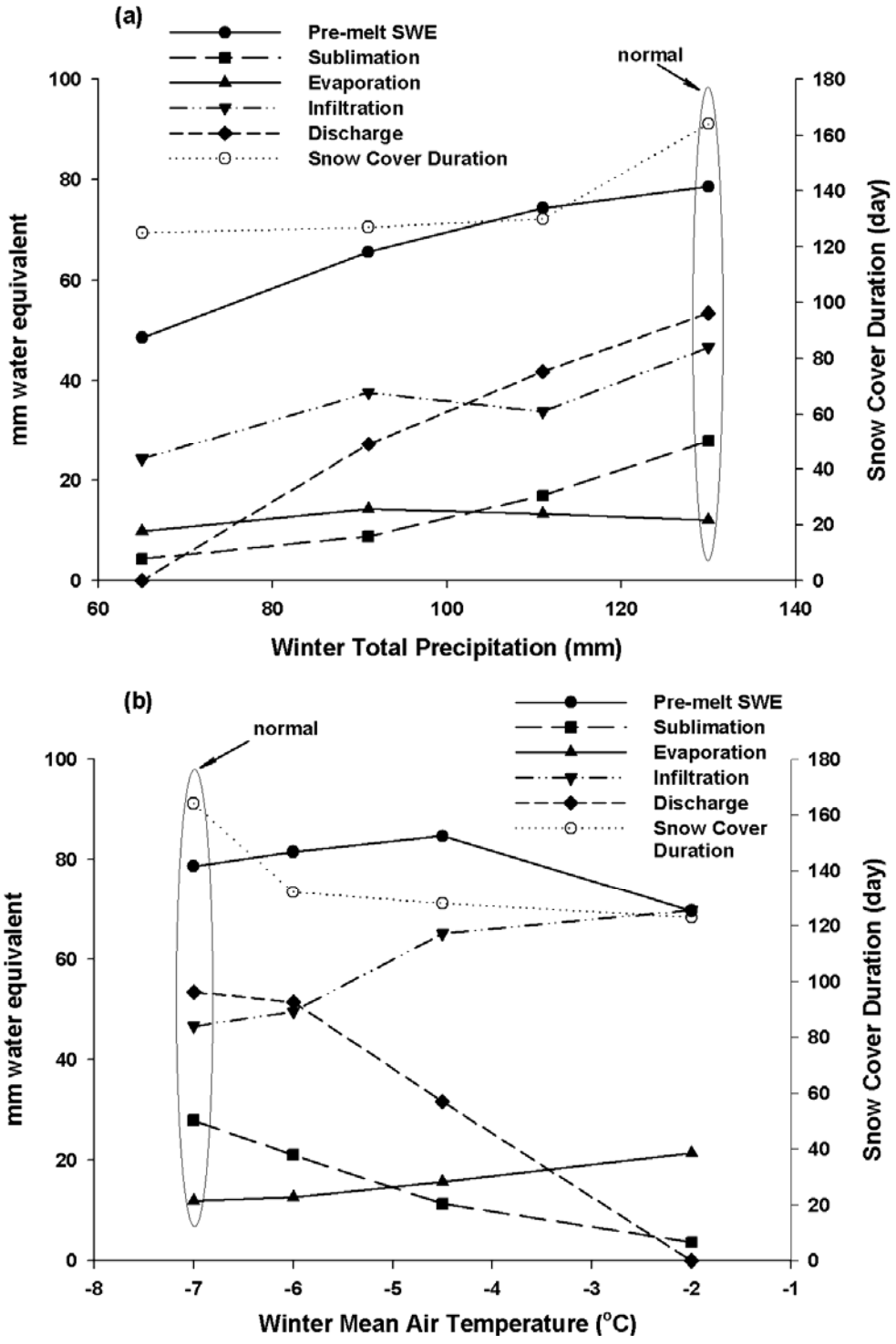

Figure 6.3 Simulated drought sensitivity of basin-wide snowmelt runoff-related processes to individual parameters. (a) precipitation, (b) mean air temperature, (c) initial (fall) volumetric soil moisture content, (d) vegetation height. 'normal' denotes the values during hydrological winter of 1974-75.

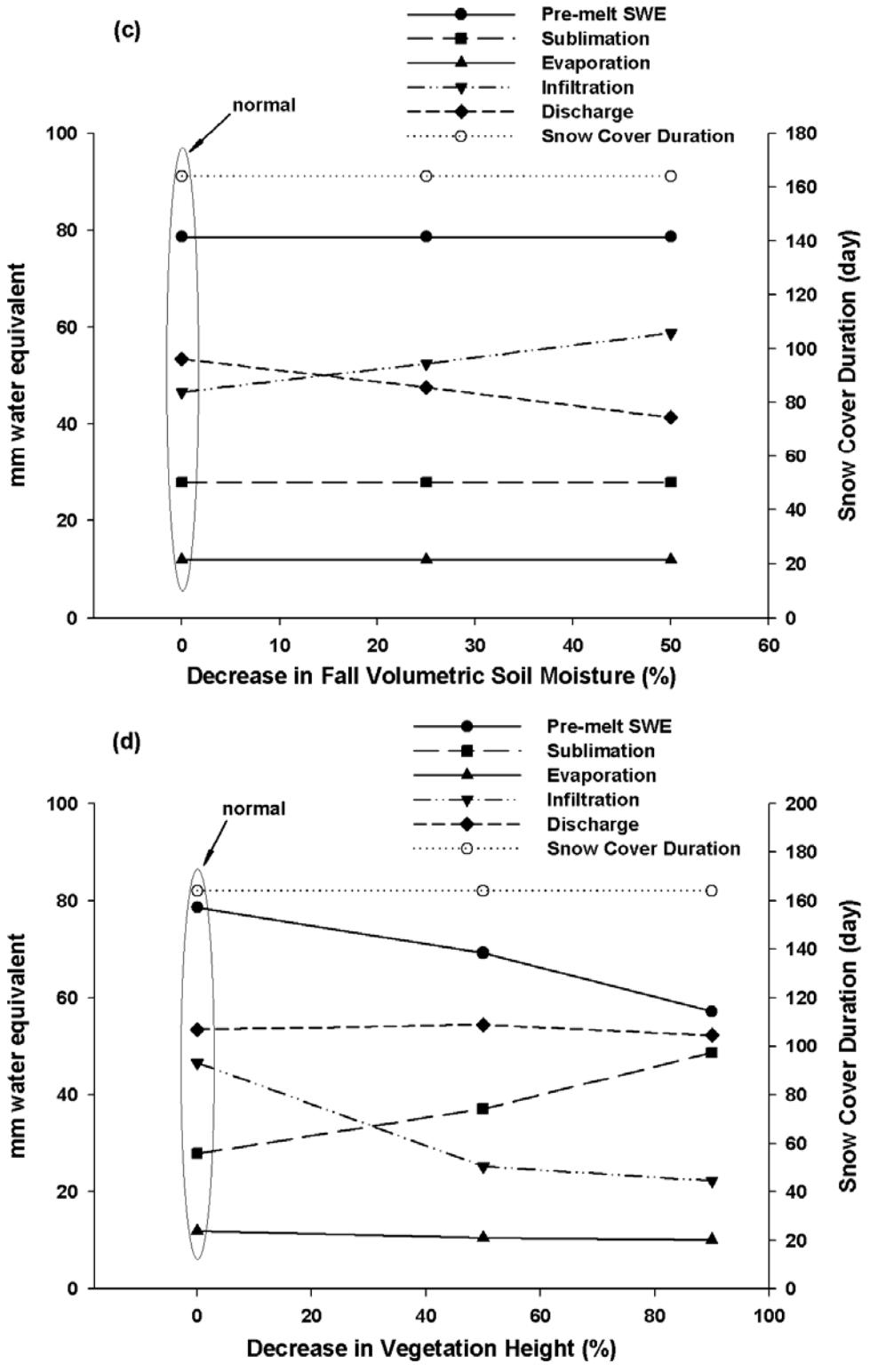

Figure 6.3 *Concluded*.

The basin blowing snow sublimation was sensitive to changing precipitation, air temperature and vegetation height and insensitive to changes in soil moisture (Figure 6.3). Blowing snow sublimation relies on the occurrence of blowing snow and undersaturated conditions in the atmosphere. The frequency of blowing snow declined as the precipitation decreased, which resulted in suppression of blowing snow sublimation. The basin sublimation of blowing snow decreased by more than 80% when the precipitation declined by 50%. The basin sublimation also decreased as air temperature increased, with decreases of more than 60% and 85% as the temperature rose by 2.5 ºC and 5 ºC, respectively. This implies that the influence of enhancing atmospheric undersaturation at warmer conditions was overcome by the suppression of blowing snow with higher temperatures. Basin sublimation almost doubled when vegetation heights declined by 90%. This is associated with a higher frequency of blowing snow with shorter vegetation covers.

The winter evaporation for the basin was insensitive to changes in soil moisture and vegetation height and somewhat sensitive to the precipitation and air temperature (Figure 6.3). Winter evaporation increased slightly with an initial drop in precipitation due to the shorter snow-covered season, but decreased as the precipitation was reduced by 50% resulting in the shortage of available water, which overwhelmed the effect of a longer period of bare surface to the evaporation. The reduced vegetation height contributed to lower snow accumulation and lower aerodynamic roughness height and thus decreased the winter evaporation for the shorter vegetation area (fallow and

stubble), but overall the basin winter evaporation responded little to the decreased vegetation height. The insensitivity of the winter evaporation to the initial fall soil moisture implies that the evaporation was not subject to the limitations of moisture supply provided that precipitation was normal.

Snow cover duration was very sensitive to precipitation and air temperature and showed no sensitivity to the soil moisture and vegetation height (Figure 6.3). Either the initial decrease in the precipitation by 15% or increase in air temperature by 1 ºC resulted in a sharp decline of snow-covered period from 165 to 125 days, but no further large decreases as precipitation declined or air temperature warmed. This is attributed to reduction in the length of winter, with the greatest effect on the shoulder seasons of early and late winter.

Infiltration was sensitive to changes in each of precipitation, air temperature, soil moisture, and vegetation height (Figure 6.3). The sensitivity was complex because infiltration is the combination of snowmelt infiltration to frozen soils and rainfall infiltration to unfrozen soils. Infiltration decreased as precipitation declined, with about a 50% decrease for a 50% decrease in precipitation. Infiltration increased by 45% as air temperature rose by 5 ºC. This was due to the winter precipitation shifting to rainfall with warmer conditions and then relatively rapid rainfall infiltration to unfrozen soils dominating over relatively slow snowmelt infiltration to frozen soils. Infiltration increased as initial fall soil moisture declined. This is consistent with Gray's theory for prairie snowmelt infiltration (Gray *et al.*, 1985).

Infiltration declined by 45% as vegetation height decreased by 50% due to decreased snow accumulation, but little decrease was found as vegetation height reduced further.

Snowmelt runoff from the different HRUs within the basin flowed to the deeply-incised coulee (grassland), discharging at the outlet of Creighton Tributary. The basin discharge showed dramatic responses to changes in precipitation and air temperature (Figure 6.3). Snowmelt runoff decreased almost linearly to zero when the precipitation decreased by 50% to 65 mm or when air temperature increased by 5 ºC to -2 ºC. The decline in discharge with declining precipitation was due to winter precipitation infiltrating and evaporating preferentially to forming surface runoff. The decline in discharge with increasing air temperature was due to the conversion of winter snowfall to rainfall, mid winter melting of the snowpack, greater infiltration into unfrozen soils and greater evaporation losses over the winter due to the shorter snow season. Discharge declined linearly with decreasing soil moisture as more melt water infiltrated. The response of discharge to the changes in vegetation height was within 1% to 2% of the original 'normal' discharge.

6.1.2.2 Prairie Hydrological Drought Progression

Major hydrological processes during the hydrological winter were simulated corresponding to the hypothetical prairie hydrological drought progression summarized in Table 6.3 and are shown in Figure 6.4. The figure shows that how typical combinations of meteorological, soil and land cover

conditions may progress during drought and also shows the response of each HRU to these conditions. Hydrological Winter 1 is the 'normal' winter with no drought; while Hydrological Winters 2 and 3 are progressively stronger 'severe drought' and Hydrological Winters 4 and 5 have progressively recovering state parameters ('recovery'). Figure 6.4(a) shows that snow accumulation dropped during the severe drought as results of rising temperature and decreasing precipitation. Interestingly, the grassland HRU had slightly less snow accumulation than on stubble HRU during the severe drought. This is due to the suppression of blowing snow redistribution to the grassland from the stubble. There was some snow redistribution from fallow to stubble, but not enough to "fill" the stubble. Figure 6.4(b) illustrates that the differences in snow-covered period among the HRUs became smaller in the severe drought period. Blowing snow sublimation was heavily suppressed during severe drought and only occurred in short vegetation area (fallow HRU); while it increased during the recovery period as precipitation and temperature returned to normal but vegetation still stayed short. Figure 6.4(d) shows that increasing winter evaporation in severe drought was more prominent in taller vegetation areas (stubble and grassland HRUs). For all HRUs, infiltration declined during the severe drought period, started to increase in the first recovery winter (Hydrological Winter 4) and returned to normal in the second year of recovery. It should be noted that changes in infiltration for grassland HRU were relatively small throughout the drought progression compared to other HRUs. Figure 6.4(f) shows that surface

snowmelt runoff entirely ceased for all HRUs in the severe drought period and almost recovered for fallow and stubble HRUs at the end of recovery period.

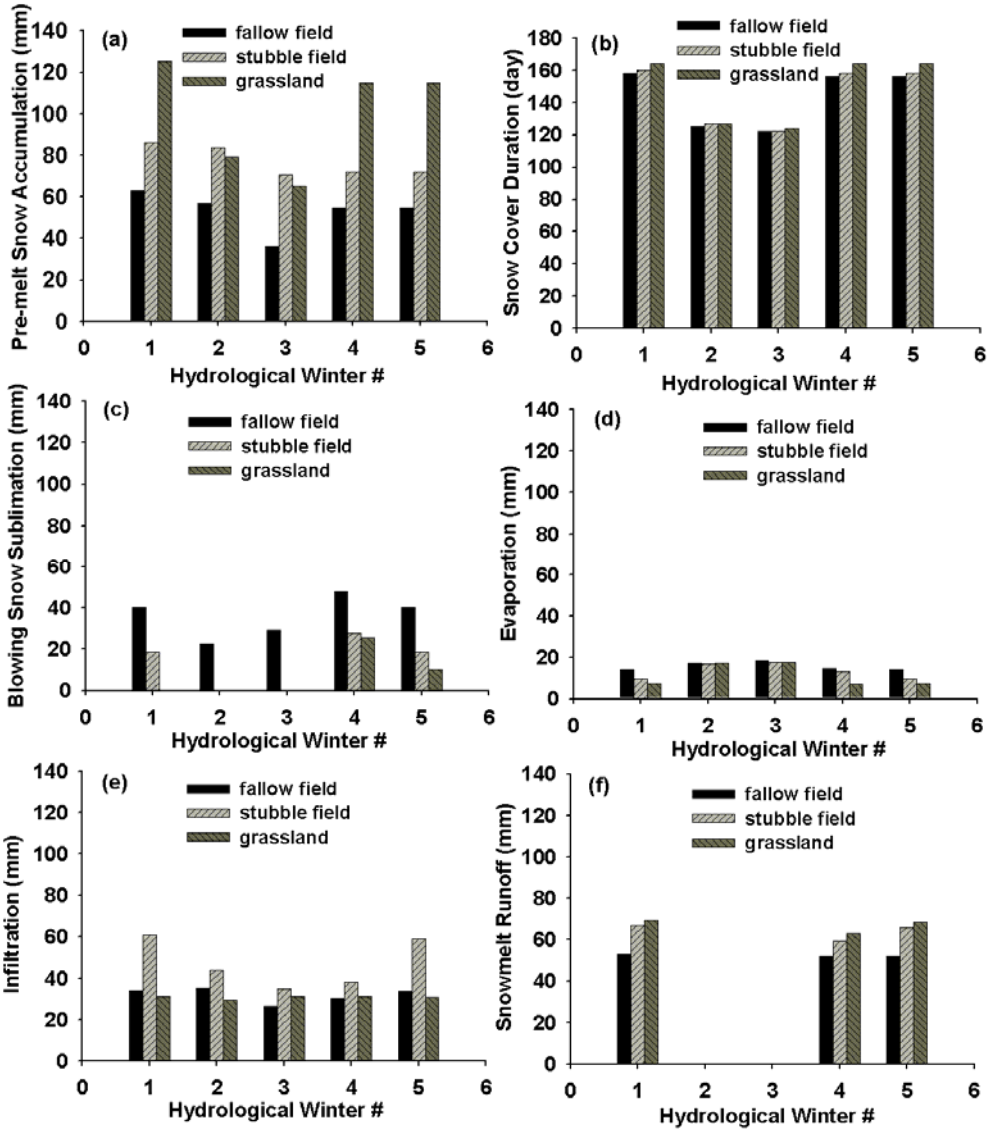

Figure 6.4 Simulated hydrological processes for individual HRU at Creighton Tributary in prairie winter hydrological drought progression. Changing processes from normal (hydrological winter 1) to severe drought (hydrological winter 2, 3) to recovery (hydrological winter 4, 5): (a) pre-melt snow accumulation (b) snow cover duration (c) blowing snow sublimation (d) evaporation (e) infiltration (f) snowmelt runoff.

The responses in hydrological processes to the combined conditions of meteorology, soil, and land cover in the prairie hydrological drought progression were estimated for Creighton Tributary basin based on the area-weighted response in each HRU (Figure 6.5). Sublimation of blowing snow was largely suppressed during severe drought, but it was enhanced during recovery when snowfall returned but vegetation heights remained low. As a result, even though snowfall returned to normal after the severe drought period, snow accumulation did not rebound until the very end of the recovery period when vegetation (stubble, some grass) had grown to its former height and density. Interestingly, rainfall declined only slightly during the severe drought as rising air temperatures increased the proportion of precipitation falling as rain and this compensated for the overall decrease in precipitation amount. A shorter snow-covered period developed in the severe drought due to the combined effects of lowered snowfall and higher temperature. Evaporation increased slightly during severe drought and somewhat during the first year of recovery (Hydrological Winter 4) but was not strongly affected by the drought progression. Infiltration was more strongly affected by drought and declined progressively through severe drought and started to bounce back during the recovery period. Basin streamflow discharge from the surface melting water runoff showed the greatest response to the drought progression, ceasing completely during the severe drought and not fully recovering until the end of the recovery period. The results show that although the winter meteorological drought only occupied Hydrological Winters 2 and

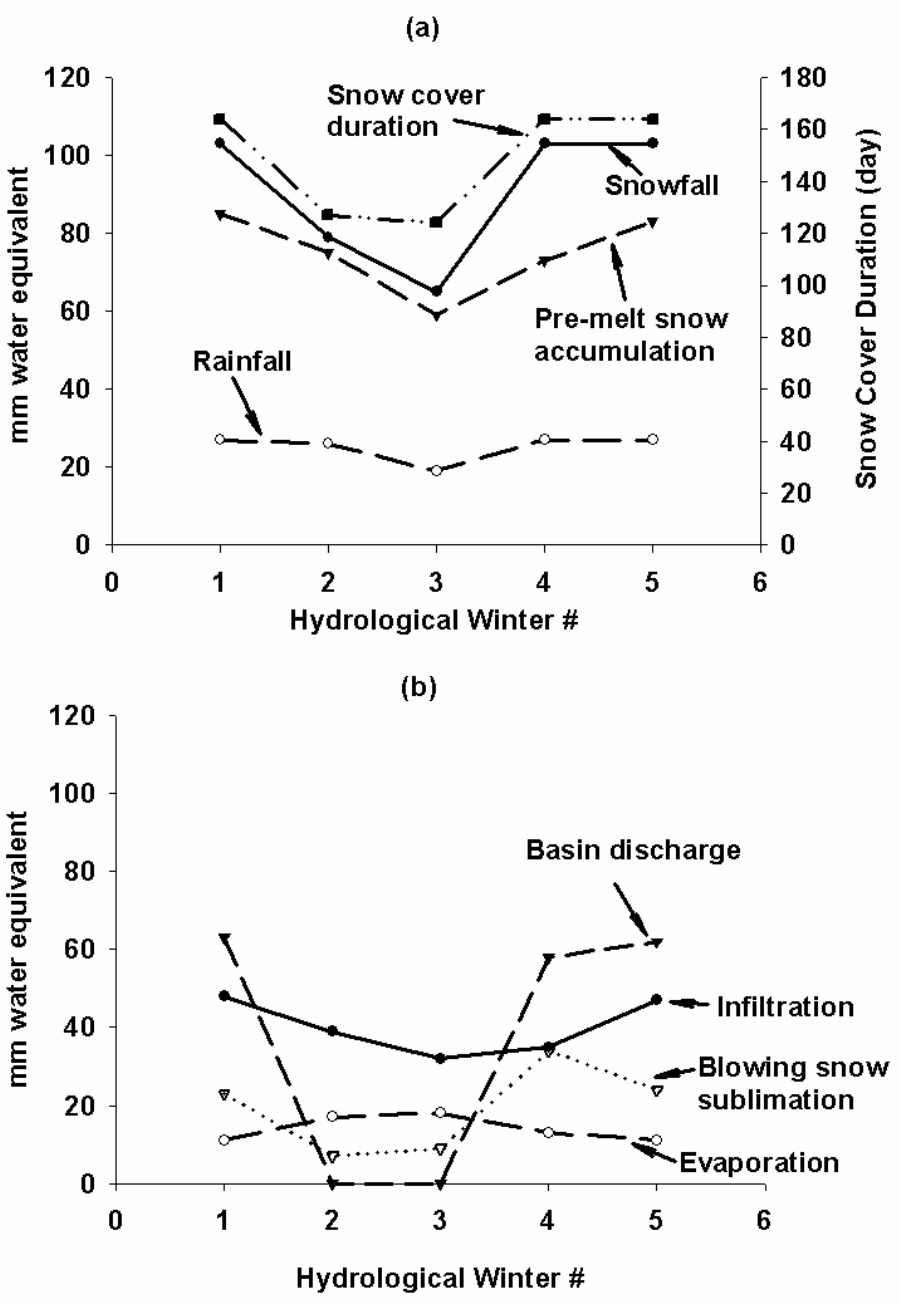

Figure 6.5 Simulated hydrological processes for Creighton Tributary basin in prairie winter hydrological drought progression. Changing processes from normal (hydrological winter 1) to severe drought (hydrological winter 2, 3) to recovery (hydrological winter 4, 5): (a) snowfall, rainfall, pre-melt snow accumulation, snow cover duration (b) blowing snow sublimation, evaporation, infiltration, basin discharge. It should be noted that lines connecting points among years are only for visual purpose and do not imply interpolation.

3, the system required two more winters for the hydrological drought to end. This shows that how the system responded to effect of summer drought on soil moisture storage and the growth cycle of crops and native vegetation.

6.1.3 Discussion

There are several interesting and somewhat non-intuitive results from the sensitivity of winter hydrology to the individual drought parameters. Snow accumulation was affected by the winter precipitation, air temperature and vegetation height but did not show a particularly strong sensitivity to any of them. This resilience was due to wind redistribution of snow being very sensitive to drought meteorology and more snowfall remaining on the ground during drought as a result of suppression of blowing snow by meteorological conditions in a drought. Winter evaporation did not show great enhancement with drought conditions and any increase in evaporation was more than balanced out by the decrease in blowing snow sublimation. No strong trend was found for infiltration in a drought because so many processes controlled the fluxes and offset each other for specific drought conditions. A shorter snow-covered period developed under drought meteorology and this resulted in earlier spring snowmelt runoff. Snowmelt runoff showed a dramatic decrease with drought meteorology and this was exacerbated by decreased soil moisture during drought. That snow accumulation was not strongly affected by drought but that snowmelt runoff can easily cease under typical drought meteorology and soil conditions has important implications. It indicates that

the prairie winter hydrological system magnifies the impact of drought in translating it to streamflow generation in springtime. This has severe implications for the prairie wetlands, ponds, lakes and the recharge of groundwater systems from these areas during drought. These implications have been described and confirmed by van der Kamp *et al.* (2003) and the mechanisms discussed by Hayashi *et al*. (2003).

The prairie drought progression scenario provides insight into the sequential development of drought and the hydrological impact when many meteorological variables and surface parameters vary in a consistent temporal pattern. The early suppression and then later amplification of blowing snow sublimation serves to reduce the variability of snow accumulation during a drought. The main effect of the synthetic drought is complete cessation of snowmelt runoff and streamflow discharge due to the combination of lower precipitation, warmer winter temperatures and drier soils. It should be noted that this combination does not always develop during a Canadian Prairie drought. The behaviour of streamflow discharge as a drought develops in this scenario is very non-linear, because all meteorological and surface factors work to diminish runoff generation at once. The observed departures from average conditions at Rosetown (Figure 6.2) show some association between decreased precipitation and decreased temperature during hydrological winter in the recent drought. Perhaps the synoptic patterns resulting in low precipitation also cause low temperatures in the hydrological winter. This is

different from summer drought where higher temperatures are associated with lower precipitation.

6.2 Impact of 1999–2004/05 Drought at St. Denis, Saskatchewan

6.2.1 Methods

6.2.1.1 Field Observations

At the St. Denis NWA, extensive measurements of air temperature, relative humidity, wind speed (2 metre and 10 metre), precipitation, radiation, and vapour pressure along with field observations of land cover, soil properties, and wetland water level were conducted by University of Saskatchewan and Environment of Canada in the 1990s and 2000s. The methods used for collecting these variables and parameters are described in Appendix C. The soil properties and land cover information for the basin of Wetland 109 during the recent drought period were summarized and shown in Table 6.4.

6.2.1.2 Drought Impact Simulations

CRHM was used to estimate the water balance during winter and spring period for the basin of Wetland 109 during 1999-2006. Two HRU (cultivated and wetland) shown in Table 6.4 were built to run the simulations for the basin. Meteorology during hydrological winter period (November 1-April 30) and soil and land cover conditions described in Table 6.4 were used in CRHM to simulate the drought impact on the wetland snowmelt hydrology.

Table 6.4 Observed soil properties and land cover information at the Wetland 109 during 1999-2006.

HRU	Area (km^2)	Vegetation Height (m)	Fall Soil Moisture (m^3 water/m^3 soil)	Porosity (ratio)
		1999 - 2000		
Cultivated (stubbles)	0.01601	0.3	0.21	0.48
Wetland	0.00412	5	0.23	0.54
		2000 - 2001		
Cultivated (stubbles)	0.01601	0.1	0.19*	0.48
Wetland	0.00412	5	0.22*	0.54
		2001 - 2002		
Cultivated (stubbles)	0.01601	0.15	0.19	0.48
Wetland	0.00412	5	0.22	0.54
		2002 - 2003		
Cultivated (fallows)	0.01601	0.001	0.19	0.48
Wetland	0.00412	5	0.22	0.54
		2003 - 2004		
Cultivated (stubbles)	0.01601	0.1	0.22	0.48
Wetland	0.00412	5	0.25	0.54
		2004 - 2005		
Cultivated (stubbles)	0.01601	0.1	0.19	0.48
Wetland	0.00412	5	0.22	0.54
		2005 - 2006		
Cultivated (stubbles)	0.01601	0.2	0.27	0.48
Wetland	0.00412	5	0.32	0.54

Note: * unlimited soil infiltrability corresponding to macropore development was set up and used for the CRHM simulations.

6.2.2 Results

6.2.2.1 Air Temperature and Precipitation Anomalies

The observed cumulative precipitation (rainfall and snowfall) and air temperature for the hydrological winters during 1999-2006 are shown in Figure 6.6 and Figure 6.7. Figure 6.6 shows that precipitation was consistently low for hydrological winters of 1999-2000, 2000-01, 2001-02, 2003-04, and

2004-05 with cumulative values of 73.6 mm, 71.2 mm, 58.8 mm, 84.8 mm, and 77.5 mm, respectively. Precipitation in the hydrological winter of 2002-03 was high with total of 123.8 mm. The highest cumulative precipitation for the period of 1999-2006 was 148.1 mm, in the winter of 2005-06. Figure 6.7 shows that air temperatures were cold during the hydrological winters of 2000-01, 2001-02, 2002-03, and 2003-04 with the average temperature below -8 °C for all these 4 winters. Air temperatures during hydrological winters of 1999-2000 and 2004-05 slightly increased, with the average temperature of -6.2 °C and -7.3 °C, respectively. The highest average temperature for the period 1999-2006 was -5.4 °C, in the winter of 2005-06.

Observed cumulative precipitation and observed air temperature were compared to the long term average precipitation and long term air temperature (Figure 6.8). Figure 6.8(a) shows that 30-year (1975-2005) average precipitation during the hydrological winter (November 1-April 30) was very close between Saskatoon and Humboldt, 85.4 mm and 86.1 mm, respectively (Environment Canada, 2006a). Compared to the 30-year average precipitation in Saskatoon, the precipitation was 14%, 17%, and 31% lower for the hydrological winters of 1999-2000, 2000-01, and 2001-02, respectively, with similar values for Humboldt. Compared to the 30-year average in Saskatoon, the precipitation was 45% and 73% higher for the hydrological winters of 2002-03 and 2005-06, respectively, with similar values for Humboldt. The precipitation in the hydrological winter of 2003-04 was very near the average in Saskatoon and Humboldt. In the hydrological winter of 2004-05, the

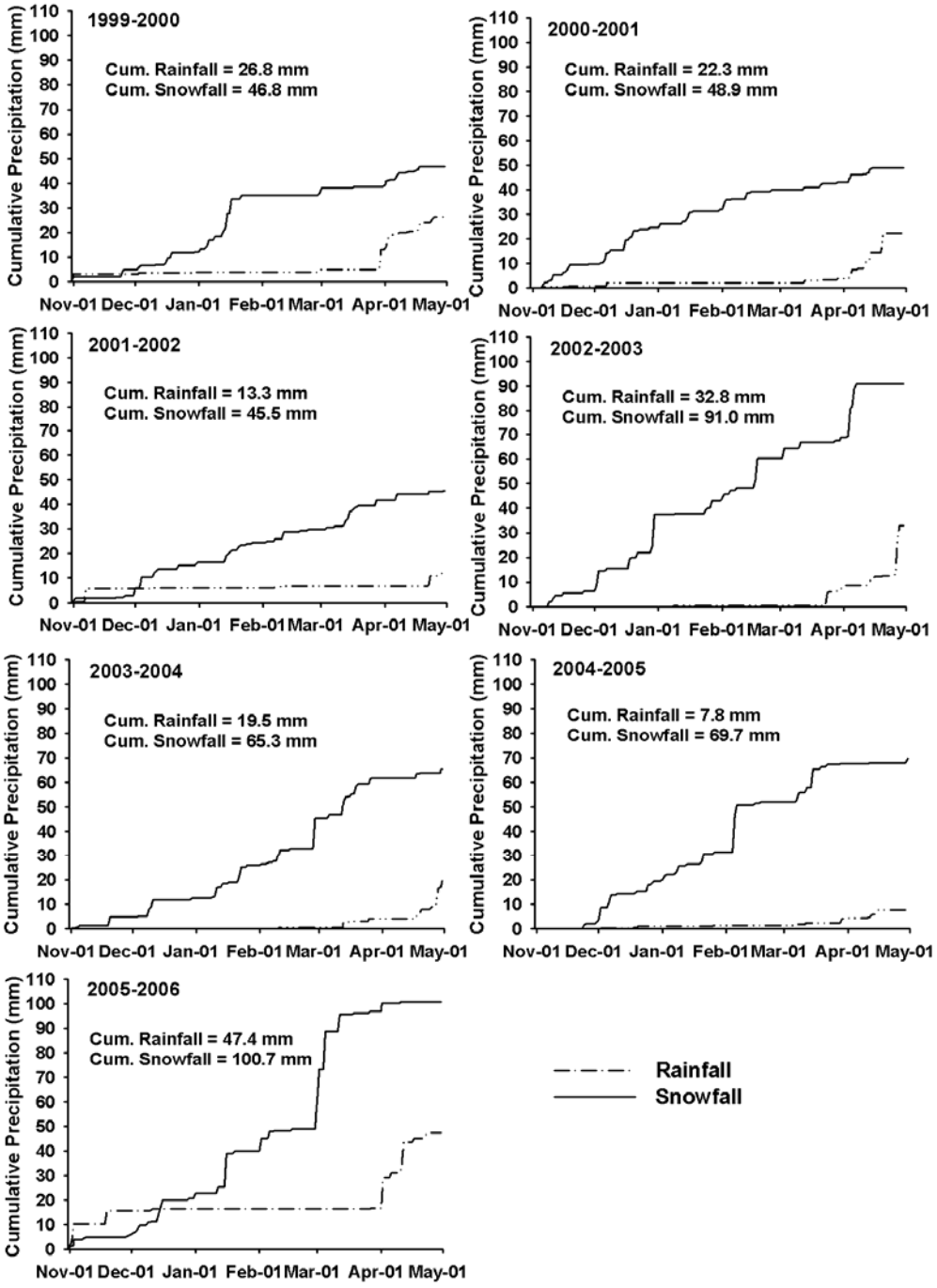

Figure 6.6 Observed cumulative precipitation for hydrological winters during 1999-2006 at St. Denis NWA.

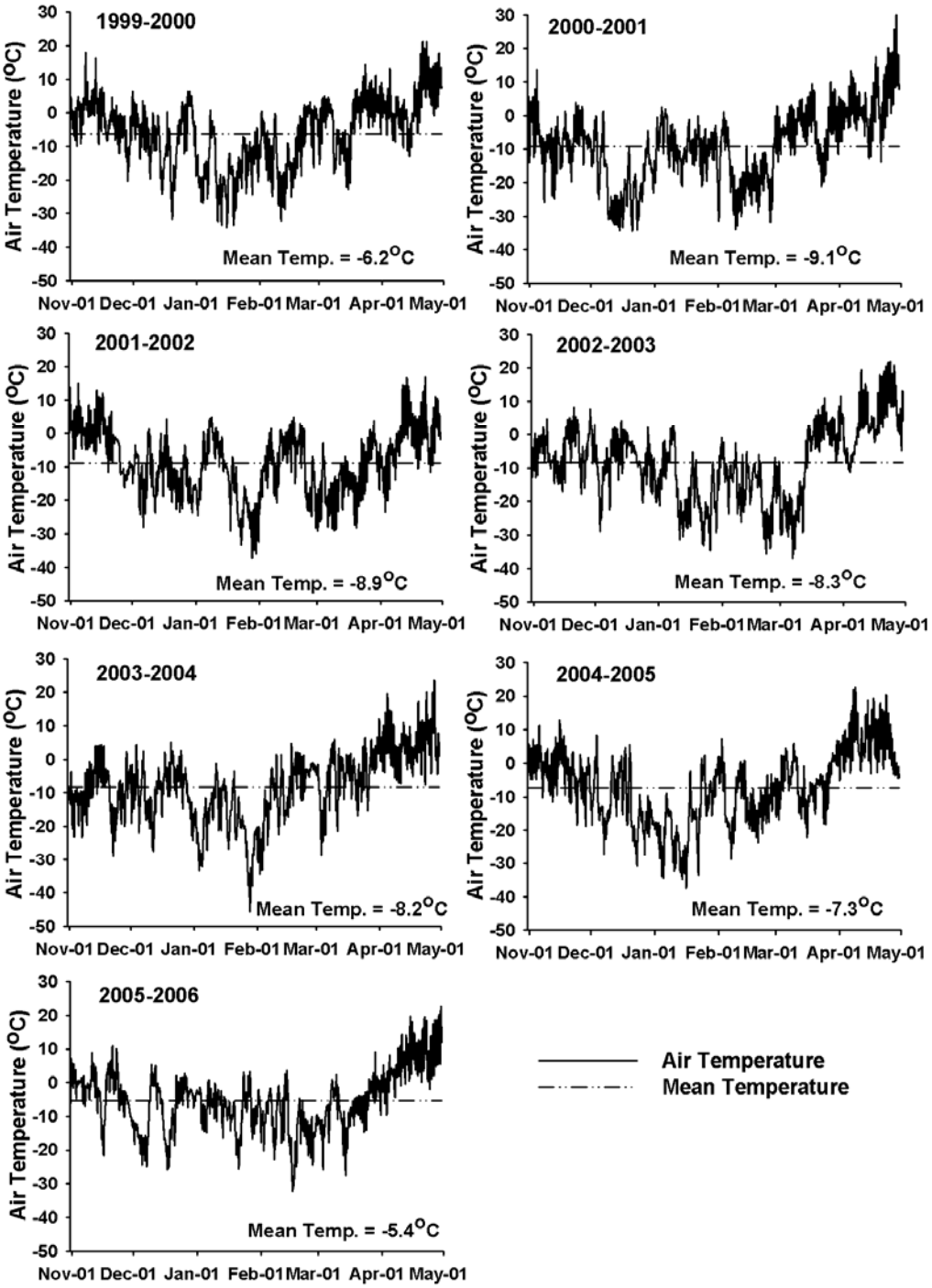

Figure 6.7 Observed air temperature for hydrological winters during 1999-2006 at St. Denis NWA.

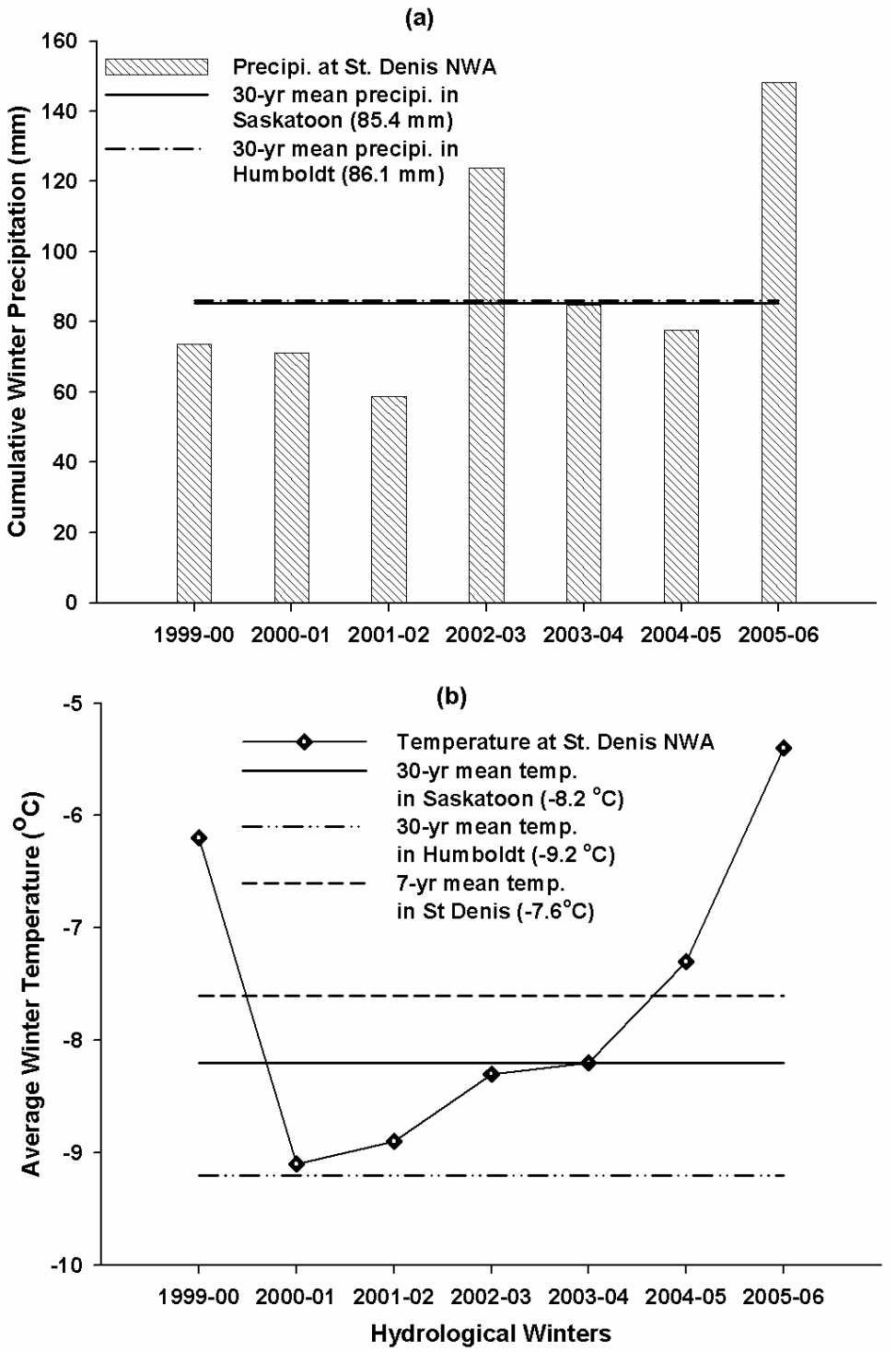

Figure 6.8 Comparisons of winter precipitation and temperature to 30-year (1975-2005) mean precipitation and temperature during hydrological winters of 1999-2006. 30-year mean precipitation and temperature derived from Environment Canada, 2006a.

precipitation was slightly below the average, about 9% less than the 30-year average in Saskatoon and Humboldt. It should be noted that the winter precipitation collected from the ten-metre station at St. Denis during 1999-2005 was replaced by the winter precipitation from a nearby Meteorological Service of Canada station at Humboldt.

Figure 6.8(b) shows that 30-year (1975-2005) average temperature during hydrological winter (November 1-April 30) was -8.2 °C and -9.2 °C for Saskatoon and Humboldt, respectively (Environment Canada, 2006a). The seven-year (1999-2006) mean hydrological winter temperature at St. Denis was -7.6 °C. This implies that slightly warmer than average conditions developed during the drought. The standard deviation for the temperature during 1975-2005 was 1.9 °C for both Saskatoon and Humboldt; that for the temperature during 1999-2006 was 1.4 °C at St. Denis. This indicates the winter temperature has less variability during the seven-year period (1999-2006) compared to the winter temperature during 30-year period (1975-2005).

6.2.2.2. Drought Impact on Wetland Snow Hydrology

Major wetland snow hydrology processes during the hydrological winter were simulated for the individual HRU at Wetland 109 during 1999-2006 (Figure 6.9). The figure shows the combined effects of changing meteorology and changing soil and land cover conditions on the Canadian prairie wetland snowmelt hydrology during the drought. The figure also

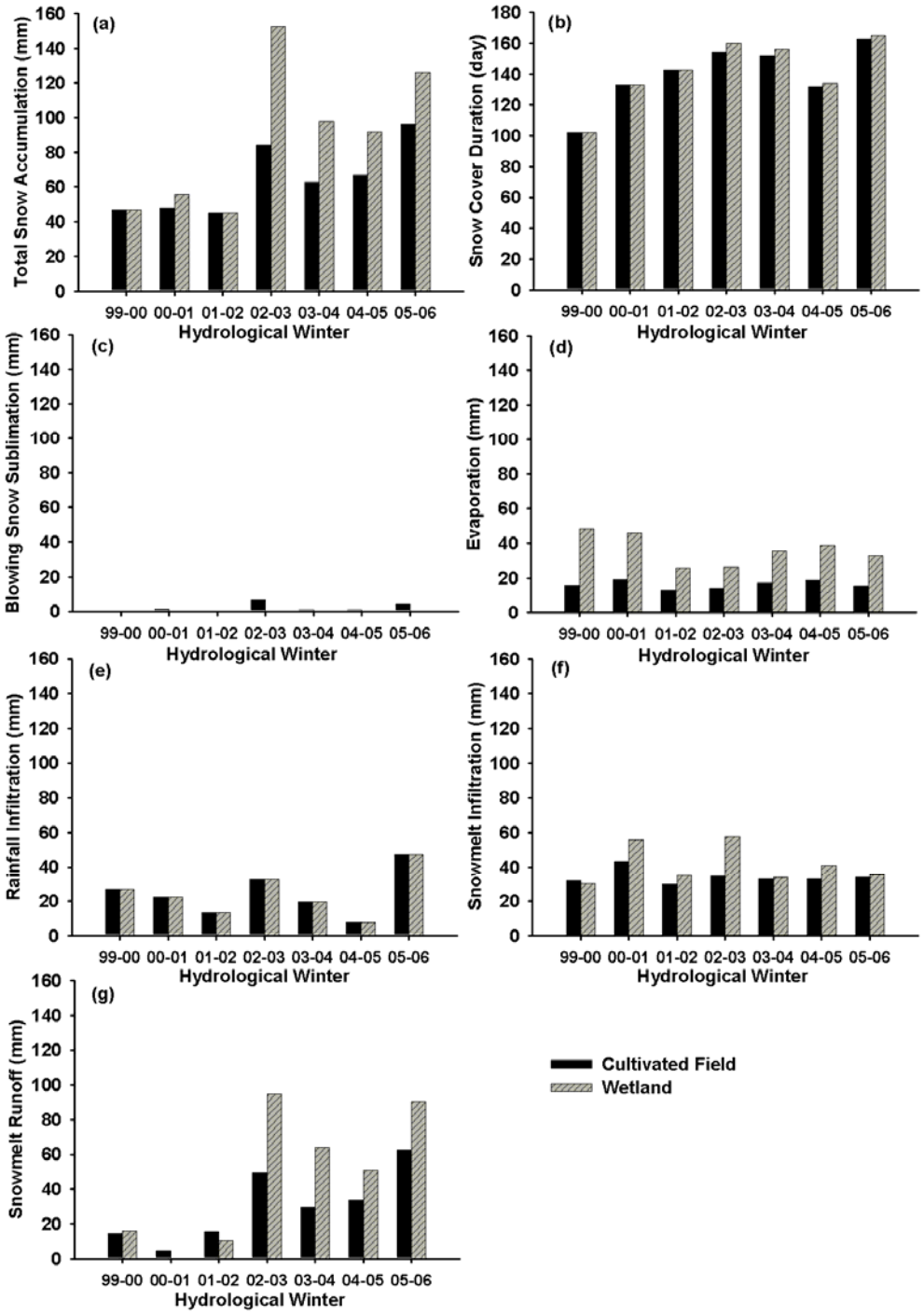

Figure 6.9 Simulated hydrological processes for individual HRU at the Wetland 109 during 1999-2006. Changing processes: (a) total snow accumulation (b) snow cover duration (c) blowing snow sublimation (d) evaporation (e) rainfall infiltration (f) snowmelt infiltration (g) snowmelt runoff.

illustrates the response of each HRU (cultivated field and wetland) to these conditions.

Figure 6.9(a) shows that the cumulative snow accumulation (SWE) was consistently low for both cultivated field and wetland during the hydrological winters of 1999-2000, 2000-01, and 2001-02; 'severe drought' periods. There was only 46%-57% of SWE in the cultivated field and 30%-45% of SWE in the wetland compared to the snow accumulation during 2002-03 and 2005-06; 'normal' periods. There were moderate amounts of SWE during the hydrological winters of 2003-04 and 2004-05; 'recovery' periods. There was great snow accumulation in the wetland HRU during 2002-03 when compared to that during 2005-06; this is because the summer-fallowed field in 2002 resulted in more blowing snow redistributed to the wetland ('sink'). Figure 6.9(b) shows that the snow-covered periods of the two HRUs were similar during the severe drought periods, with much shorter duration in the hydrological winter of 1999-2000 compared to the recovery and normal periods. Figure 6.9(c) shows that sublimation of blowing snow was persistently low, nearly zero for the severe drought periods, due to suppression of blowing snow. Winter evaporation in the cultivated field was not very sensitive to the changing conditions during drought; compared to the normal periods (2002-03 and 2005-06), evaporation in the wetland tended to be higher during some severe drought periods, 1999-2000 and 2000-01, due to the shorter snow-covered season and earlier occurrence of evaporation in the spring. Figure 6.9(e) shows that there was no difference in rainfall infiltration

into unfrozen soils between HRUs. Snowmelt infiltration into frozen soils was sensitive to the amount of snow accumulation and soils conditions. Figure 6.9(a) and Figure 6.9(f) show that snowmelt infiltration in the wetland during 2002-03 increased as snow accumulation increased; snowmelt infiltration in both HRUs increased when macropores developed during 2000-01. Figure 6.9(g) demonstrates that compared to the normal periods (2002-03 and 2005-06), there was much lower surface runoff from melting snow during the severe drought periods, with decreases of 35-58 mm and 75-90 mm snowmelt runoff for the cultivated field and wetland, respectively. During drought, lower snow accumulation, enhanced evaporation, and higher ratio of snowmelt infiltration to snow accumulation all affect the runoff generation in Canadian prairie wetlands.

The evolution of major wetland snow hydrology processes during the hydrological winters was simulated for the basin of Wetland 109 during 1999-2006 (Figure 6.10). The cumulative responses of these processes to the combined conditions of meteorology, soil, and land cover were estimated at end of the winter (Figure 6.11). Compared to the 'normal' periods, 2002-03 and 2005-06, both snowfall and rainfall during the hydrological winter were consistently low for the 'severe drought' periods, 1999-2002. As a result, compared to the normal periods, snow accumulation was 50-55% lower for the basin during the severe drought periods. Snow accumulation was moderate for the hydrological winters of 2003-04 and 2004-05, 'recovery' periods. Basin snow-cover season was 17-63 days shorter during the severe drought

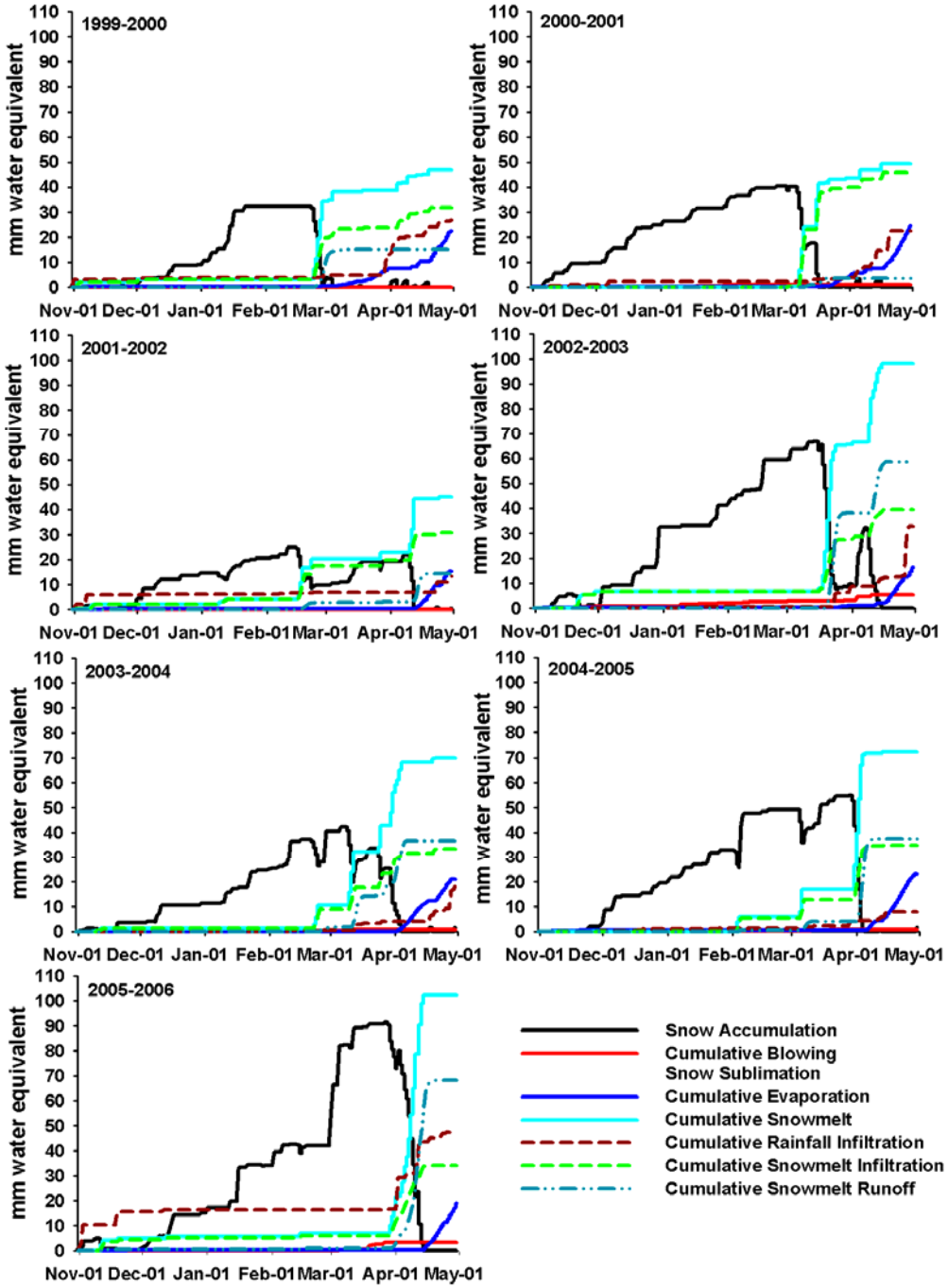

Figure 6.10 The simulated evolution of wetland snow hydrology processes during the hydrological winters of 1999-2006 at the Wetland 109.

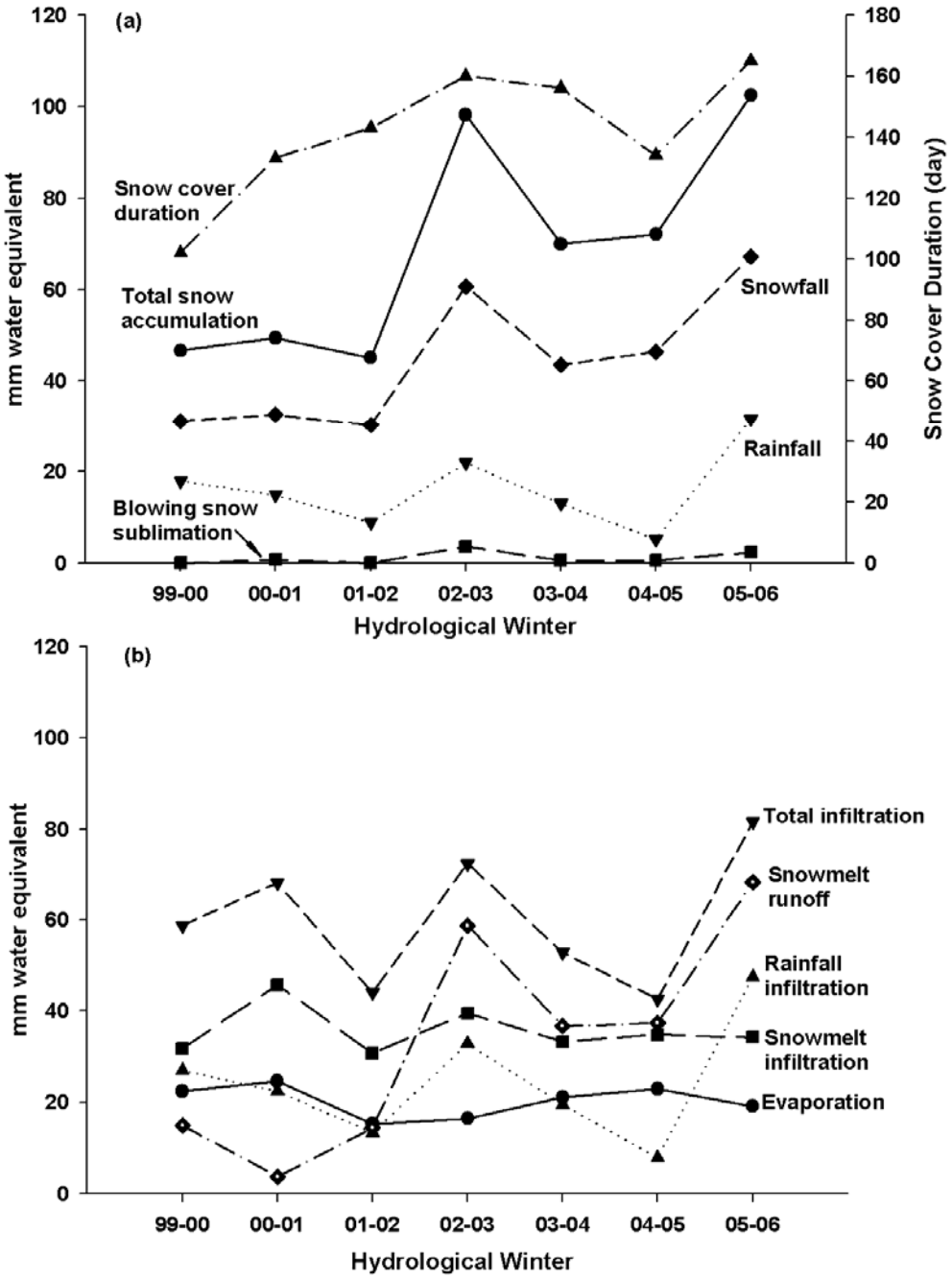

Figure 6.11 Simulated hydrological processes for the basin of Wetland 109 during 1999-2006. Changing processes: (a) snowfall, rainfall, total snow accumulation, snow cover duration, blowing snow sublimation (b) evaporation, rainfall infiltration, snowmelt infiltration, total infiltration, snowmelt runoff. It should be noted that lines connecting points among years are only for visual purpose and do not imply interpolation.

periods compared to the normal periods. Sublimation of blowing snow was low for the basin throughout the period of 1999-2006; this is due to lack of blowing snow occurrence from low snowfall and relatively tall vegetation cover. Basin winter evaporation was not strongly sensitive to the changing conditions during 1999-2006, with increases of 3 to 8 mm during severe drought periods. Basin infiltration did not show a strong trend with changing conditions during 1999-2006. This is because infiltration comprises both rainfall infiltration into unfrozen soils and snowmelt infiltration into frozen soils; both are complex processes controlled by combinations of hydro-meteorological condition and soil status. Basin surface runoff from snowmelt was much lower during the severe drought periods, approximately 45-65 mm less compared to that in the normal periods. Snowmelt runoff was very low in 2000-01 and this is related to the formation of macropores in dry soils (Bodhinayake and Si, 2004; van der Kamp *et al.*, 2003), causing unlimited soil infiltrability that allowed all melt water to infiltrate into soils (Gray *et al.*, 2001). Similar results were found in the springtime water level during the drought. Figure 6.12 shows the maximum spring water level observed in Wetland 109 during 1997-2005; the water level was much lower during the severe drought periods compared to the non-drought periods.

6.2.3 Discussion

Severe winter drought occurred during 1999-2002. It began with an inadequate precipitation during the hydrological winter (November 1-April 30)

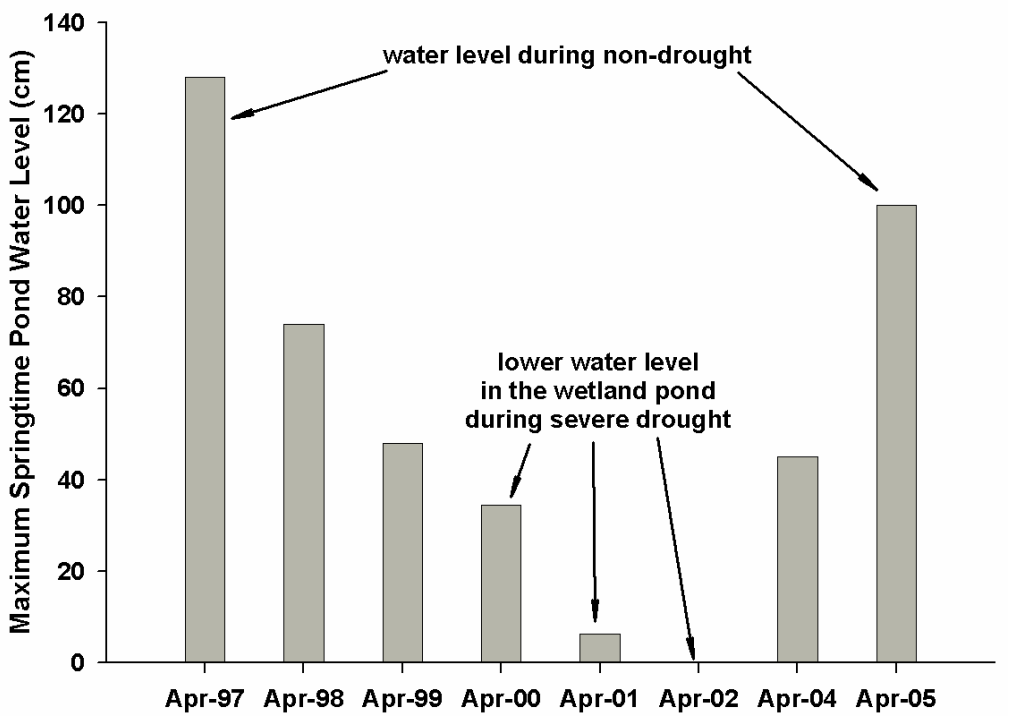

Figure 6.12 Observed springtime water levels at the Wetland 109, St. Denis NWA during 1997-2005. Note that water level was not measured in April 2003. Water level data acquired from van der Kamp *et al.*, 2006b.

of 1999-2000. This is a meteorological drought characterized by below average precipitation over an extended period of time (Wilhite and Glantz, 1985). The occurrence of meteorological drought on the Canadian Prairie during 1999-2002 was related to large-scale disruptions of atmospheric circulation pattern and displacement of air mass (Liu *et al.*, 2004; Bonsal and Wheaton, 2005; Shabbar, 2006). As a result, low soil moisture developed during this period, leading to reduced availability of soil water to support crops, an agricultural drought. With these atmospheric and soil conditions, hydrological drought emerged during the hydrological winters of 1999-2002,

resulting in much less springtime discharge of snowmelt to wetland area and subsequently drying out of wetland.

Compared to the synthetic prairie drought progression described earlier, the recent multi-year drought of 1999-2004/05 has distinctive characteristics. A three-year (1999-2002) severe winter drought period was followed by a normal year (2002-03) and then a two-year (2003-05) recovery period, with slightly below average precipitation and somewhat lower snowmelt runoff and wetland water level, and then returning to normal (2005-06). This is related to the nature of drought; that is, drought is a gradual process and its beginning and end is hard to define (Wilhite and Buchanan-Smith, 2005). Wetland 109 at St. Denis represents a sub-humid, partly wooded and relatively poorly-drained site on the Canadian Prairies; the drought impact on snowmelt hydrology and response in surface water supplies to the drought was specific to such a site.

The winter season discussed here is the hydrological winter, extending from November to end of April, during which hydrological processes such as snowfall, snowmelt, and snowmelt runoff occur. Below average air temperature developed during the hydrological winter on the Canadian prairie regions (e.g. Rosetown, St. Denis), while positive temperature anomalies were found during the meteorological winter (i.e. Dec, Jan, and Feb) in these regions (Environment Canada, 2007). This suggests that for cold regions such as the Canadian Prairies, the conventional definition of winter by meteorology sometimes is not accurate enough to provide information for analyzing the

effects of drought on hydrology. More study is needed using a functional definition of winter in order to improve the understanding of drought impacts on the hydrological processes over the Prairies.

Chapter 7

7.0 Conclusions

Spatially distributed and spatially aggregated approaches were used to examine the modelling scale for snow accumulation (SWE) and snowmelt at a Canadian prairie basin – St. Denis NWA. The simulated results of pre-melt SWE evolution, end of winter SWE, and daily snowmelt were compared with the observed pre-melt SWE, cumulative SWE, and daily snowmelt on seven Hydrological Response Units (HRUs). Both approaches simulated the development and timing of pre-melt SWE well with relatively small differences with observations, and both approaches generated end of winter SWE that was close to the observations on most HRU. Both approaches were able to estimate large amounts of snow transport to and accumulation on the wetland HRU, which is critical to the water balance.

Comparisons of areal average end of winter SWE, areal daily snowmelt, snowmelt duration, and snow-covered area were also made between the two modelling approaches. Results showed that both approaches had similar levels of accuracy. This is because models with similar physics were used in both approaches. However, the spatially aggregated approach had a computational advantage; the computational time for the spatially

aggregated approach was about one minute, while the spatially distributed approach took over 30 minutes. Thus, the spatially aggregated approach was selected for estimation of sow accumulation and snowmelt on the Canadian Prairies.

The Cold Regions Hydrological Modelling platform (CRHM) was used to derive a snow hydrology model for the Canadian Prairies and was run at two drainage basins: Creighton Tributary of Bad Lake, Saskatchewan and Wetland 109 at St. Denis, Saskatchewan. The snow hydrology model scheme in CRHM used the spatially aggregated modelling approach to calculate the water balance during winter and spring. Simulated results of pre-melt SWE and springtime snowmelt runoff were compared to the field observations, showing a reasonable performance of CRHM in estimating the snowmelt runoff on the prairies. Due to the importance of wetlands, ponds, and dugouts in prairie hydrological systems, addition of a surface storage model to CRHM would make a significant improvement to this prairie snowmelt runoff model.

A drought sensitivity study of winter hydrological processes to individual components of meteorological, soil and land cover conditions during a drought was conducted at Bad Lake. Results showed that blowing snow accumulation and sublimation were very sensitive to winter precipitation and air temperature as well as to the changing land covers. Snow cover duration initially decreased when drought meteorology was induced but showed little sensitivity to the onset of severe drought conditions. Winter evaporation was relatively insensitive to drought conditions. Infiltration was

sensitive to changes in each of winter precipitation, air temperature, soil moisture, and land covers during the drought. Snowmelt runoff showed a dramatic response to drought and ceased when winter precipitation dropped by 50% or air temperature rose by 5 °C.

A multi-year prairie winter hydrological drought progression was proposed and simulated at Bad Lake. In this drought progression, severe winter drought meteorology developed for the first two years of drought but fall soil moisture and vegetation recovered after the winter meteorology returned to normal. The combined condition of winter precipitation dropping by 15% and air temperature increasing by 2.5 °C was sufficient to cause the cessation of snowmelt runoff and streamflow discharge.

A study of impact of the 1999-2005 drought conducted at the Wetland 109, St. Denis showed that winter precipitation was largely reduced during 1999-2002, the severe drought periods. During these periods, snow accumulation was low due to decreasing frequency of blowing snow; winter evaporation slightly increased due to shorter snow-covered season and earlier occurrence of evaporation in the spring. The sensitivity of infiltration to drought was complex because infiltration comprises rainfall infiltration into unfrozen soils and snowmelt infiltration into frozen soils and is affected by both winter precipitation and soil conditions. Snowmelt runoff was much lower during the severe drought periods, leading to a drying out of the wetland.

List of References

Agriculture and Agri-Food Canada. 1998. *Drought in the Palliser Triangle*. PFRA Publications. Retrieved: March 20, 2007. [Web Page]. Available at: http://www.agr.gc.ca/pfra/publications_e.htm.

Alley, W.M. 1984. The Palmer Drought Severity Index: Limitations and assumptions. *Journal of Climate and Applied Meteorology* **23**: 1100-1109.

Andersland, O.B., Wiggert, D.C. and Davies, S.H. 1996. Hydraulic conductivity of frozen granular soils. *Journal of Environmental Engineering* **122**: 212-216.

Anderson, E.A. 1973. National Weather Service River Forecast System – Snow Accumulation and Ablation Model. Silver Springs, Maryland: National Oceanic and Atmospheric Administration (NOAA), Technical Memorandum NWS HYDRO-17.

Bagnold, R.A. 1954. *The Physics of Blown Sand and Desert Dunes*. Chapman & Hall: London, 265p.

Bodhinayake, W. and Si, B.C. 2004. Near-saturated surface soil hydraulic properties under different land uses in the St Denis National Wildlife Area, Saskatchewan, Canada. *Hydrological Processes* **18**: 2835-2850.

Bonsal, B.R. 2005. Atmospheric circulation patterns associated with the 2001 and 2002 Canadian Prairie Droughts. In Sauchyn, D. Khandekar, M. and Garnett, E.R. (Eds.), *The Science, Impacts and Monitoring of Drought in Western Canada: Proceedings of the 2004 Prairie Drought Workshop*. Canadian Plains Research Centre, University of Regina, pp. 11-16.

Bonsal, B.R. and Wheaton, E.E. 2005. Atmospheric circulation comparison between the 2001 and 2002 and the 1961 and 1988 Canadian Prairie droughts. *Atmosphere-Ocean* **43**:163-172

Clark, C.O. 1945. Storage and the unit hydrograph. *Proceedings of the American Society of Civil Engineering* **69**: 1419-1447.

Dingman, S.L. 1994. *Physical Hydrology*. Prentice-Hall, Inc: Englewood Cliffs, New Jersey, 575p.

Division of Hydrology. 1977. An examination of U.S. NWS River Forecast System snow and ablation model under Prairie conditions. Internal Report, Division of Hydrology, University of Saskatchewan, Saskatoon. 26pp.

Donald, J.R., Soulis, E.D., Kouwen N. and Pietroniro, A. 1995. A land cover-based snow cover representation for distributed hydrologic models. *Water Resources Research* **31**: 995-1009.

Dornes, P.F., Pomeroy, J.W., Pietroniro, A., Carey, S.K., Quinton, W.L. 2006. The use of inductive and deductive reasoning to model snowmelt runoff from northern mountain catchments. In: Voinov, A., Jakeman, A.J. and Rizzoli, A.E. (Eds). *Proceedings of the iEMSs Third Biennial Meeting: "Summit on Environmental Modelling and Software"*. International Environmental Modelling and Software Society, Burlington, USA, July 2006. CD ROM. Internet: http://www.iemss.org/iemss2006/sessions/all.html

Engelmark, H. 1984. Infiltration in unsaturated frozen soil. *Nordic Hydrology* **15**: 243-252.

Engelmark, H. and Svensson, U. 1993. Numerical modelling of phase change in freezing and thawing unsaturated soil. *Nordic Hydrology* **24**: 95-110.

Environment Canada. 2006a. *Climate data online* [Web Page]. Retrieved: December 12, 2006. Available at: http://www.climate.weatheroffice.ec.gc.ca/climateData/canada_e.html.

Environment Canada. 2006b. *Temperature and Precipitation in Historical Perspective* [Web Page]. Retrieved: December 14, 2006.Available at: http://www.msc-smc.ec.gc.ca/ccrm/bulletin/national_e.cfm.

Environment Canada. 2007. *Climate Trends and Variations Bulletin* [Web Page]. Retrieved: February 20, 2007. Meteorological Service of Canada, Climate Research Branch. Available at: http://www.msc-mc.ec.gc.ca/ccrm/bulletin/archive_e.cfm.

Essery, R., Li, L. and Pomeroy, J.W. 1999. A distributed model of blowing snow over complex terrain. *Hydrological Processes* **13**: 2423-2438.

Essery, R. and Pomeroy, J. 2004. Vegetation and topographic control of wind-blown snow distributions in distributed and aggregated simulations for an arctic tundra basin. *Journal of Hydrometeorology* **5**: 735-744.

Essery, R. 2006. Portable version of Distributed Blowing Snow Model. Personal Communication.

Essery, R., Granger, R. and Pomeroy, J. 2006. Boundary-layer growth and advection of heat over snow and soil patches: modelling and parameterization. *Hydrological Processes* **20**: 953-967.

Evans, B.M., Sheeder, S.A. and Lehning, D.W. 2003. A spatial technique for estimating streambank erosion based on watershed characteristics. *Journal of SpatialHydrology* **3**(1): 1-13.

Flerchinger, G.N. and Saxton, K.E. 1989a. Simultaneous heat and water model of a freezing snow-residue-soil system I. Theory and Development. *Transactions of the ASAE* **32**: 565-571.

Flerchinger, G.N. and Saxton, K.E. 1989b. Simultaneous heat and water model of a freezing snow-residue-soil system II. Field Verification. *Transactions of the ASAE* **32**: 573-578.

Flerchinger, G.N. 2000. The simultaneous heat and water (SHAW) model: technical documentation. Technical Report NWRC 2000-09. Northwest Watershed Research Center, USDA agricultural Research Service, Boise, Idaho.

Garnier, B.J. and Ohmura, A. 1970. The evaluation of surface variations in solar radiation income. *Solar Energy* **13**: 21-34.

Godwin, R.B. and Martin, F.R.J. 1975. Calculation of gross and effective drainage areas for the Prairie Provinces. In: *Canadian Hydrology Symposium - 1975 Proceedings, 11-14 August 1975, Winnipeg, Manitoba.* Associate Committee on Hydrology, National Research Council of Canada, pp. 219-223.

Granger, R.J., Chanasyk, D.S., Male, D.H. and Norum, D.I. 1977. Thermal regime of prairie snowcover. *Soil Science Society of America Journal* **41**: 839-842.

Granger, R.J. and Male, D.H. 1978. Melting of a prairie snowpack. *Journal of Applied Meteorology* **17**: 1833-1842.

Granger, R.J., Gray, D.M. and Dyck, G.E. 1984. Snowmelt infiltration to frozen Prairie soils. *Canadian Journal of Earth Science* **21**: 669-677.

Granger, R.J. and Gray, D.M. 1989. Evaporation from natural non-saturated surfaces. *Journal of Hydrology* **111**: 21-29.

Granger, R.J. and Gray, D.M. 1990. A net radiation model for calculating daily snowmelt in open environments. *Nordic Hydrology* **21**: 217-234.

Granger, R.J. and Pomeroy, J.W. 1997. Sustainability of the western Canadian boreal forest under changing hydrological conditions - 2- summer energy and water use. In *Sustainability of Water Resources under Increasing Uncertainty*, Rosjberg, D., Boutayeb, N., Gustard, A., Kundzewicz, Z. and Rasmussen, P. (Eds.) IAHS Publ No. 240. IAHS Press: Wallingford, UK; 243-250.

Granger, R.J., Pomeroy, J.W. and Parviainen, J. 2002. Boundary-layer integration approach to advection of sensible heat to a patchy snow cover. *Hydrological Processes* **16**: 3559-3569.

Gray, D.M., Norum, D.I. and Wigham, J.M. 1970. Infiltration and the physics of flow of water through porous media. In Gray, D.M. (Ed.), *Handbook on the Principles of Hydrology: with special emphasis directed to Canadian conditions in the discussions, applications and presentation of data.* New York: Water Information Center, Inc., Section V.

Gray, D.M., Landine, P.G. and Granger, R.J. 1985. Simulating infiltration into frozen Prairie soils in stream flow models. *Canadian Journal of Earth Science* **22**: 464-474.

Gray, D.M. and Granger, R.J. 1986. In situ measurements of moisture and salt movement in freezing soils. *Canadian Journal of Earth Sciences* **23**: 696-704.

Gray, D.M., Granger, R.J. and Landine, P.G. 1986. Modelling snowmelt infiltration and runoff in a prairie environment. In Kane, D.L. (Ed.), *Proceedings of the Symposium: Cold Regions Hydrology.* Maryland: American Water Resources Association, pp. 427-438.

Gray, D.M. and Landine, P.G. 1987. Albedo model for shallow prairie snow covers. *Canadian Journal of Earth Sciences* **24**: 1760-1768.

Gray, D.M. and Landine, P.G. 1988. An energy-budget snowmelt model for the Canadian Prairies. *Canadian Journal of Earth Sciences* **25**: 1292-1303.

Gray, D.M., Pomeroy, J.W. and Granger, R.J. 1989. Modelling snow transport, snowmelt and meltwater infiltration in open, northern regions. In *Northern Lakes and Rivers*, Mackay, W.C. (Ed.). Occasional Publication No. 22. Boreal Institute for Northern Studies, University of Alberta, Edmonton; 8-22.

Gray, D.M., Toth, B., Zhao, L., Pomeroy, J.W. and Granger, R.J. 2001. Estimating areal snowmelt infiltration into frozen soils. *Hydrological Processes* **15**: 3095-3111.

Guttman, N.B., Wallis, J.R. and Hosking, J.R.M. 1992. Spatial comparability of the Palmer Drought Severity Index. *Water Resources Bulletin* **28**: 1111-1119.

Hayashi, M., van der Kamp, G. and Rudolph, D.L. 1998. Water and solute transfer between a prairie wetland and adjacent uplands, 1. Water balance. *Journal of Hydrology* **207**: 42-55.

Hayashi, M. and van der Kamp, G. 2000. Simple equations to represent the volume-area-depth relations of shallow wetlands in small topographic depressions. *Journal of Hydrology* **237**: 74-85.

Hayashi, M., van der Kamp, G. and Schmidt, R. 2003. Focused infiltration of snowmelt water in partially frozen soil under small depressions. *Journal of Hydrology* **270**: 214-229.

Hillel, D. 2004. *Introduction to Environmental Soil Physics*. Elsevier Academic Press: Amsterdam, 494p.

Jackson, P.S. and Hunt, J.C.R. 1975. Turbulent wind flow over a low hill. *Quarterly Journal of the Royal Meteorological Society* **101**: 929-955.

Kane, D.L. 1980. Snowmelt infiltration into seasonally frozen soils. *Cold Regions Science and Technology* **3**: 153-161.

Kane, D.L. and Stein, J. 1983. Water movement into seasonally frozen soils. *Water Resource Research* **19**: 1547-1557.

Karl, T.R. 1986. The sensitivity of the Palmer Drought Severity Index and Palmer's Z-Index to their calibration coefficients including potential evapotranspiration. *Journal of Climate and Applied Meteorology* **25**: 77-86.

Lapen, D.R. and Martz, L.W. 1996. An investigation of the spatial association between snow depth and topography in a Prairie agricultural landscape using digital terrain analysis. *Journal of Hydrology* **184**: 277-298.

Lawford, R.G. 1992. Research implications of the 1988 Canadian Prairie provinces drought. *Natural Hazards* **6**: 109-129.

Leavesley, G.H., Lichty, R.W., Troutman, B.M. and Saindon, L.G. 1983. Precipitation-runoff modelling system: user's manual. US Geological Survey Water Resources Investigations Report 83-4238. 207 pp.

Li, L. and Pomeroy, J.W. 1997a. Estimates of threshold wind speed for snow transport using meteorological data. *Journal of Applied Meteorology* **36**: 205-213.

Li, L. and Pomeroy, J.W. 1997b. Probability of occurrence of blowing snow. *Journal of Geophysical Research* **102**: 21,955-21,964.

Liu, J., Stewart, R.E. and Szeto, K.K. 2004. Moisture Transport and other hydrometeorological features associated with the severe 2000/01 drought over the western and central Canadian Prairies. *Journal of Climate* **17**: 305-319.

Male, D.H. and Gray, D.M. 1981. Snowcover ablation and runoff. In Gray, D.M. and Male, D.H. (Eds.), *Handbook of Snow: principles, processes, management & use.* Ontario: Pergamon Press Canada Ltd., pp. 360-436.

Marks, D., Kimball, J., Tingey, D. and Link, T. 1998. The sensitivity of snowmelt processes to climate conditions and forest cover during rain-on-snow: a case study of the 1996 Pacific Northwest flood. *Hydrological Processes* **12**: 1569-1587.

Marsh, P. and Woo, M.K. 1984. Wetting front advance and freezing of meltwater within a snowcover. 1. Observations in the Canadian Arctic. *Water Resources Research* **20**: 1853-1864.

Mason, P.J. and Sykes, R.I. 1979. Flow over an isolated hill of moderate slope. *Quarterly Journal of the Royal Meteorological Society* **105**: 383-395.

Maybank, J., Bonsal, B., Jones, K., Lawford, R., O'Brien, E.G., Ripley, E.A. and Wheaton E. 1995. Drought as a natural disaster. *Atmosphere-Ocean* **33**: 195-222.

McKee, T.B., Doesken, N.J. and Kleist, J. 1993. The relationship of drought frequency and duration to time scale. Anaheim, CA: Preprints, Eighth Conference on Applied Climatology, pp. 179-184.

Motovilov, Yu.G. 1978. Mathematical model of water infiltration into frozen soil. *Soviet Hydrology* **17**: 62-66.

Musgrave, G.W. and Holtan, H.N.1964. Infiltration. In Chow, V.T. (Ed.), *Handbook of Applied Hydrology: A Compendium of Water-resources Technology*. New York: McGraw-Hill, Inc., Section 12.

Nash, J.E. and Sutcliffe, J.V. 1970. River flow forecasting through conceptual models. Part I – A discussion of principles. *Journal of Hydrology* **10**: 282-290.

Nkemdirim, L. and Weber, L. 1999. Comparison between the Droughts of the 1930s and the 1980s in the Southern Prairies of Canada. *Journal of Climate* **12**: 2434-2450.

Norum, D.I., Gray, D.M. and Male, D.H. 1976. Melt of shallow prairie snowpacks: basis for a physical model. *Canadian Agricultural Engineering* **18**: 2-6.

Palmer, W.C. 1965. Meteorological drought. Research Paper No. 45, U.S. Department of Commerce Weather Bureau, Washington, D.C., 58 pp.

Pennock, D. 2004. Integrated catchment assessment of carbon sequestration and trace gas emissions in Saskatchewan, Project 4036-1. Project Report: Department of Soil Science, University of Saskatchewan.

Pennock, D., Braidek, J., Yates, T. and Bedard-Haughn, A. 2005. Greenhouse gas assessment from agricultural landscapes St. Denis National Wildlife Area, Saskatchewan. Project Report: Department of Soil Science, University of Saskatchewan.

Pomeroy, J.W. 1988. Wind transport of snow. Ph.D. Thesis, University of Saskatchewan, Saskatoon, Saskatchewan. 226 pp.

Pomeroy, J.W. 1989. A process-based model of snow drifting. *Annals of Glaciology* **13**: 237-240.

Pomeroy, J.W. and Gray, D.M. 1990. Saltation of snow. *Water Resources Research* **26**: 1583-1594.

Pomeroy, J.W., Nicholaichuk, W., Gray, D.M., McConkey, B., Granger, R.J. and Landine, P.G. 1990. Snow management and meltwater enhancement final report. NHRI Contribution No. CS-90021.

Pomeroy, J.W. and Male, D.H. 1992. Steady-state suspension of snow. *Journal of Hydrology* **136**: 275-301.

Pomeroy, J.W., Gray, D.M. and Landine, P.G. 1993. The prairie blowing snow models: characteristics, validation, operation. *Journal of Hydrology* **144**: 165-192.

Pomeroy, J.W. and Gray, D.M. 1995. *Snowcover Accumulation, Relocation and Management.* NHRI Science Report No. 7, Environment Canada, Saskatoon. 144 pp.

Pomeroy, J.W. and Goodison, B.E. 1997. Winter and snow. In Bailey, W.G., Oke, T.R. and Rouse, W.R. (Eds.). *The Surface Climates of Canada*. Montreal: McGill-Queen's University Press, pp. 68-100.

Pomeroy, J.W., Marsh, P. and Gray, D.M. 1997. Application of a distributed blowing snow model to the arctic. *Hydrological Processes* **11**: 1450-1464.

Pomeroy, J.W., Gray, D.M., Shook, K.R., Toth, B., Essery, R.L.H., Pietroniro, A. and Hedstrom, N. 1998. An evaluation of snow accumulation and ablation processes for land surface modelling. *Hydrological Processes* **12**: 2339-2367.

Pomeroy, J.W., Essery, R., Gray, D.M., Shook, K.R., Toth, B. and Marsh, P. 1999. Modelling snow-atmosphere interactions in cold continental environments. In Tranter, M. (Ed.). *Interactions between the Cryoshere, Climate and Greenhouse Gases*. IAHS Publication 256. Wallingford: International Association of Hydrological Sciences Press, pp. 91-102.

Pomeroy, J.W. and Li, L. 2000. Prairie and Arctic areal snow cover mass balance using a blowing snow model. *Journal of Geophysical Research* **105**: 26619-26634.

Pomeroy, J.W., de Boer, D. and Martz, L.W. 2007a. Hydrology and water resources. In Thraves, B., Lewry, M.L., Dale, J.E. and Schlichtmann, H. (Eds.), *Saskatchewan: Geographic Perspectives*. Regina: CRRC, pp. 63-80.

Pomeroy, J.W., Gray, D.M., Brown, T., Hedstrom, N.R., Quinton, W., Granger, R.J. and Carey, S. 2007b. The Cold Regions Hydrological Model, a platform for basing process representation and model structure on physical evidence. *Hydrological Processes* **21**: 2650-2667.

Rannie, W.F. 2006. A comparison of 1858-59 and 2000-01 drought patterns on the Canadian Prairies. *Canadian Water Resources Journal* **31**: 263-274.

Ripley, E.A. 1988. *Drought Prediction on the Canadian Prairies*, Report No. 88-4, Canadian Climate Centre, AES, National Hydrology Research Centre, Saskatoon, SK. 137 pp.

Sauchyn, D.J., Stroich, J. and Beriault, A. 2003. A paleoclimatic context for the drought of 1999-2001 in the northern Great Plains of North America. *The Geographical Journal* **169**: 158-167.

Shabbar, A., Bonsal, B. and Khandekar, M. 1997. Canadian precipitation patterns associated with the Southern Oscillation. *Journal of Climate* **10**: 3016-3027.

Shabbar, A. 2006. The impact of El Niño-Southern Oscillation on the Canadian climate. *Advances in Geosciences* **6**: 149-153.

Shafer, B.A. and Dezman, L.E. 1982. Development of a Surface Water Supply Index (SWSI) to assess the severity of drought conditions in snowpack runoff areas. Fort Collins, CO, Proceedings of the Western Snow Conference, pp. 164-175.

Schmidt, R.A. 1991. Sublimation of snow intercepted by an artificial conifer. *Agricultural and Forest Meteorology* **54**: 1-27.

Shook, K. 1995. Simulation of the ablation of prairie snowcovers. Ph.D. Thesis, University of Saskatchewan, Saskatoon, Saskatchewan. 189 pp.

Shook, K. and Gray, D.M. 1997. Snowmelt resulting from advection. *Hydrological Processes* **11**: 1725-1736.

Soulis, E.D., Snelgrove, K.R., Kouwen, N., Seglenieks, F. and Verseghy, D.L. 2000. Towards closing the vertical water balance in Canadian atmospheric models: Coupling of the land surface scheme CLASS with the distributed hydrological model WATFLOOD. *Atmosphere-Ocean* **38**: 251-269.

Steinemann, A.C., Hayes, M.J. and Cavalcanti, L.F.N. 2005. Drought indicators and triggers. In *Drought and Water Crises: Science, Technology, and Management Issues*, Wilhite, D.A. (ed.). Florida: CRC Press, Taylor & Francis Group, pp. 71-92.

Steppuhn, H. 1981. Snow and agriculture. In Gray, D.M. and Male, D.H. (Eds.). *Handbook of Snow: principles, processes, management & use.* Ontario: Pergamon Press Canada Ltd., pp. 60-125.

Su, M., Stolte, W.J. and van der Kamp, G. 2000. Modelling Canadian prairie wetland hydrology using a semi-distributed streamflow model. *Hydrological Processes* **14**: 2405-2422.

Thornthwaite, C.W. 1947. Climate and moisture conservation. *Annals of the Association of American Geographers* **37**: 87-100.

Töyrä, J. 2005. *Metadata for Preliminary LiDAR DEM – St. Denis NWA*. The National Water Research Institute, Environment Canada, Saskatoon, Canada.

van der Kamp, G., Stolte, W.J. and Clark, R.G. 1999. Drying out of small prairie wetlands after conversion of their catchments from cultivation to permanent brome grass. *Hydrological Sciences Journal* **44**: 387-397.

van der Kamp, G., Hayashi, M. and Gallén, D. 2003. Comparing the hydrology of grassed and cultivated catchments in the semi-arid Canadian prairies. *Hydrological Processes* **17**: 559-575.

van der Kamp, G. 2006. Personal Communication.

van der Kamp, G., Schmidt, R., Bayne, D. and Su, M. 2006a. Snow surveys at St. Denis NWA. Personal Communication.

van der Kamp, G., Schmidt, R., and Bayne, D. 2006b. Pond water levels at St. Denis NWA. Personal Communication.

Walmsley, J.L., Taylor, P.A. and Salmon, J.R. 1989. Simple guidelines for estimating windspeed variations due to small-scale topographic features – an update. *Climatological Bulletin* **23**: 3-14.

Wheaton, E.E., Arthur, L.M., Chorney, B., Shewchuk, S., Thorpe, J., Whiting, J. and Wittrock, V. 1992. The Prairie drought of 1988. *Climatological Bulletin* **26**: 188-205.

Wheaton. E., Wittrock, V., Kulshreshtha, S., Koshida, G., Grant, C., Chipanshi, A. and Bonsal. B., with the rest of the Canadian Drought Study Steering Committee, Adkins, P., Bell, G., Brown, G., Howard, A. and MacGregor, R. 2005. *Lessons Learned from the Canadian Drought Years 2001 and 2002: Synthesis Report. Publication No. 11602-46E0.* Prepared for Agriculture and Agri-Food Canada, SRC, Saskatoon, Saskatchewan. 38 pp.

Whitmore, J.S. 2000. *Drought Management on Farmland*. Kluwer Academic Publishers: Dordrecht, The Netherlands; 360.

Wilhite, D.A. and Glantz, M.H. 1985. Understanding the drought phenomenon: The role of definitions. *Water International* **10**: 111-120.

Wilhite, D.A. and Buchanan-Smith, M. 2005. Drought as hazard: understanding the natural and social context. In *Drought and Water Crises: Science, Technology, and Management Issues*, Wilhite, D.A. (ed.). CRC Press, Taylor & Francis Group: Florida; 3-29.

Woo, M.K. and Rowsell, R.D. 1993. Hydrology of a prairie slough. *Journal of Hydrology* **146**: 175-207.

Zhao, L., Gray, D.M. and Male, D.H. 1997. Numerical analysis of simultaneous heat and mass transfer during infiltration into frozen ground. *Journal of Hydrology* **200**: 345-363.

Zhao, L. and Gray, D.M. 1997. A parametric expression for estimating infiltration into frozen soils. *Hydrological Processes* **11**: 1761-1775.

Zhao, L. and Gray, D.M. 1999. Estimating snowmelt infiltration into frozen soils. *Hydrological Processes* **13**: 1827-1842.

Zhao, L., Gray, G.M. and Toth, B. 2002. Influence of soil texture on snowmelt infiltration into frozen soils. *Canadian Journal of Soil Science* **82**: 75-83.

APPENDIX A – FIELD TRANSECTS PHOTOS


Photo A.1 Field transect 1 north end (left) and south end (right).


Photo A.2 Field transect 2 north end (left) and south end (right).


Photo A.3 Field transect 2 wetland area (left) and field transect 3 (right).

Photo A.4 Field transect 4 north end (left) and south end (right).

APPENDIX B – MEAN VALUES OF VOLUMETRIC SOIL MOISTURE, VEGETATION HEIGHT, SWE, AND SNOW DENSITY

Table B.1 Mean observed fall volumetric soil moisture and mean vegetation height on field transects, St. Denis.

Transect #	Mean Volumetric Soil Moisture (%)	Mean Vegetation Height (m)
1	26.7	0.18
2	25.4	0.79
3	31.1	0.60
4	30.1	0.30

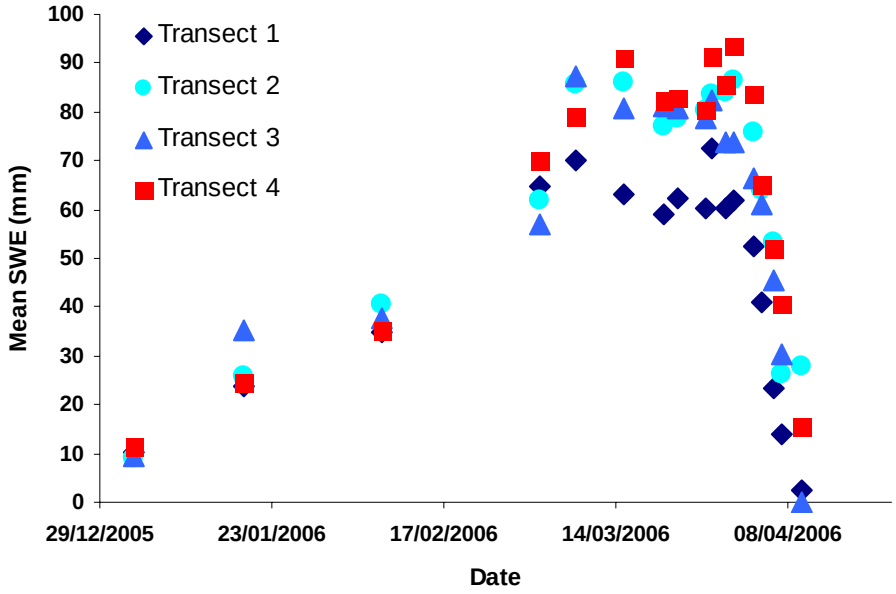

Figure B.1 Mean observed SWE on field transects, St. Denis.

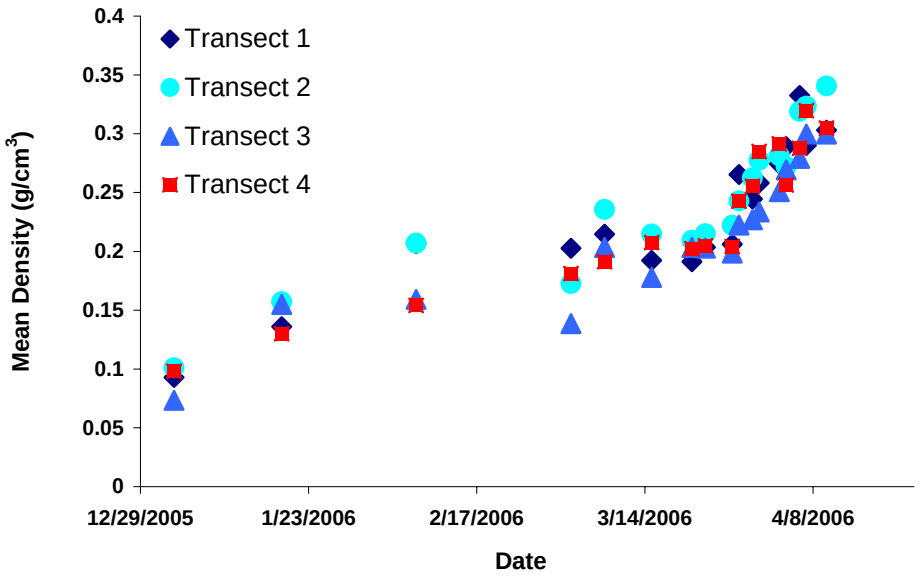

Figure B.2 Mean observed snow density on field transects, St. Denis.

APPENDIX C – METHODS FOR FIELD DATA COLLECTION

C.1 Field observations at Bad Lake

At Bad Lake IHD Research Basin, an instrumentation station was installed and maintained to measure air temperature, relative humidity, and wind at 2 metre height as well as radiation. Air temperature was measured with nickel-iron resistance thermometers, which were housed in double radiation shields with natural ventilation. Measurements of relative humidity were obtained with the Honeywell dewcells (Li-C1 type), which were shielded against solar radiation and naturally ventilated. The Rimco 'Miniature-cup' impulse type anemometers were used for wind speed measurements; a potentiometer attached to a wind vane was used to measure wind direction. The net all-wave radiation was measured with a Funk (Middleton) Pyrradiometer. Copper-constantan thermocouples placed in the snowpack and placed in the underlying soil provided measurements of snow temperature and soil temperature, respectively. These measurements described above were automatically recorded by a Hewlett-Packard mini-computer which was housed in the instrument box.

In addition, Meteorological Service of Canada Nipher gauges were used to provide point measurements of snowfall data. Both depth and density of snow were measured on snow survey courses on different land uses to provide measurements of areal snow water equivalent. The snow depth was determined by ruler; the snow density was decided by gravimetric method. Also, Tipping Buckets attached with Solid State Recorders were used to record rainfall data. For the fall soil moisture, two probe gamma density meter in PVC tube was used to monitor the changes in density of the soil and to estimate soil moisture. For the streamflow monitoring, stage recorder at a weir by the outlet of Creighton Tributary of Bad Lake was used to estimate streamflow discharge.

C.2 Field observations at St. Denis

At St. Denis NWA, measurements of air temperature, relative humidity, wind speed, wind direction, and radiation were collected from ten-metre tower stations and station with eddy correlation system. The instrumentations included Campbell Scientific RM Young 6-Plate and 10-Plate Gill Radiation Shield sensors for measuring air temperature and relative humidity; Campbell Scientific RM Young Wind Monitor was used to measure wind speed and wind direction. The net radiation was measured using Campbell Scientific Kipp & Zonen Net Radiometer, which consists of two pyranometers to measure short-wave radiation and two pyrgeometers to measure long-wave radiation. Measurements of precipitation were acquired from precipitation gauges station, which consists of Meteorological Service of

Canada Nipher gauge for snowfall measurement and Tipping Bucket for rainfall measurement. The above stations all had measuring sensors connected to Campbell Scientific datalogger that allows automatic data recording.

In addition, vegetation surveys were taken to determine vegetation type and vegetation height on field transects with different land uses: cultivated field, grassland, and wetland; simple measurements by metre stick were used in the vegetation surveys. Soil surveys were conducted to determine fall soil moisture on field transects with different land uses. Soil core samples (0-40 cm) were taken and oven-drying method was used to estimate the volumetric soil moisture and bulk density. Total porosity of soil was calculated from bulk density (g/cm^3) and particle density (g/cm^3) as:

$$Total\ Porosity = 1 - \frac{Bulk\ Density}{Particle\ Density} \qquad [C.1]$$

Campbell Scientific TDR soil probes were also used for additional measurements of fall volumetric soil moisture. On the field transects, snow surveys of depth and density were taken to determine snow water equivalent (SWE). The snow depth was determined by ruler; the snow density was decided by gravimetric method. SWE (mm) was calculated as:

$$SWE = 10D\bar{\rho} \qquad [C.2]$$

where D (cm) is the snow depth at each point of a transect and $\bar{\rho}$ (g/cm^3) is the mean snow density of a transect. For the wetland water level, a graduated stick with a 4 cm diameter circular plate at the bottom was used for water depth measurements.

APPENDIX D – C++ PROGRAMMING CODE FOR THE SIMPLIFIED WINDFLOW MODEL

Simplified windflow model (Walmsley *et al.*, 1989) was programmed in C++ code and integrated into CRHM as 'wind_adjust' module to calculate windspeed due to local topographic change. The coding is complied in Borland C++ Builder and is shown as follow:

Part I – NewModules_withwind.cpp file

```
// 09/18/06
//---------------------------------------------------------------------------
#include <vcl.h>
#pragma hdrstop
#include "NewModules_withwind.h"
#include "DefCRHMGlobal.h"
#include "common.h"
#include <algorithms>
//---------------------------------------------------------------------------
#pragma package(smart_init)

using namespace std;

extern double xLimit;
extern long lLimit;

Administer DLLModules("09/18/06", "Modules_New");

void MoveModulesToGlobal(String DLLName){
  DLLModules.AddModule(new Classwind_adjust("wind_adjust", 09/18/06"));
  DLLModules.LoadCRHM(DLLName);
}

// WindAdjust module that adjusts the wind speed due to topographic feature

void Classwind_adjust::decl(void) {

  declvar("hru_Uadjust", NHRU, "adjusted wind speed", "(m/s)", hru_Uadjust);
  declvar("hru_Uchange", NHRU, "wind speed change due to topography",
  "(m/s)", &hru_Uchange);
  declvar("WR", NHRU, "wind ratio", "()", &WR);
  declparam("Zwind", NHRU, "[10.0]", "0.0", "100.0", "wind instrument
  height", "(m)", &Zwind);
  declparam("A", NHRU, "0.0", "0.0", "4.4", "coefficient for wind speed
  change due to topography, 0.0 = flat terrain, 2.5 = 2D escarpments, 3.0 = 2D
```

```
 hills, 3.5 = 2D rolling terrain, 4.0 = 3D hills, 4.4 = 3D rolling terrain", "()",
 &A);
 declparam("B", NHRU, "0.0", "0.0", "2.0", "coefficient for wind speed
 change due to topography, 0.0 = flat terrain, 0.8 = 2D escarpments, 1.1 = 3D
 rolling terrain, 1.55 = 2D rolling terrain, 1.6 = 3D hills, 2.0 = 2D hills", "()",
 &B);
 declparam("L", NHRU, "[40.0]", "40.0", "300.0", "upwind half-width at half
 height", "(m)", &L);
 declparam("obs_elev", NHRU, "[637]", "0.0", "100000.0", "measurement
 altitude", "(m)", &obs_elev);
 declparam("hru_elev", NHRU, "[637]", "0.0", "100000.0", "altitude", "(m)",
 &hru_elev);
 declgetvar("obs",     "hru_u", "(m/s)", &hru_u);

}

void Classwind_adjust::init(void) {
 nhru = getdim(NHRU);
}

void Classwind_adjust::run(void) {

/*Walmsley, Talor and Salmon's simple guidelines for estimating wind speed
variations due to topographic features*/

 for (int hh = 0; hh < nhru; hh++) {
  double h = hru_elev[hh] - obs_elev[hh]; /* topgraphic feature height*/
  double Smax = B[hh] * h / L[hh]; /* maximum decay of fractional speed-up
                                      ratio*/
  double S = Smax * exp(-A[hh]*Zwind[hh]/L[hh]); /* decay of fractional
                                                    speed-up ratio*/

  hru_Uchange[hh] = S * hru_u[hh];
  hru_Uadjust[hh] = hru_Uchange[hh] + hru_u[hh];
  WR[hh] = hru_Uadjust[hh] / hru_u[hh];
 }

}
```

Part II – NewModules_withwind.h file

```
//---------------------------------------------------------------------------
#ifndef OurModulesH
#define OurModulesH
//---------------------------------------------------------------------------
```

```
#include "ClassModule.h"

using namespace std;

extern "C" void __declspec(dllexport) MoveModulesToGlobal(String
DLLName = "CRHM new");

class Classwind_adjust : public ClassModule {
public:

Classwind_adjust(string Name, String Version = "undefined") :
ClassModule(Name, Version) {};

long nhru;

// declared variables
float *hru_Uadjust;
float *hru_Uchange;
float *WR;

// declared parameters
const float *Zwind;
const float *A;
const float *B;
const float *L;
const float *obs_elev;
const float *hru_elev;

// varaible inputs
const float *hru_u;

void decl(void);
void init(void);
void run(void);
};
#endif
```

APPENDIX E – CHARACTERISTICS OF PARAMETER FOR 19 HRUS IN SPATIALLY AGGREGATED MODELLING APPROACH

HRU Name	Symbols	Area (km^2)	Slope Aspect (°)	Slope Angle (°)	Elevation (m)	Vegetation Height (m)	Fetch Distance (m)
Stubble South Steep Slope	SSSS	0.1	180	8	550	0.15	300
Stubble South Gentle Slope	SSGS	0.1	180	5	548	0.15	300
Stubble North Steep Slope	SNSS	0.1	0	8	550	0.15	300
Stubble North Gentle Slope	SNGS	0.1	0	5	548	0.15	300
Stubble Level	SL	1.05	0	0	555	0.15	300
Stubble Steep Slope Hilltop	SSSH	0.1	0	8	565	0.15	300
Stubble Gentle Slope Hilltop	SGSH	0.1	0	5	563	0.15	300
Stubble Steep Slope Valley	SSSV	0.1	0	8	540	0.15	300
Stubble Gentle Slope Valley	SGSV	0.1	0	5	542	0.15	300
Grass South Steep Slope	GSSS	0.1	180	8	550	0.5	300
Grass South Gentle Slope	GSGS	0.1	180	5	548	0.5	300
Grass North Steep Slope	GNSS	0.1	0	8	550	0.5	300
Grass North Gentle Slope	GNGS	0.1	0	5	548	0.5	300
Grass Level	GL	1.05	0	0	555	0.5	300
Grass Steep Slope Hilltop	GSSH	0.1	0	8	565	0.5	300
Grass Gentle Slope Hilltop	GGSH	0.1	0	5	563	0.5	300
Grass Steep Slope Valley	GSSV	0.1	0	8	540	0.5	300
Grass Gentle Slope Valley	GGSV	0.1	0	5	542	0.5	300
Wetland	W	0.15	0	0	542	5	300

APPENDIX F – SCHMATICS FOR SNOW HYDROLOGY MODEL AT CREIGHTON TRIBUTARY

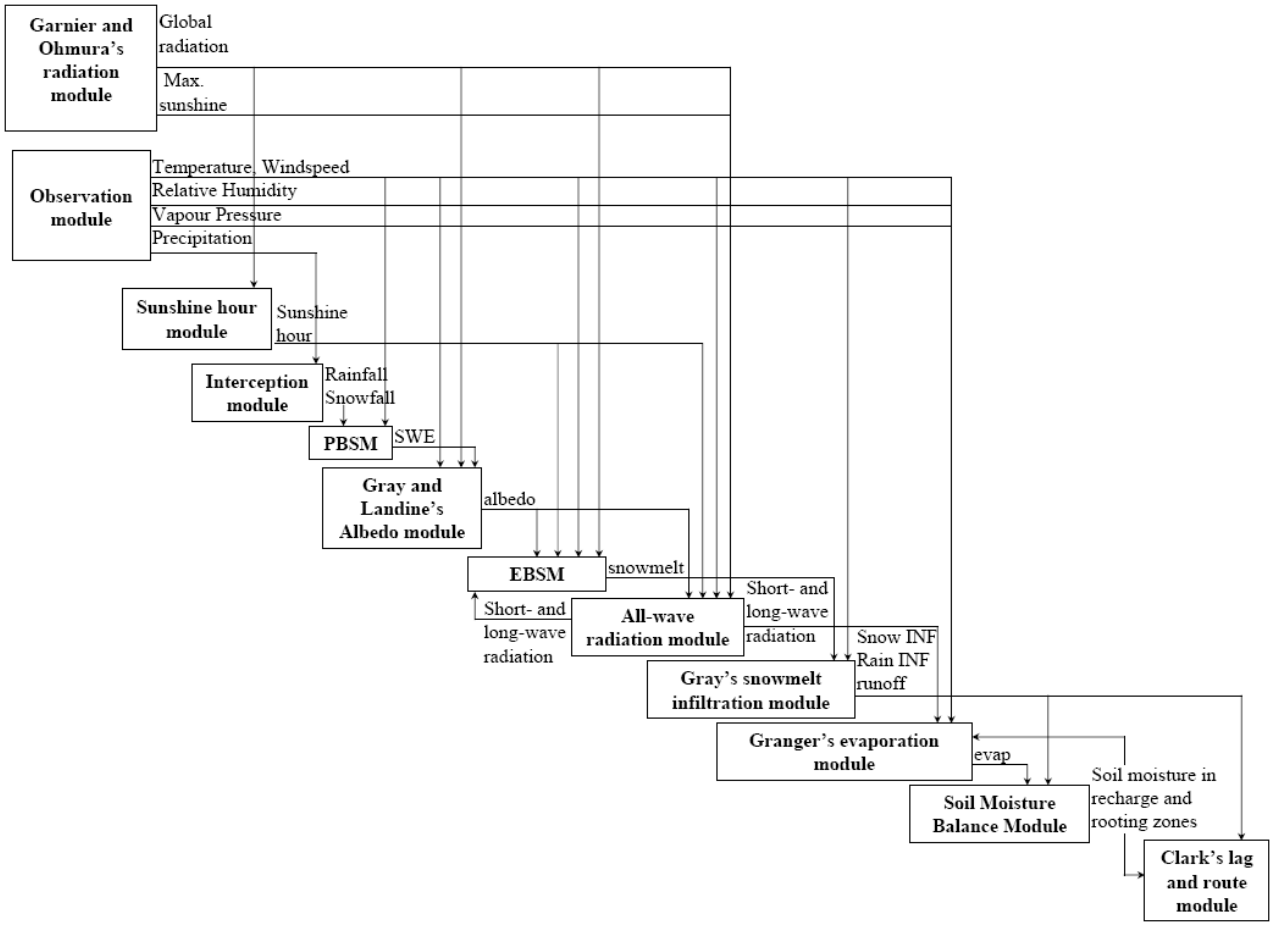

APPENDIX G – SCHMATICS FOR SNOW HYDROLOGY MODEL AT WETLAND 109